



University of Kentucky  
UKnowledge

---

University of Kentucky Master's Theses

Graduate School

---

2008

## PRODUCTION OF LOW-ENERGY, 100% BY-PRODUCT CEMENT UTILIZING COAL COMBUSTION PRODUCTS

David E. Rust  
*University of Kentucky*, [rustde@gmail.com](mailto:rustde@gmail.com)

[Right click to open a feedback form in a new tab to let us know how this document benefits you.](#)

---

### Recommended Citation

Rust, David E., "PRODUCTION OF LOW-ENERGY, 100% BY-PRODUCT CEMENT UTILIZING COAL COMBUSTION PRODUCTS" (2008). *University of Kentucky Master's Theses*. 541.  
[https://uknowledge.uky.edu/gradschool\\_theses/541](https://uknowledge.uky.edu/gradschool_theses/541)

This Thesis is brought to you for free and open access by the Graduate School at UKnowledge. It has been accepted for inclusion in University of Kentucky Master's Theses by an authorized administrator of UKnowledge. For more information, please contact [UKnowledge@lsv.uky.edu](mailto:UKnowledge@lsv.uky.edu).

## ABSTRACT OF THESIS

### PRODUCTION OF LOW-ENERGY, 100% BY-PRODUCT CEMENT UTILIZING COAL COMBUSTION PRODUCTS

The ever-increasing quantity of by-products generated from burning coal in the production of electricity has brought about the need for new areas of utilization. This study examined the use of FGD gypsum and fluidized bed combustion ash along with Class F fly ash in the production of low-energy, 100% by-product cement blends. The cement blends used the advantageous properties of the by-product materials to create cementing properties rather than energy intensive clinker used in ordinary portland cement. The FGD gypsum was converted to hemihydrate which rapidly hydrated to provide the cement with early strength gains, whilst the fluidized bed combustion ash reacted with the Class F fly ash to form pozzolanic cementitious phases which provided the longer-term compressive strength and possibly resistance to weathering. The rate of compressive strength gains and minimizing detrimental expansion were two properties of particular interest in the study. Chemical admixtures were used to improve the compressive strengths of the cement mortars and decrease their solubility.

KEYWORDS: FGD Gypsum, Fluidized Bed Combustion Ash, Fly Ash, Ettringite,  
Low-Energy Cement

---

David E. Rust

---

July 22, 2008

---

PRODUCTION OF LOW-ENERGY, 100% BY-PRODUCT CEMENT  
UTILIZING COAL COMBUSTION PRODUCTS

By

David Edward Rust

Kamyar C. Mahboub

---

Director of Thesis

Kamyar C. Mahboub

---

Director of Graduate Studies

July 22, 2008

---



THESIS

David Edward Rust

The Graduate School  
University of Kentucky

2008

PRODUCTION OF LOW-ENERGY, 100% BY-PRODUCT CEMENT  
UTILIZING COAL COMBUSTION PRODUCTS

---

THESIS

---

A thesis submitted in partial fulfillment of the requirements  
for the degree of Master of Science in the  
College of Engineering at the University of Kentucky

By

David Edward Rust

Lexington, Kentucky

Director: Dr. Kamyar C. Mahboub, Professor of Civil Engineering

Lexington, Kentucky

2008

Copyright© David Edward Rust 2008

## ACKNOWLEDGEMENTS

The following thesis, while an individual work, benefited from the insights and directions of several people. First, my Thesis Chair, Dr. Kamyar Mahboub, exemplifies the high quality of scholarship to which I aspire. In addition, Mr. Robert Rathbone and Dr. Tom Robl provided timely and instructive comments and evaluation at every stage of the thesis process, allowing me to complete this project on schedule. Instrumental assistance was provided by Kevin Henke who performed the X-ray Diffraction analysis, and Aurora Rubel who performed the Thermogravimetric Analysis. Their assistance resulted in a more thorough analysis of the data presented in the following thesis. Next, I wish to thank the complete Thesis Committee: Dr. Kamyar C. Mahboub, Dr. Issam E. Harik, and Dr. Tom Robl. Each individual provided insights that guided and challenged my thinking, substantially improving the finished product.

In addition to the technical and instrumental assistance above, I received equally important assistance from family and friends. My girlfriend, Chelsea Elam, provided on-going support throughout the thesis process. My parents, Tom and Mary Rust, instilled in me, from an early age, the desire and skills to obtain a Master's Degree. They have taught me that with hard work, anything can be accomplished. Bob Jewell, Jack Groppo, John Wiseman, and Dong Li provided help and support throughout the project.

## TABLE OF CONTENTS

Acknowledgements.....	iii
List of Tables .....	vi
List of Figures.....	vii
List of Files .....	x
Section 1: Introduction.....	1
Section 2: Literature Review .....	5
Section 3: Materials Used in the Study.....	9
Section 4: Equipment Used in the Study .....	14
Section 5: Cement Experiments.....	20
5.1 “Clinkerless” Cement Research Methodology.....	20
5.1.1 Preliminary “Clinkerless” Cement Blends .....	21
5.1.2 Establishing a Standard Prehydration Technique.....	22
5.1.3 “Clinkerless” Cement Blends Utilizing Standard Prehydration Technique .....	23
5.2 Reproducing Previous Research.....	24
5.3 Introducing Hemihydrate to the By-Product Cement System.....	25
5.4 Expansion Studies .....	27
5.5 Mortar Paste Study .....	28
5.6 Procedure for Producing Hemihydrate from FGD Gypsum .....	30
5.7 Preliminary “Low-Energy, 100% By-Product Cement” Blends.....	34
5.8 High Strength and Low Expansion “Low-Energy, 100% By-Product Cement” .....	35
Section 6: Results and Discussion of the Cement Experiments .....	37
6.1 “Clinkerless” Cement Blends .....	37
6.1.1 Preliminary “Clinkerless” Cement Blends .....	37
6.1.2 Confirmation of the Prehydration Technique.....	38
6.1.3 “Clinkerless” Cement Blends to Reduce Expansion .....	39
6.1.4 High Strength and Low Expansion “Clinkerless” Cement Blends .....	44
6.2 Reproducing Previous Research.....	46
6.3 Introducing Hemihydrate to the By-Product Cement System.....	49
6.4 Expansion Studies .....	52
6.5 Mortar Paste Study .....	59
6.5.1 X-ray Diffraction Analysis.....	59
6.5.2 Thermogravimetric Analysis.....	62
6.6 Procedure for Producing Hemihydrate from FGD Gypsum .....	64
6.7 Preliminary “Low-Energy, 100% By-Product Cement” Blends.....	70
6.7.1 Compressive Strength Results.....	70



6.7.2 Expansion Results .....	74
6.8 High Strength and Low Expansion “Low-Energy, 100% By-Product Cement” .....	76
Section 7: Conclusions.....	81
Section 8: Recommendations for Future Research.....	84
Appendices.....	85
Appendix A: Glossary of Terms Used in this Report.....	85
Appendix B: Raw Experimental Data of Cement Blends Produced in the Study.....	87
Appendix C: Two Sample t-Tests Performed in the Study .....	98
References.....	108
Vita.....	111

## LIST OF TABLES

Table 3.1 – Chemical composition of FGD gypsum used in the study .....	9
Table 3.2 – Chemical composition of the spent bed ash used in the study .....	10
Table 3.3 – Chemical composition of the Class F ultra fine ash used in the study .....	11
Table 3.4 – Chemical composition of <u>Hydro-Stone®</u> .....	12
Table 3.5 – Chemical composition of <u>Duracal®</u> .....	12
Table 5.1 – Composition of the preliminary “Clinkerless” cement blends prepared in the research project .....	22
Table 5.2 – Composition of the “Clinkerless” cement blends prepared using prehydrated spent bed .....	24
Table 5.3 – <i>No-Cement #1</i> mix design .....	24
Table 5.4 – <i>Sandless #1</i> mix design .....	25
Table 5.5 – Composition of cement blends containing <u>Hydro-Stone®</u> .....	27
Table 5.6 – Composition of the preliminary “low-energy, 100% by-product cement” blends .....	35
Table 5.7 – Mix design of the <i>0.5HH/0.5CL6 #1</i> cement blend to produce a 500 g (17.64 oz) batch of mortar cement .....	36
Table 5.8 – Mix design of the <i>0.5HH/0.5CL6 w/Silica Fume</i> cement blend to produce a 500 g (17.64 oz) batch of mortar cement .....	36
Table 6.1 – Calcium hydroxide content of cement blends at different curing ages .....	64
Table 7.1 – Mortar mix design of the <i>0.5HH/0.5CL6 #1</i> cement blend .....	83
Table 7.2 – Mortar mix design of the <i>0.5HH/0.5CL6 w/Silica Fume</i> cement blend .....	83

## LIST OF FIGURES

Figure 4.1 – Photograph of the disk mill used to grind raw materials.....	14
Figure 4.2 – Photograph looking down into the ball mill showing its cross-section and steel media used for grinding action .....	15
Figure 4.3 – Photograph of the ball mill situated on its base.....	16
Figure 4.4 – Photograph of the <i>Malvern Mastersizer 2000 Particle Analyzer</i> used to determine the size distribution of cement candidate materials .....	17
Figure 4.5 – Photograph of the <i>All American Model 75X Pressure Steam Sterilizer</i> used in the production of hemihydrate.....	17
Figure 4.6 – Photograph of the <i>VWR Scientific Model 1370 FM Forced Air Oven</i> used for the drying phase of the hemihydrate processing.....	18
Figure 4.7 – Photograph of the mortar mixer conforming to ASTM C 305 used in the 100% by-product cement project.....	19
Figure 4.8 – Photograph of the compression machine used to test mortar specimen in the study .....	19
Figure 5.1 – Photograph of sealed plastic containers with moist paper towels stored at room temperature used in the refined method of curing the cement paste samples.....	29
Figure 5.2 – Photograph of the items used to form the gypsum into molded bodies. Pictured from left: Proctor mold with moist FGD gypsum, short cylinder, and tall cylinder .....	31
Figure 5.3 – Photograph of the molding system situated in the compression machine with the tall cylinder extending above the Proctor mold to allow the load to be applied to the gypsum .....	31
Figure 5.4 – Photograph of the Proctor mold base with gypsum puck, short cylinder, and tall cylinder stacked on top. The cylindrical portion of the Proctor mold had been removed .....	32
Figure 5.5 – Photograph of 16 gypsum pucks in the autoclave .....	33
Figure 5.6 – Photograph showing hemihydrate pucks broken up with a hammer and being ground in the disk mill .....	34
Figure 6.1 – Compressive strengths of mortar cubes prepared using the preliminary “Clinkerless” cement blends .....	37
Figure 6.2 – Compressive strengths of mortar cubes prepared using the 70/30 spent bed / ultra fine ash cement blend prehydrated with 10% and 20% water by weight of spent bed.....	39
Figure 6.3 – Photograph of map cracking on a mortar cube prepared using the <i>Clinkerless #3</i> cement blend after 56 days in the moist curing room.....	40
Figure 6.4 – Average edge lengths of mortar cubes prepared using the preliminary “Clinkerless” cement blends.....	41
Figure 6.5 – Average compressive strengths of mortar cubes prepared using the “Clinkerless” cement blends that were produced to reduce expansion .....	42
Figure 6.6 – Average edge lengths of mortar cubes prepared using the “Clinkerless” cement blends that were produced to reduce expansion.....	44

Figure 6.7 – Compressive strengths of mortar cubes prepared using the high strength and low expansion “Clinkerless” cement blends .....	45
Figure 6.8 – Compressive strengths of mortar cubes prepared using the mortar mixes that reproduced previous research by Bland et al. (1987) .....	47
Figure 6.9 – Average edge lengths of mortar cubes prepared using the mortar mixes that reproduced previous research by Bland et al. (1987) .....	48
Figure 6.10 – Compressive strengths of mortar cubes prepared using the cement blends that contained <u>Hydro-Stone®</u> .....	50
Figure 6.11 – Expansion data of length-change prisms prepared using the high strength and low expansion “Clinkerless” cement blends .....	53
Figure 6.12 – Expansion data of length-change prisms prepared using a 70/30 ratio of spent bed / pozzolan .....	55
Figure 6.13 – Expansion data of length-change prisms prepared using the two <u>Hydro-Stone®</u> / <i>Clinkerless</i> #2 cement blends and <u>Duracal®</u> cement.....	56
Figure 6.14 – Expansion data of length-change prisms prepared using the <i>Clinkerless</i> #2 and <i>HSCL2</i> #2 cement blends .....	58
Figure 6.15 – XRD plots of <i>Clinkerless</i> #2 at different curing ages.....	59
Figure 6.16 – XRD plots of <i>Clinkerless</i> #6 at different curing ages.....	60
Figure 6.17 – XRD plots of <i>HSCL2</i> #2 at different curing ages.....	61
Figure 6.18 – TGA plot of <i>Clinkerless</i> #2 .....	62
Figure 6.19 – TGA plot of <i>Clinkerless</i> #6 .....	63
Figure 6.20 – TGA plot of <i>HSCL2</i> #2.....	63
Figure 6.21 – SEM photograph of gypsum crystals before the conversion to hemihydrate .....	65
Figure 6.22 – SEM photograph of hemihydrate crystals produced from un-pressed gypsum autoclaved four hours .....	66
Figure 6.23 – SEM photograph of hemihydrate crystals produced from gypsum that was pressed into pucks with 24.47 kN (5500 lbs) of force, and autoclaved four hours.....	66
Figure 6.24 – SEM photograph of hemihydrate crystals produced from gypsum that was pressed into pucks with 48.93 kN (11000 lbs) of force, and autoclaved four hours.....	67
Figure 6.25 – Compressive strengths of mortar cubes prepared using hemihydrates produced from the different FGD gypsum pressing techniques .....	68
Figure 6.26 – Compressive strengths of mortar cubes prepared using hemihydrates that were produced from FGD gypsum mixed with chemical additives, and pressed with 24.47 kN (5500 lbs) of force.....	69
Figure 6.27 – Setting time of the mortar prepared using the <i>0.5HH/0.5CL2</i> #1 cement blend .....	71
Figure 6.28 – Compressive strengths of mortar cubes prepared using the preliminary “low-energy, 100% by-product cement” blends.....	72
Figure 6.29 – Expansion data of length-change prisms prepared using the preliminary “low-energy, 100% by-product cement” blends.....	75

Figure 6.30 – Compressive strengths of mortar cubes prepared using the high strength and low expansion “low-energy, 100% by-product cement” mortar mix designs.....	78
Figure 6.31 – Expansion data of length-change prisms prepared using the high strength and low expansion “low-energy, 100% by-product cement” mortar mix designs .....	80

LIST OF FILES

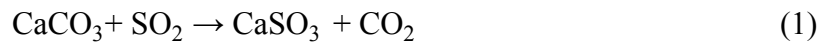
David\_Rust\_2008 ..... 5.0 MB PDF

## Section 1: Introduction

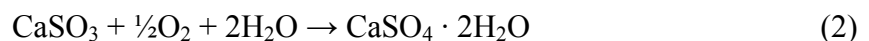
Sulfur dioxide (SO<sub>2</sub>), a by-product of the combustion of sulfur contained in coal used in power generation, is a harmful gas to both humans and the environment. When inhaled by humans, sulfur dioxide can cause throat irritation, coughing, and labored breathing. Acid rain is a major threat to the environment and is caused by the reaction of sulfur dioxide with moisture in the air to form sulfuric acid. Typical results from acid precipitation are damage to forests, surface water, soils, and man-made materials such as buildings and monuments.

In 1990, the United States Environmental Protection Agency (EPA) made amendments to its 1970 Clean Air Act to curb sulfur dioxide emissions as a solution to the acid rain problem (EPA 1990). Two common methods employed to reduce sulfur dioxide emissions from the generation of electricity are flue gas desulfurization and circulating fluidized bed combustion.

The first and more traditional method of sulfur dioxide reduction in coal power generation is flue gas desulfurization (FGD). In the FGD scrubbing process, sulfur dioxide is removed from the flue gas after coal combustion has occurred. As coal is combusted, the sulfur present in the coal reacts with oxygen in the air, and it forms sulfur dioxide that exits the combustor in the flue gas. The flue gas containing sulfur dioxide is an acidic gas; therefore, alkaline materials such as limestone slurries or lime are used to remove the sulfur as the gas passes through the scrubber system. The following equation is an example of a chemical reaction which takes place in the scrubber system.



Early on in the FGD scrubbing technology, the by-product produced was a calcium sulfite (CaSO<sub>3</sub>) sludge that was not of much use. However, as the technology advanced it was discovered that the sludge could be oxidized and converted into a marketable gypsum product.

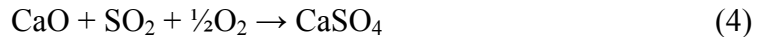


The majority of FGD scrubbing systems installed and in use in the United States are wet scrubber systems because of their ability to remove large quantities (more than 90%) of sulfur dioxide from flue gas.

A second method of sulfur dioxide pollution control is a technology called circulating fluidized bed combustion (CFBC). CFBC is gaining acceptance for the utilization of “problem fuels”, such as low-grade or high-sulfur coals, for thermal power generation (Berry 1991). In the CFBC process, sulfur dioxide removal takes place inside the coal combustion zone rather than using expensive post combustion scrubber systems to clean the flue gas as it passes through. The sulfur dioxide removal is achieved by burning the coal in the presence of limestone resulting in two desired chemical reactions. The first reaction that occurs is the limestone calcining in the combustor, as described by the reaction below.



The second reaction results in the sulfur dioxide removal as the unslaked lime (CaO) reacts with sulfur dioxide to form anhydrite (CaSO<sub>4</sub>) which is the mineral form of gypsum, as shown by the following reaction.



There are advantages of using the CFBC technology other than sulfur dioxide control that are contributing to their usage in power generation. CFBC technology operates at a lower temperature of 800-900°C (1472-1652°F) compared to ordinary pulverized coal combustion (PCC) units and thus reduces NO<sub>x</sub> emissions. The reduction in NO<sub>x</sub> is attributed to the dominant NO<sub>x</sub> source being fuel nitrogen oxidation in CFBC units as opposed to air nitrogen oxidation in ordinary PCC units. A significant amount of the fuel-nitrogen remains in the char in the CFBC unit after devolatilization instead of escaping into the air (Gungor 2008).

One major cost advantage to using CFBC technology is the ability to burn coal that is higher in ash and sulfur than that used in ordinary PCC units. The fuel flexibility



is attributed to the unique combustion and heat transfer environment present in the fluidized bed (Basu 1999). Coal is burned in the presence of non-combustible granular solids such as limestone that are maintained in a fast-fluidized condition. This condition enables intense mixing of fresh coal particles with the hot bed material. The hot bed material easily raises the temperature of the coal particles, regardless of their quality, above their ignition temperature. Some of the heat generated by the combusted coal particles then goes back to the bed solids and the process continues. The ability of CFBC units to burn lower quality coal results in a lower fuel cost compared to ordinary PCC units.

Even though CFBC technology has many advantages, it does not come without some problems that need to be addressed. CFBC produces more ash and carbon dioxide (CO<sub>2</sub>) than conventional PCC units. Carbon dioxide is a common greenhouse gas that is generally believed to contribute to global warming. The ash generated in the CFBC process is problematic because of the large quantity that needs to be landfilled (which comes with a significant cost) as well as the exothermic and expansive phenomena associated with the hydration of the large quantity of unslaked lime present in the spent bed material. Additionally, the spent bed material is characterized by poor pozzolanic activity and is therefore unsuitable for traditional recycling such as concrete manufacturing (Montagnaro 2008).

According to the American Coal Ash Association (ACAA 2007), in 2006 over 30.2 million tons of FGD scrubber by-products were produced in the United States of which just over 10.6 million tons were utilized for a 35% utilization rate. FGD gypsum was the most heavily utilized FGD material with 79% of the material utilized, the majority of which was used in the production of gypsum wallboard (7.6 million tons). Also in 2006, 1.6 million tons of FBC ash were produced with 1.1 million tons utilized for a 68% utilization rate.

Because of the implementation of sulfur control technologies, according to the Energy Information Administration (EIA 2008), electric power sulfur dioxide emissions are expected to decrease from 9.39 million tons in 2006 to 4.67 million tons and 3.71 million tons in 2015 and 2030 respectively. The effort of the utility companies is even more significant than the overall 61% reduction in sulfur dioxide emissions suggests.

Over the same time period, the EIA expects the amount of electric power generated from coal to grow 42%. Therefore, the quantity of sulfur-containing by-products will likely increase dramatically over the next several years. New alternative applications for their use will be needed to address the increase in production.

The research presented in this report was devoted to utilizing sulfur dioxide removal waste products as well as Class F fly ash in the production of low-energy, 100% by-product cement. There were two main components of the by-product cement that were developed in the research.

The first component of the by-product cement was calcium sulfate hemihydrate ( $\text{CaSO}_4 \cdot 0.5\text{H}_2\text{O}$ ), which is produced by partially dehydrating FGD gypsum. Hemihydrate, also commonly referred to as Plaster of Paris, has a very fast set time and was responsible for providing the by-product cement products with early compressive strength. Contributing to the goal of the project, the production of hemihydrate only requires 15% of the energy input required to produce portland cement (Mehta 1980).

The second component of the by-product cement was a blend of CFBC spent bed ash and Class F fly ash that reacted to produce ettringite and other cementitious hydrates. This second component was responsible for providing the by-product cement compound with long-term strength while lowering its solubility. Further contributing to the goal of producing low-energy by-product cement, no energy was required to heat the CFBC spent bed ash and Class F fly ash in preparation for their use.

As in any situation where new uses for a particular by-product are being investigated, there were problems that needed to be addressed throughout the study. Two of the major problems were obtaining sufficient early strength in a cement blend that was formulated entirely from by-products, and eliminating detrimental expansion caused by the reaction of the CFBC spent bed ash and the Class F fly ash. This report explains the experimental process devised to overcome these challenges as well as create a “green cement” which was based entirely on by-product materials and had a smaller carbon footprint when compared to ordinary portland cement.

## **Section 2: Literature Review**

The literature review revealed that there are many applications where coal combustion products (CCPs) are being utilized. However, there is much room for new areas of utilization. According to the American Coal Ash Association (ACAA 2007), 124.8 million tons of CCPs were produced in 2006. Of the CCPs produced, slightly more than 43% were used beneficially rather than landfilled. A goal of 50% beneficial use by 2011 has been jointly established by the EPA and industry which provides incentive to research and develop new applications for CCPs.

Wallboard production is a major area of flue gas desulfurization (FGD) gypsum utilization. In the wallboard process, the FGD gypsum crystals are subjected to a flash drying and deagglomeration process to eliminate the free moisture present. The dried FGD gypsum is then flash calcined to a hemihydrate. The hemihydrate is ground and formed into an aqueous slurry along with a lightweight foam solution or other lightweight aggregate. The slurry is placed on the inner surface of a paper face sheet, and a paper back sheet is placed on the top surface (Burkard 1985).

In the 1980's, the marketing potential of FGD gypsum was evaluated for use in the wallboard industry. Results showed that producing a marketable gypsum product would be cheaper than landfilling the FGD by-product. In some cases relocation of wallboard plants close to power plants producing FGD gypsum was feasible (O'Brien 1984). The process became very popular and in 2006, 79% of FGD gypsum utilized was used in the production of wallboard (ACAA 2007).

Another "traditional" area of CCP utilization is the addition of fly ash to concrete. Many benefits are realized by such a combination and they include: enhanced workability due to the spherical shape of fly ash particles, reduced bleeding and a lower water : cement ratio, increased ultimate strength, reduced permeability and chloride ion penetration, greater resistance to sulfate attack, greater resistance to alkali-aggregate reactivity, reduced drying shrinkage, and increased ultimate strength (ACAA 1995). In 2006, nearly 50% of fly ash utilized was used as an addition to concrete and grouts. Another 13% was used as cement or raw feed for clinker (ACAA 2007).

In addition to these two common areas of CCP utilization, there has been much research into the utilization of CCPs in newer areas of the construction industry. The

expansive nature of some CCP materials allows for their use in mine backfill and expansive grout. The high free lime content of FBC waste enables it to be used to neutralize acidic waste forms. Several soil applications including soil-cements, stabilization, deep soil mixing, slurry walls, and jet grouting are areas where CCPs can be employed. Fluidized bed combustion (FBC) ash and fly ash have been used to make concrete without the need of traditional portland cement, thus producing an inexpensive concrete (Berry 1991; Hemmings 2007).

Much research has been done investigating the use of CCPs in mine back-filling and mine contamination barriers. Use of FGD material in a grout pumped into an underground coal mine (Walker 2005), and the use of FGD compacted as a seal in an open pit mine (Stuart 1999) were successful in preventing acid mine drainage. Similar research was done on compacted fly ash (Shang 2005), and it was found that its low hydraulic conductivity could make it a candidate for an acid mine drainage barrier. Use of a FBC ash grout also proved to be successful in reducing the problems associated with acid mine drainage in an underground coal mine (Siriwardane 2003) as well as providing cost savings over conventional grout (Giacinto 2007). The acid mine drainage does not appear to increase the weathering of the FGD grout (Warner 2007).

Using CCPs in soil-related applications has been the topic of several studies with mixed results. Hopkins and Beckham investigated the use of FBC material as a chemical admixture for soil subgrade stabilization of a highway in Kentucky. Within two months of placement of the bituminous base courses, severe differential swelling had occurred (Hopkins and Beckham 1999). Deschamps experienced more severe results in a study on using FBC and Stoker Ashes in a roadway embankment (Deschamps 1998). The compacted FBC material exhibited significant swell stresses, and it was still expanding two years after construction. Wolfe et al. (2001) examined CCPs that were used as structural fill for a shopping center constructed in a wetland in Virginia. Shortly after construction, distress on the structures was observed causing one to be closed and reconstructed. It was concluded that the damage observed was a result of differential settlement of the compressible clays that made up the subgrade. However, some researchers believe that the damage was caused by expansive reactions in the CCPs.

On a more positive note, when FGD material was used to repair a failed highway embankment, it significantly improved the stability and safety of the hillside (Payette 1996). Weinberg and Hemmings focused research on using CCPs in landfills. In their study, the authors found that the addition of Class F fly ash to FBC ash in landfill cells increased the unconfined compressive strength and reduced the permeability over the cell containing FBC ash alone by an order of magnitude (Weinberg and Hemmings 1997).

A more specific application where CCPs have been utilized is in flowable fill, often called controlled low strength material (CLSM). The American Concrete Institute (ACI) Committee 229 has defined CLSM as a self-compacted, cementitious material that is self-leveling and has a compressive strength of less than 8.27 MPa (1200 psi). Most applications require strengths of less than 2.07 MPa (300 psi) and are used in backfills in place of compacted clays or sand (ACI 1994). Typically, flowable fills are a blend of cement, fly ash, sand, and water, but the substitution of a dry FGD material for fly ash has been studied and results comparable with traditional mixes were obtained (Butalia 2001). In an attempt to increase the amount of CCPs utilized and reduce the amount of cement used in flowable fills, a study was performed on flowable fills that contained high volumes of fly ash, reduced volume of cement, and no sand. The results indicated that high volumes of coal ash can successfully be used in flowable fills (Swan 2007). There has not been much research into the use of circulating FBC spent bed ash in flowable fills, but fly ash from CFBC boilers has been blended with portland cement to create structural fill grade and excavatable trench fill grade flowable fills (Bland 1997).

Research that was especially pertinent to the current research investigated the use of FBC ash and fly ash as a substitute for river sand and cement in concrete (Bland 1987). Using a no-sand, no-cement concrete cost less than portland cement concrete, and it allowed for use of the atmospheric FBC ash in construction applications rather than paying for its disposal. The spent bed ash used in the study was a granular material with a size distribution similar to ASTM C 33 river sand making it an ideal replacement. The spent bed also contained a large amount of unslaked lime that, when hydrated, reacted with the fly ash to form cementitious materials, thus allowing for the elimination of portland cement. The fly ash was composed of very fine siliceous and aluminous glassy phases and has been recognized as a pozzolan.

The optimal “no cement” concrete produced by Bland et al. (1987) consisted of a blend of spent bed and fly ash along with water and coarse aggregate. The cementitious component comprised 73% spent bed and 27% fly ash by weight. The “no cement” concrete and control mix (i.e. portland cement concrete) had similar compressive strengths at 90 days, but the “no cement” concrete had much slower early-age strength gains. The “no cement” concrete had a modulus of elasticity of about half that of normal concrete indicating it is a less brittle material that produces similar compressive strength results.

There are other environmental advantages to using CCPs in construction materials apart from avoiding the need to landfill them. Gartner (2004) discussed the practicality of replacing portland cement with other hydraulic cements that could result in lower carbon dioxide emissions and energy use per unit volume of concrete. In the article, it was stated that the most promising alternatives were based on three known classes of cementing systems: Pozzolan-based cements, calcium (sulfo)aluminate-based cements, and calcium sulfate-based cements. The research presented in this report falls in the categories of pozzolan-based cements and calcium sulfate-based cements.

In addition to areas of application for CCPs, much research has been devoted to the cementitious reactions and hydration products associated with them. Ettringite, a hydrated calcium aluminum sulfate, has been identified as being important to the engineering properties of FBC materials as well as mixtures of FGD gypsum, fly ash, and lime. Many studies indicate that swelling or the potential for swelling can result from ettringite formation (Mehta 1973; Hansen 1973; Solem-Tishmack 1995; Wolfe 2001; Hemmings 2007). In fact, destructive expansion reactions can preclude the use of these materials in construction applications. The research presented in this report therefore focused on minimizing expansion to develop a practical product employing the use of CCPs.

### Section 3: Materials Used in the Study

The research presented in this report focused on using combinations of cementing agents derived from three coal combustion products (CCPs) to make “low-energy, 100% by-product cement”: flue gas desulfurization (FGD) gypsum, circulating fluidized bed combustion (CFBC) spent bed ash, and Class F ultra fine ash. One consistent and uniform sample of each cementing material was used throughout the study to maintain consistent results. Both the ultra fine ash and the FGD gypsum were obtained from the Kentucky Utilities Ghent Power Plant located in Carroll County, Kentucky. The spent bed material was obtained from the East Kentucky Power Cooperative Gilbert Unit at Spurlock Power Station in Maysville, Kentucky. All three samples represented typical by-products from their respective applications. Their chemical compositions were determined in the Analytical Lab at the University of Kentucky Center for Applied Energy Research (UK CAER).

The Ghent FGD gypsum was representative of flue gas desulphurization materials generated by coal-fired power plants. The chemical composition of the FGD gypsum used in this study was as follows:

Table 3.1 – Chemical composition of FGD gypsum used in the study.

<b>Chemical Composition (Wt. %)</b>	
Ash	80.56
Loss on Ignition	19.44
<b>Elemental Analysis (Wt. %)</b>	
SiO <sub>2</sub>	4.54
TiO <sub>2</sub>	0.13
Al <sub>2</sub> O <sub>3</sub>	1.09
Fe <sub>2</sub> O <sub>3</sub>	0.60
CaO	40.15
MgO	0.37
K <sub>2</sub> O	0.06
Na <sub>2</sub> O	< 0.01
P <sub>2</sub> O <sub>5</sub>	0.04
SO <sub>3</sub>	53.67

Two dry ash materials are generated at the Gilbert plant: spent bed ash and fly ash. The Gilbert spent bed ash was of particular interest in this project because of the large quantity produced in the CFBC process, and because of its high percentage of lime. Currently, the spent bed material is being landfilled. The chemical composition of the Gilbert Unit spent bed ash was as follows:

Table 3.2 – Chemical composition of the spent bed ash used in the study.

<b>Chemical Composition (Wt. %)</b>	
Ash	98.26
Loss on Ignition	2.00
<b>Elemental Analysis (Wt. %)</b>	
SiO <sub>2</sub>	12.77
TiO <sub>2</sub>	0.26
Al <sub>2</sub> O <sub>3</sub>	5.25
Fe <sub>2</sub> O <sub>3</sub>	3.15
CaO	48.23
MgO	2.47
K <sub>2</sub> O	0.36
Na <sub>2</sub> O	0.05
P <sub>2</sub> O <sub>5</sub>	0.13
SO <sub>3</sub>	27.83
Free lime	23.0

The third and final coal by-product which was investigated in the project was a processed Class F fly ash obtained from the Ghent Power Plant in Carroll County, Kentucky. The ultra fine ash was obtained using a hydraulic classifier that produced a very fine ash product with a median particle size of five microns. The primary purpose for its use was its high aluminum and silica content that would react with the lime in the spent bed to form ettringite and calcium silicate hydrates as cementitious phases. The chemical composition of the ultra fine ash used in the study was as follows:



Table 3.3 – Chemical composition of the Class F ultra fine ash used in the study.

<b>Chemical Composition (Wt. %)</b>	
Ash	96.64
Loss on Ignition	2.32
<b>Elemental Analysis (Wt. % oxides)</b>	
SiO <sub>2</sub>	54.34
TiO <sub>2</sub>	1.56
Al <sub>2</sub> O <sub>3</sub>	31.47
Fe <sub>2</sub> O <sub>3</sub>	5.21
CaO	1.35
MgO	1.1
K <sub>2</sub> O	2.66
Na <sub>2</sub> O	0.41
P <sub>2</sub> O <sub>5</sub>	0.28
SO <sub>3</sub>	0.07

In addition to the three CCPs investigated in the study, there were other materials that were utilized in the research that were used to predict and/or explain the overall behavior of the by-product cement. Determining the best method of making cements from the CCPs, and waiting for the results took a great deal of time. By using commercial materials of similar composition as those produced from by-products to predict behavior, benchmark comparisons could be made when the CCP material protocols were devised. A brief description of why the materials were used in the study and their chemical compositions are provided below:

Hydro-Stone® is a calcium sulfate hemihydrate product with a trace of portland cement distributed by United States Gypsum Company. The product was used to compare strengths and behavior of the hemihydrate produced from the FGD gypsum at the UK CAER to a commercial material. Table 3.4 contains the chemical composition of Hydro-Stone® as released by the United States Gypsum Company (US Gypsum 2003). However, results from the CAER Analytical lab showed that the product was almost 100% calcium sulfate hemihydrate (CaSO<sub>4</sub>·0.5H<sub>2</sub>O), commonly referred to as Plaster of Paris.

Table 3.4 – Chemical composition of Hydro-Stone®.

Plaster of Paris	> 0.90
Portland Cement	< 0.05
Crystalline Silica	< 0.05

Duracal® is a calcium sulfate hemihydrate and portland cement product distributed by the United States Gypsum Company. The product is marketed as a rapid setting roadway patching material, but its application was not of particular interest in the study. The composition of 50% hemihydrate (Plaster of Paris) provided an indication of the behavior of cements containing significant amounts of hemihydrate. The following table contains the chemical composition of Duracal® as released by the United States Gypsum Company (US Gypsum 2003).

Table 3.5 – Chemical composition of Duracal®.

Plaster of Paris	> 0.50
Portland Cement	> 0.40
Crystalline Silica	< 0.05

In addition to commercial material products, there were chemical admixtures typically used in portland cement applications that were used in the study. The admixtures were used to gain the same desired effects on the cement blends as if they were used with portland cement.

Recover® is a Type D retarder distributed by Grace Construction Products used to stabilize mixer wash water and leftover concrete for an extended period of time. It is also used in situations where controlled set of concrete is desired. When used as a traditional ASTM Type D retarder, Recover® is added to concrete mix at a suggested rate of 130 - 390 mL per 100 kg portland cement (4.40 - 13.19 oz per 220.5 lb portland cement) (Grace 2007).

Glenium® 3030 NS is a full-range water-reducing admixture distributed by BASF Construction Chemicals under the Master Builders brand name that was used in the study to lower the water : cement ratio of various cements to increase their strength. The

product meets ASTM C 494 / C 494M requirements for Type A water-reducing and Type F high-range water-reducing admixtures (BASF 2007). The suggested mid-range application dosage of 195 - 390 mL per 100 kg portland cement (6.60 – 13.19 oz per 220.5 lb portland cement) was used in the study to achieve the desired water reduction and increase the compressive strengths of various cement blends.

Chryso® Pave 100 is a plasticizing, pore blocking and water repelling admixture distributed Chryso, Inc. In dry-mix portland cement applications, the product is used to increase the compressive strength without the need of using another water-reducing admixture and to reduce the potential for efflorescence (Chryso 2007). The suggested dosage of 300 – 600 mL per 100 kg portland cement (10.14 – 20.29 oz per 220.5 lb portland cement) was used to increase the strength of the cement blends produced in the study in addition to keeping excess water from entering the cement systems.

#### Section 4: Equipment Used in the Study

All of the experiments in the study were performed at the University of Kentucky Center for Applied Energy Research (UK CAER) located in Lexington, Kentucky. The following equipment was used in the preparation and testing of the materials that were used as part of the “low-energy, 100% by-product cement” research project.

A disk mill was used to grind raw materials to a minus 1.18 mm (16-mesh) particle size before they were milled in a ball mill. This step improved the efficiency of the ball mill. In addition, if the raw materials going into the ball mill were too large, they would “smooth” rather than mill to a smaller particle size. The disk mill used in the study was a 1/3 HP *Straub Grinding Mill Model 4E*.

Figure 4.1 – Photograph of the disk mill used to grind raw materials.



The ball mill used was a rubber-lined, 18.14 kg (40 lb) capacity *Covington Rock Tumbler*. To convert the tumbler into a cement mill, three different sizes of spherical steel media were combined for the grinding action. The smallest media were approximately 1.25 cm (0.5 in) in diameter and they each weighed about 9.2 g (0.325 oz). There were 4.34 kg (9.57 lb) total of the small size media with an estimated 470 balls. The middle size media were approximately 1.9 cm (0.75 in) in diameter and they each weighed 28.5 g (1 oz). There were 4.26 kg (9.39 lb) total of the medium size media with

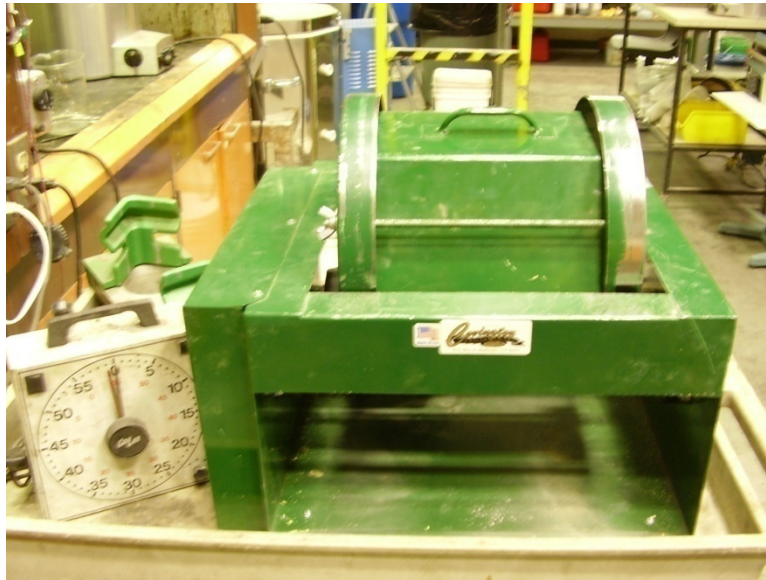
an estimated 150 balls. The largest size media had a diameter of about 2.54 cm (1 in) and weighed about 75 g (2.65 oz) each. There were 8.77 kg (19.33 lb) total of the large size media with an estimated 120 balls.

The mill had a hexagonal cross-section measuring 25.4 cm (10 in) side-to-side, 30.5 cm (12 in) vertex-to-vertex, and its overall length (top to bottom) was 31.75 cm (12.5 in). The top and bottom of the mill were circles measuring 31.75 cm (12.5 in) in diameter which allowed it to spin at  $27 \frac{3}{4}$  revolutions per minute.

Figure 4.2 – Photograph looking down into the ball mill showing its cross-section and steel media used for grinding action.

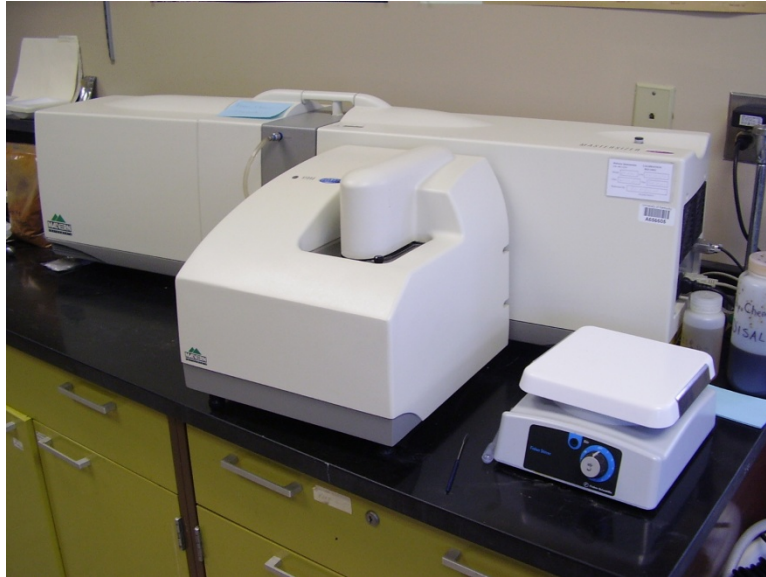


Figure 4.3 – Photograph of the ball mill situated on its base.



A *Malvern Mastersizer 2000 Particle Analyzer* was used to determine the particle size distribution of the raw materials and cements used in the study. The particle size distribution of the cement candidate materials milled in the study was close to that of portland cement because the goal of the research was to create cement that could replace portland cement in certain applications. Consistent particle sizes between the cements in the study would provide consistent strength results and allow for comparison between the different cement blends. If the particle size of the cements were too large, the compressive strength would suffer as the result. Conversely, if the particle sizes of the cements were made to be very fine, this would come at a higher processing cost.

Figure 4.4 – Photograph of the *Malvern Mastersizer 2000 Particle Analyzer* used to determine the size distribution of cement candidate materials.



A consistent hemihydrate product was obtained by dehydrating FGD gypsum under saturated steam. In the project, a 38.8 L (41 qt) capacity *All American Model 75X Pressure Steam Sterilizer* was used as an autoclave to prepare the hemihydrate.

Figure 4.5 – Photograph of the *All American Model 75X Pressure Steam Sterilizer* used in the production of hemihydrate.





A *VWR Scientific Model 1370 FM Forced Air Oven* was used for several applications throughout the research project. Its primary use was in drying the FGD gypsum product upon its removal from the autoclave to complete the conversion to hemihydrate.

Figure 4.6 – Photograph of the *VWR Scientific Model 1370 FM Forced Air Oven* used for the drying phase of the hemihydrate processing.



A 4.73 L (5 qt) *Hobart Model N50* commercial mixer conforming to ASTM C 305 (ASTM 2000) was used to mix all the mortar used in the study. It was very important that the mixing equipment conformed to the ASTM standard so the experiments were valid and could be easily repeated.

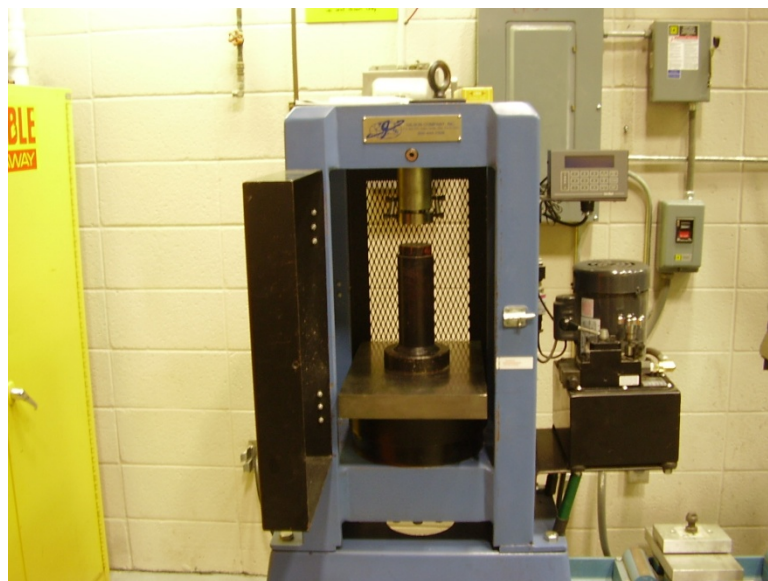


Figure 4.7 – Photograph of the mortar mixer conforming to ASTM C 305 used in the 100% by-product cement project.



An 181,437 kg (400,000 lb) capacity *Gilson Model MC-407 Compression Machine* was used to measure the compressive strength of mortar and concrete specimens tested in the study.

Figure 4.8 – Photograph of the compression machine used to test mortar specimen in the study.



Copyright© David Edward Rust 2008

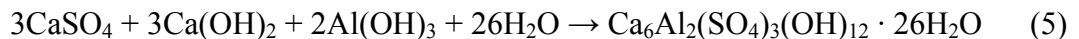
## Section 5: Cement Experiments

### 5.1 “Clinkerless” Cement Research Methodology

The overarching goal of the project was to produce a durable, low-energy cementitious material from flue gas desulfurization (FGD) gypsum that was converted to hemihydrate, circulating fluidized bed combustion (CFBC) spent bed ash, and Class F fly ash. Hemihydrate would give the by-product cement early strength development, whilst the spent bed / ultra fine ash blend would provide the by-product cement with long-term strength (gaining slowly at first) and make it less soluble.

The first step of the experimental procedure was to determine the spent bed / ultra fine ash ratio, called “Clinkerless” cement, to blend with the hemihydrate to form by-product cements that obtained high compressive strengths while keeping expansion at a minimum. The cement blends were called “Clinkerless” because cement clinker was not required for their cementitious action. Clinker is a hydraulic material consisting of at least two-thirds calcium silicates by mass with the remainder consisting of aluminum oxide, iron oxide, and other oxides (Hewlett 2001). The preparation of portland cement clinker is an energy-intensive process in which the raw materials are fired in a kiln at 1450°C (2642°F) until they sinter into lumps.

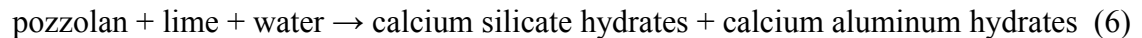
A kiln was never used in the low-energy, by-product cement research project. The principal strength-gaining reaction between the spent bed and ultra fine ash was in the formation of a complex and sometimes unpredictable mineral called ettringite. Ettringite is a white, highly insoluble mineral with good cementitious properties. There are three main components to the formation of ettringite: lime (Ca(OH)<sub>2</sub>), sulfate, and reactive alumina (Hemmings 2007). As can be seen from the chemical compositions of the two materials in Section 3 of this report, the spent bed provided the lime and sulfate, and the ultra fine ash provided the reactive alumina for ettringite. The following equation shows the ideal reaction for ettringite:



In addition to ettringite formation, there were other secondary pozzolanic reactions that took place between the spent bed and ultra fine ash to provide additional

long-term strength. By definition, a pozzolan is a siliceous or siliceous and aluminous material which in itself possesses little or no cementitious value but will, in finely divided form and in the presence of moisture, chemically react with calcium hydroxide at ordinary temperatures to form compounds possessing cementitious properties (ASTM 2000).

The Class F ultra fine ash is a known pozzolan, and the lime was provided by the spent bed. The classic “pozzolanic reaction” consumes lime, pozzolans, and water to make new cementitious hydrated phases that occupy more volume than the original solid phases (Gartner 2004):



Before “Clinkerless” cement blends could be produced from the combination of spent bed and ultra fine ash, the spent bed needed to be prehydrated. As noted by Bland et al. (1987), a substantial amount of heat was generated as the result of the hydration reaction of unslaked lime (CaO) and anhydrite (CaSO<sub>4</sub>). If the spent bed ash was prehydrated with 10%-20% water by weight, the peak temperature was reduced from 46.1 °C (115°F) to 23.9°C (75°F), which was close to the 21.7°C (71°F) temperature of the control portland cement mix.

By prehydrating the “Clinkerless” cement blends with 10% water by weight of spent bed material, which was the lower-limit of the range suggested by Bland et al. (1987), the exothermic unslaked lime (CaO) hydration reaction was completed before mortar was prepared. Thermal cracking was minimized by the prehydration step.

### **5.1.1 Preliminary “Clinkerless” Cement Blends**

The preliminary cement blends were produced to determine which ratio of spent bed / ultra fine ash would produce the best strength results. Similar research using materials with similar chemical composition determined that a spent bed / fly ash ratio of 70/30 provided optimum strength in mortar and concrete (Bland 1987). Therefore, the initial experimentation focused around the 70/30 ratio of spent bed / ultra fine ash, and three different ratios were examined: 80/20, 70/30, and 60/40.

To save time and material, the experimentation was conducted on a bench-scale, and the cement blends were compared by preparing 50 mm (2.0 in) mortar cube specimen per ASTM C 109 (ASTM 2000). A slight modification to the specification was made in that 525 g (18.52 oz) of cement were used per batch of mortar instead of the standard 500 g (17.64 oz). This slight modification was made because about 25 g (0.88 oz) of additional water weight were expected per 500 g (17.64 oz) of “Clinkerless” cement due to the unslaked lime (CaO) in the spent bed hydrating to calcium hydroxide (Ca(OH)<sub>2</sub>). A cement content more comparable to portland cement mortar was obtained by making the modification.

From each “Clinkerless” blend, 12 mortar cubes were prepared to measure the 7, 28, 56, 112, and 224-day compressive strengths, with two tests per age. The two remaining cubes were left in the moist curing room to monitor their volume stability beyond 224 days of curing. Due to the slow strength gains of the “Clinkerless” cement blends, the cubes were de-molded after seven days in the curing room as opposed to one day with traditional portland cement-based mortar cubes.

Table 5.1 summarizes the preliminary “Clinkerless” cement blends that were produced and tested in the research project. Results of the cement blends have been included in Section 6.1 of this report.

Table 5.1 – Composition of the preliminary “Clinkerless” cement blends prepared in the research project.

<b>Cement Name</b>	<b>Spent Bed</b>	<b>Ultra Fine Ash</b>	<b>Hemihydrate</b>	<b>d<sub>50</sub> (µm)</b>	<b>w/c Ratio</b>
Clinkerless #1	0.80	0.20	-	15	0.47
Clinkerless #2a	0.70	0.30	-	14	0.45
Clinkerless #3	0.60	0.40	-	14	0.44

### **5.1.2 Establishing a Standard Prehydration Technique**

The prehydration method used in the preliminary cement blends was adequate, but longer drying and milling times were required as the result of prehydrating the spent bed and ultra fine ash together. This process added unnecessary energy consumption which conflicted with the overall goal of the research which was the production of low-energy cement.

Before future “Clinkerless” cement blends were produced, an improved prehydration technique was developed which is described below:

1. The spent bed was first ground in the disk mill until it passed a 1.18 mm (No. 16) sieve.
2. The spent bed was prehydrated in the *Hobart N50* mixer, 1.0 kg (2.20 lb) at a time, with 100 mL (3.38 oz) (10% by weight) deionized water. The water was added slowly to the spent bed in the mixer on its low speed.
3. The spent bed and water were mixed for 15 minutes on the low speed, stopping once to scrape down the sides of the mixing bowl approximately ten minutes into the mixing cycle.
4. The prehydrated spent bed was then removed from the mixer and was given adequate time to cool. It was then stored in a sealed container.

The new prehydration technique allowed for easier production of cement blends because the prehydrated spent bed could be milled with ultra fine ash in the ball mill without a drying step.

### **5.1.3 “Clinkerless” Cement Blends Utilizing Standard Prehydration Technique**

The remaining “Clinkerless” cement blends were produced by milling prehydrated spent bed and ultra fine ash in the ball mill for two hours. 12 mortar cubes were prepared following the same procedure as the preliminary “Clinkerless” cement blends. Due to slow early-strength gains, the cubes were de-molded after seven days in the curing room. The 7, 28, 56, and 112-day compressive strengths were measured, with three cube tests per age. 12 mortar cubes were prepared using the *Clinkerless #5* cement blend like the other cement blends, but only two cubes were available to test at each curing age.

The following table summarizes the “Clinkerless” cement blends implementing the standard prehydration technique that were produced and tested in the research project. Results of the cement blends have been included in Section 6.1 of this report.

Table 5.2 – Composition of the “Clinkerless” cement blends prepared using prehydrated spent bed.

Cement Name	Spent Bed	Ultra Fine Ash	Hemihydrate	d <sub>50</sub> (µm)	w/c Ratio
Clinkerless #2	0.70	0.30	-	14	0.45
Clinkerless #4	0.90	0.10	-	14	0.50
Clinkerless #5	0.10	0.90	-	15	0.39
Clinkerless #6	0.40	0.60	-	14	0.42

## 5.2 Reproducing Previous Research

As mentioned previously, Bland et al. (1987) prepared “no cement” concrete by replacing fine aggregate with an unground spent bed / fly ash blend (approximately 70/30) because spent bed had a size and consistency similar to sand. No detrimental cracking was noted in the research; therefore, a replication of their mix was prepared on a mortar scale and named *No-Cement #1*. The concrete mix design was the following percent by weight:

Table 5.3 – *No-Cement #1* mix design.

Water	0.114
Ultra Fine Ash	0.109
Spent Bed (As Received)	0.294
ASTM C 33 Sand	0.483

The ASTM C 33 sand was used to replace the coarse aggregate used in the concrete mix produced by Bland et al. (1987). Mortar cubes were prepared to monitor expansion and cracking behavior; additionally, compressive strengths were measured at 7, 28, 56, and 112-days. Flow was not measured. The cubes were de-molded after seven days of moist curing.

A second mix was produced using a spent bed / ultra fine ash ratio of 70/30. Pre-hydrated spent bed was mixed with ultra fine ash and water in the mortar mixer without any sand. The mix was the following percent by weight:

Table 5.4 – *Sandless #1* mix design.

Water	0.173
Ultra Fine Ash	0.223
Spent Bed (As Received)	0.603
ASTM C 778 Sand	0.000

The flow was 121% which was higher than the 110% ± 5% specified in ASTM C 109, but it was difficult to gauge workability of the mix because it contained no mortar sand. Because the cement blend was prepared for comparative purposes only, and it had suitable workability, the flow was deemed acceptable. Eight mortar cubes were prepared to measure the 7, 28, 56, and 112-day compressive strengths of the mix with two tests per curing age. As was the case with *No-Cement #1*, *Sandless #1* was prepared to monitor expansion, cracking, and compressive strength of a mix containing a high cement content. Results of the two mixes have been included in Section 6.2 of this report.

### 5.3 Introducing Hemihydrate to the By-Product Cement System

It was previously stated that the goal of the research presented in this report was to make “low-energy, 100% by-product cement” from FGD gypsum, CFBC spent bed ash, and Class F ultra fine ash. Research had been dedicated to investigating optimal spent bed / ultra fine ash ratios, but the amount of hemihydrate to include in the by-product cement to produce high compressive strength and low expansion needed to be determined. Hydro-Stone® was used as the hemihydrate in the initial phase of the research because a technique of producing hemihydrate from FGD gypsum in the research lab had not yet been established. Early strength gain, long-term strength gain, expansion, and solubility of the cement blends were properties of interest which would dictate the proportion of hemihydrate.

The first cement blend that contained Hydro-Stone® was named *HydroStone #1* as it was 100% Hydro-Stone®. ASTM C 109 was followed to prepare 12 mortar cubes. Due to the fast set time of hemihydrate, Recover® was used as a set-retarder to allow time for the cubes to be cast properly. To monitor how moisture affected the strengths of mortar cubes prepared using hemihydrate, all 12 cubes were placed in the curing room,

and 1, 7, 28, 56, 112, and 224-day compressive strengths were measured, with two cube tests per curing age.

The first hemihydrate / “Clinkerless” combined cement blend produced in the lab contained 75% Hydro-Stone® and 25% *Clinkerless #2*. The blend was named *HSCL2 #1* because it contained Hydro-Stone® (*HS*) and *Clinkerless #2* (*CL2*), and it was the first attempt at blending the two materials into a cement. The Hydro-Stone®, pre-hydrated spent bed, and ultra fine ash were blended together in the ball mill and milled for two hours. ASTM C 109 was followed in preparing 15 mortar cubes. Because of the fast setting time of the hemihydrate, Citric acid was used as a set retarder to cast the cubes properly. Unlike the mortar cubes prepared using the “Clinkerless” cement blends, only 500 g (17.64 oz) of cement were used per batch of mortar as per the ASTM C 109 specification.

A second hemihydrate / “Clinkerless” blended cement was produced and named *HSCL2 #2*. The blend had an equal ratio of Hydro-Stone® to *Clinkerless #2*, and it was prepared in the same manner as *HSCL2 #1*.

The mortar cubes prepared for both blends were placed in the curing room immediately after they were cast, and they were removed from their molds after one day of moist-curing. Compressive strengths were measured at 1, 7, 28, 56, and 112 days of moist-curing, with three tests per age.

A separate experiment was designed to determine if the moisture of the curing room exerted an adverse effect on the cement blends containing Hydro-Stone®. Theoretically, by keeping excess moisture away from the mortar cubes, the hemihydrate cement would not dissolve, and the spent bed / ultra fine ash blend would hydrate using the mix water. In practice, this would be similar to placing a curing membrane or sealant on the concrete after it was placed.

The mortar cubes were prepared per ASTM C 109 and placed in the moist curing room for one day. They were removed from the molds, patted dry, labeled, and then sealed in polyethylene bags. The polyethylene bags were then returned to the curing room so the cubes would be cured at the correct temperature. The sealed curing technique was designated as “(Dry)” in the cement blend designation.



The following table summarizes the mortar cement blends containing Hydro-Stone® as an initial attempt to monitor the behavior of cements containing hemihydrate. Results of the cement blends have been included in Section 6.3 of this report.

Table 5.5 – Composition of cement blends containing Hydro-Stone®.

Cement Name	Spent Bed	Ultra Fine Ash	Hemihydrate	d <sub>50</sub> (µm)	w/c Ratio
HydroStone #1	-	-	1.00	20	0.43
HSCL2 #1	0.175	0.075	0.75	11	0.45
HSCL2 #2	0.35	0.15	0.50	11	0.45

#### 5.4 Expansion Studies

Up to this point, all of the expansion data collected on the different cementitious blends were obtained from the measurements of the dimensions of their mortar cubes. Although the average mortar cube lengths provided expansion information, it was not quantifiable by ASTM procedures. Length-change prisms per ASTM C 157 (ASTM 2000) were thus prepared to compare expansion for various blends. The 254 mm x 25.4 mm x 25.4 mm (10 in x 1.0 in x 1.0 in) length-change prisms were prepared using the following cementitious blends:

- *Clinkerless #2*
- *Clinkerless #6*
- *Clinkerless #2* with silica fume instead of ultra fine ash as the pozzolan
- *HSCL2 #1*
- *HSCL2 #2*
- Duracal®
- Duracal® with 25% ultra fine ash substitution

Length-change prisms were prepared using the *Clinkerless #2* and *Clinkerless #6* blends because they were the high strength and low expansion “Clinkerless” candidate cement blends. Due to the slow initial strength gains of the two blends, the length-change prisms for *Clinkerless #2* and *Clinkerless #6* were not de-molded until 14 days and 7 days respectively after they were cast.

Length-change prisms were prepared using the *HSCL2 #1* and *HSCL2 #2* cement blends because in the literature review, it was noted that swelling occurred as the result of the pozzolanic reaction between spent bed and Class F fly ash. Because *HSCL2 #1* was 75% hemihydrate, it was hypothesized to expand less than *HSCL2 #2* which was 50% hemihydrate. It was hypothesized that both mixes would experience less expansion than *Clinkerless #2* which was 100% “Clinkerless” material. Due to the initial strength gain provided by Hydro-Stone®, the length-change prisms for both cement blends were removed from their molds after one day in the curing room.

Length-change prisms were prepared using Duracal® in order to examine expansive behavior of a hemihydrate-blended cement product sold commercially. Taking the experiment a step further, 25% of the original Duracal® blend was substituted with ultra fine ash to see if the addition of aluminum to the cementing system would lead to increased expansion. With the addition of the ultra fine ash, all the ingredients for ettringite were present in the system.

### **5.5 Mortar Paste Study**

It was decided to prepare cement paste samples of a few blends from which mortar cubes and/or length-change prisms were prepared. The cement pastes of the blends that were of particular interest were examined using X-ray Diffraction (XRD) to track changes in hydrated phases during the hydration process. The results from the XRD analysis helped explain the compressive strengths and expansive behavior exhibited by the different cement blends. Four blends were selected for the XRD analysis: *Clinkerless #2*, *HSCL2 #2*, *Clinkerless #5*, and *Clinkerless #6*.

In the initial experiment, the pastes were cured in open dishes in the moist curing room. This storage resulted in excessive calcite ( $\text{CaCO}_3$ ) formation from carbonation of portlandite. The pozzolanic reactions would thus prematurely stop due to the lack of portlandite available. The cause of the excessive calcite formation was that the pastes were cast too thin and the amount of water made available to the different pastes was not held constant.

In order to obtain consistent results, the cement paste experiment was repeated using consistent samples that were cured uniformly. Mortar pastes were prepared using

three out of the four original blends (*Clinkerless #5* was omitted because the chemical reaction had not changed after the first week). Each paste sample was comprised of 40 g (1.41 oz) of cement mixed with 14 mL (0.047 oz) of water. The pastes were placed in their own plastic bottles along with a damp paper towel to promote slow hydration. The bottles were then sealed to keep the moisture in them and stored at room temperature in the laboratory. The samples were examined using XRD at 1, 7, 28, and 56 days of curing. Results have been included in Section 6.5 of this report.

Figure 5.1 – Photograph of sealed plastic containers with moist paper towels stored at room temperature used in the refined method of curing the cement paste samples.



In addition to conducting an XRD analysis to track the hydration process, a thermogravimetric analysis (TGA) was performed on the cement samples to measure the amount of calcium hydroxide ( $\text{Ca}(\text{OH})_2$ ) that was present at different curing ages. Calcium hydroxide, also called hydrated lime, is an important component for the formation of ettringite and the pozzolanic reaction with fly ash. By determining how much calcium hydroxide was present in each mortar paste at different ages, a better understanding of the potential for expansive behavior was obtained. It was hypothesized that expansion would cease when the amount of free hydrated lime was consumed.

## **5.6 Procedure for Producing Hemihydrate from FGD Gypsum**

After preparation and curing of the “Clinkerless” mortar cubes and length-change prisms, research focused on preparing hemihydrate from FGD gypsum. Based on a patent by Koslowski (1991), consistent hemihydrate can be produced by heating FGD gypsum, pressed into molded bodies at a pressure of 0.10 MPa-14 MPa (14.5 psi - 2030 psi), in an autoclave under saturated steam in a temperature range of 110°C-180°C (230°F - 356°F).

In the study, it was determined that molded gypsum bodies could be formed using the bottom portion of a Proctor mold, a steel cylinder with a diameter slightly smaller than the diameter of the Proctor mold, a taller steel cylinder to extend above the Proctor mold, and the compression testing machine. The resulting gypsum pucks had a diameter of 10.16 cm (4 in), and were 1.80 cm (0.71 in) thick. The procedure was as follows:

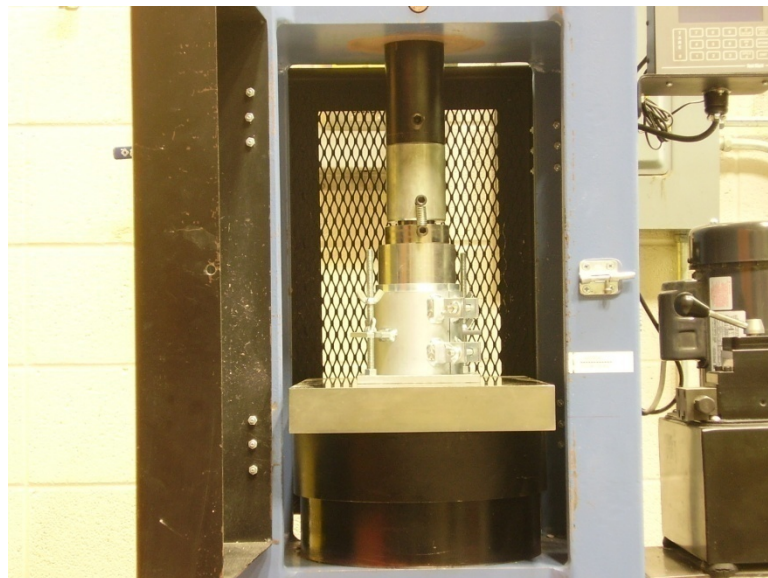
1. The Proctor mold and short cylinder were lightly coated with a releasing agent to prevent the gypsum from sticking to the surface.
2. The Proctor mold was filled with approximately 215 g (7.58 oz) of moist FGD gypsum (about 200 g (7.05 oz) of gypsum with about 15 mL (0.51 oz) of water) and topped with the short cylinder and then the tall cylinder.

Figure 5.2 – Photograph of the items used to form the gypsum into molded bodies.  
Pictured from left: Proctor mold with moist FGD gypsum, short cylinder, and tall cylinder.



3. The molding system was placed in the compression machine and pressed with 24.47 kN (5500 lbs) of force to make gypsum “pucks”.

Figure 5.3 – Photograph of the molding system situated in the compression machine with the tall cylinder extending above the Proctor mold to allow the load to be applied to the gypsum.



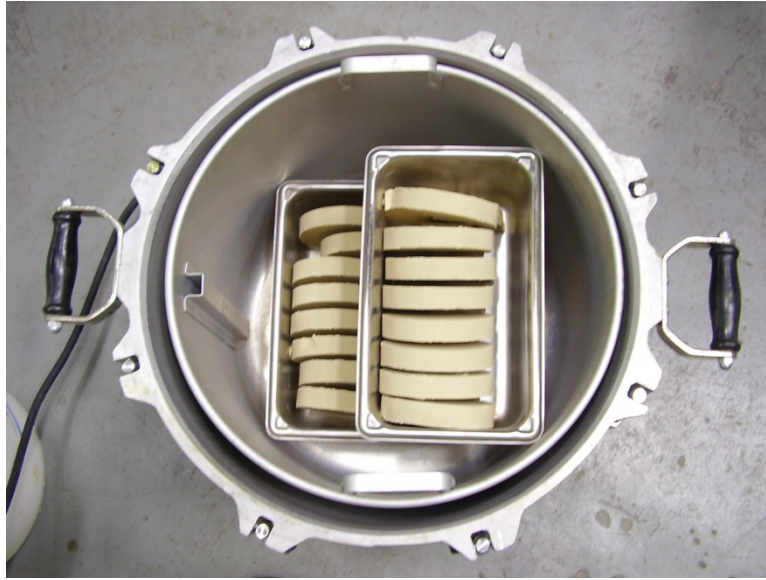
4. The pucks were removed from the Proctor mold by applying pressure to the tall cylinder and lifting upwards on the cylindrical portion of the Proctor mold. The tall cylinder, short cylinder, and gypsum puck were then removed from the Proctor mold base.

Figure 5.4 – Photograph of the Proctor mold base with gypsum puck, short cylinder, and tall cylinder stacked on top. The cylindrical portion of the Proctor mold had been removed.



5. The pucks were placed vertically in pans spaced with pieces of wood, and then they were placed in the autoclave. A total of 16 pucks were placed in the autoclave at a time, and they were autoclaved for four hours at 130°C (266°F).

Figure 5.5 – Photograph of 16 gypsum pucks in the autoclave.



6. The pucks were immediately removed from the autoclave upon completion and placed in the oven at 100°C (212°F) for a minimum of two days to dry. Care was taken to ensure the autoclaved pucks were kept above the 45°C (113°F) thermal stability of gypsum until they were dry to keep them from converting back to gypsum.
7. Upon removal from the drying oven, samples were taken from the pucks and analyzed using XRD to determine if they were hemihydrate. Upon validation of the product purity, the hemihydrate was sealed in mylar bags until a sufficient quantity was obtained to carry out planned experiments.
8. The next step in the production was to break the hemihydrate pucks with a hammer into smaller manageable pieces, and then disk-mill the product until all particles passed through a 1.18 mm (No. 16) sieve.



Figure 5.6 – Photograph showing hemihydrate pucks broken up with a hammer and being ground in the disk mill.



9. The product was then sealed in mylar bags until needed for cement production.

### **5.7 Preliminary “Low-Energy, 100% By-Product Cement” Blends**

Once the supply of hemihydrate produced from FGD gypsum had been deemed sufficient to complete experimentation, the preliminary “low-energy, 100% by-product cement” blends were produced. Using the data from the blended cements comprised of *Clinkerless #2* and *Hydro-Stone®* (discussed in Section 6.3), it was determined that equal amounts of “Clinkerless” cement and hemihydrate would be mixed together to make the 100% by-product blended cements.

The FGD hemihydrate, spent bed, and ultra fine ash were blended together and milled two hours. ASTM C 109 was followed to prepare 18 compressive mortar cubes for each blend with three tests at 1, 7, 28, 56, 112, and 224 days of curing. The 224-day data were not available at the time of this report.

Table 5.6 summarizes the preliminary “low-energy, 100% by-product cement” blends that were produced and tested in the research project. Results have been included in Section 6.7 of this report.



Table 5.6 – Composition of the preliminary “low-energy, 100% by-product cement” blends.

Cement Name	Spent Bed	Ultra Fine Ash	Hemihydrate	d <sub>50</sub> (µm)	w/c Ratio
0.5HH/0.5CL2 #1	0.35	0.15	0.50	10	0.46
0.5HH/0.5CL2 #2	0.35	0.15	0.50	10	0.40
0.5HH/0.5CL6 #1	0.20	0.30	0.50	8	0.40

Length-change prisms per ASTM C 157 were prepared to monitor the volume stability of the *0.5HH/0.5CL2 #2* and *0.5HH/0.5CL6 #1* cement blends. The prisms were de-molded three days after being cast in their molds. Measurements were recorded every 28 days.

As was the case with the cement blends prepared using Hydro-Stone®, mortar cubes prepared using the *0.5HH/0.5CL2 #2* and *0.5HH/0.5CL6 #1* cement blends were dry-cured in addition to the standard curing procedure. The dry-cured specimen were tested at the same curing ages as the moist-cured specimen.

Additionally, length-change prisms for the *0.5HH/0.5CL2 #2* and *0.5HH/0.5CL6 #1* cement blends were prepared per ASTM C 157, but they were dry-cured. The same dry-curing procedure used for the mortar cubes was used for the length-change prisms.

### **5.8 High Strength and Low Expansion “Low-Energy, 100% By-Product Cement”**

In the lab, the dry-curing method employed to keep excess water out of the cementing system may not be practical for many applications. One of the aims of the research was to develop a product that was practical and could be used for certain applications in the future. In order to succeed, a product that could repel water from concrete was needed.

The product selected as the water repellent was CHRYSO®Pave 100 which is a plasticizing, pore blocking and water repelling admixture that reacts with lime to form water repellent particles. The product is marketed for dry-mix concrete products to potentially reduce efflorescence because the hydrophobic particles inhibit the permeation of water through cement paste capillaries (Chryso 2007). A similar product is marketed by Grace Construction Products under the name Darapel®. The use of CHRYSO®Pave 100 also eliminated the need to use a separate water-reducing admixture.

Compressive mortar cubes per ASTM C 109 and length-change prisms per ASTM C 157 were prepared using the *0.5HH/0.5CL6 #1* cement blend with 2.6 mL (0.09 oz) of CHRYSO®Pave 100 used per 500 g (17.64 oz) of cement to produce a flow of 110% ± 5%. The following table shows the composition of a typical 500 g (17.64 oz) batch of mortar cement:

Table 5.7 – Mix design of the *0.5HH/0.5CL6 #1* cement blend to produce a 500 g (17.64 oz) batch of mortar cement.

<b>Material</b>	<b>Quantity (SI)</b>	<b>Quantity (US)</b>
Hemihydrate	250 g	8.82 oz
Spent Bed	100 g	3.53 oz
Ultra Fine Ash	150 g	5.29 oz
Sand	1375 g	48.5 oz
Sodium Citrate	1.0 g	0.035 oz
Water	180 mL	6.09 oz
<u>CHRYSO®Pave 100</u>	2.6 mL	0.088 oz

A second mortar cement product was prepared with a small amount of silica fume substituted for ultra fine ash in an attempt to accelerate the initial strength gain of the cement blend. Compressive mortar cubes per ASTM C 109 and length-change prisms per ASTM C 157 were prepared using the mortar cement blend with the following 500 g (17.64 oz) batch composition:

Table 5.8 – Mix design of the *0.5HH/0.5CL6 w/Silica Fume* cement blend to produce a 500 g (17.64 oz) batch of mortar cement.

<b>Material</b>	<b>Quantity (SI)</b>	<b>Quantity (US)</b>
Hemihydrate	250 g	8.82 oz
Spent Bed	100 g	3.53 oz
Ultra Fine Ash	137.5 g	4.85 oz
Silica Fume	12.5 g	0.44 oz
Sand	1375 g	48.5 oz
Sodium Citrate	1.0 g	0.035 oz
Water	180 mL	6.09 oz
<u>CHRYSO®Pave 100</u>	2.6 mL	0.088 oz

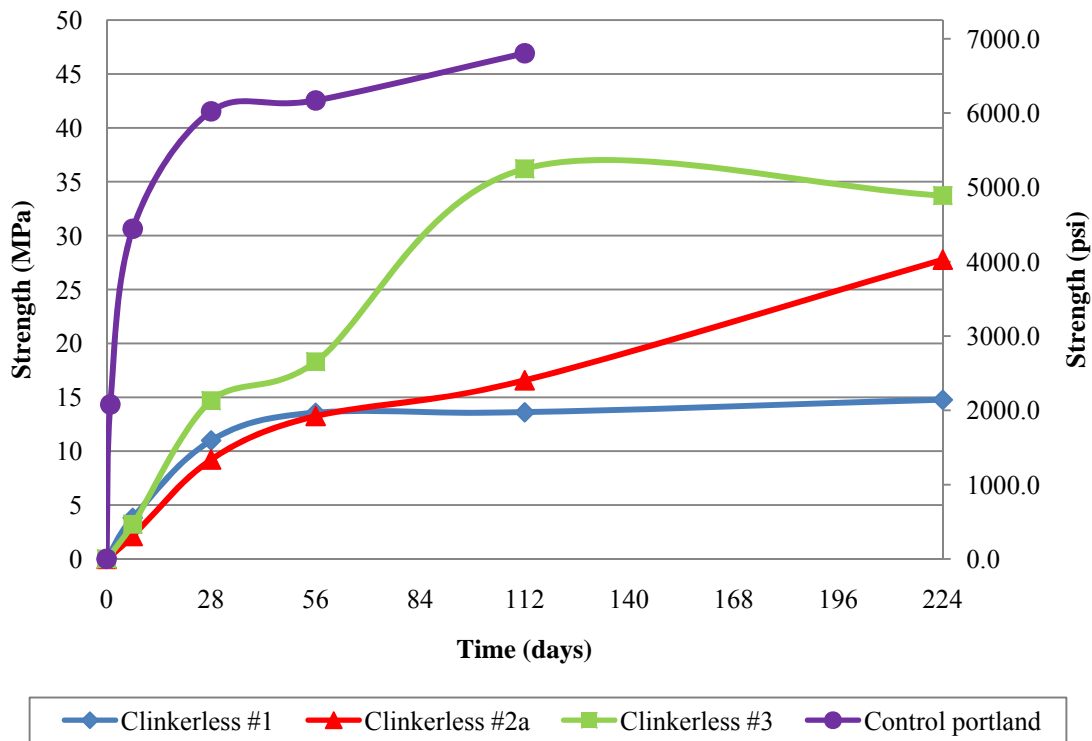
## Section 6: Results and Discussion of the Cement Experiments

### 6.1 “Clinkerless” Cement Blends

#### 6.1.1 Preliminary “Clinkerless” Cement Blends

Figure 6.1 displays the average compressive strength gains with curing time of the mortar cubes prepared using the preliminary “Clinkerless” cement blends. Each data point represents the average of two tests.

Figure 6.1 – Compressive strengths of mortar cubes prepared using the preliminary “Clinkerless” cement blends.



It can be seen from the figure that the strength gains of the mortar cubes prepared using the preliminary “Clinkerless” cement blends were very slow compared to control portland cement mortar cubes which had an average seven-day compressive strength of 30.34 MPa (4400 psi). The “Clinkerless” cement blends required seven days of curing to reach a compressive strength of 3.45 MPa (500 psi). *Clinkerless #1* and *Clinkerless #2a* required approximately 28 days of curing to reach compressive strengths of 10.34 MPa

(1500 psi) while *Clinkerless #3* had a compressive strength of 14.48 MPa (2100 psi) at 28 days of curing.

The slow strength gains of the preliminary “Clinkerless” cement blends may be attributed to the time required for the lime and sulfate present in the spent bed to react with the aluminum and silica of the ultra fine ash to form ettringite and calcium silicate hydrates. Even though the ultra fine ash was an extremely fine Class F fly ash (median particle size of five microns), it still required a few days for the particles to react and provide significant strength. If more practical Class F fly ash particle sizes were used, the delay in pozzolanic activity may have been even longer.

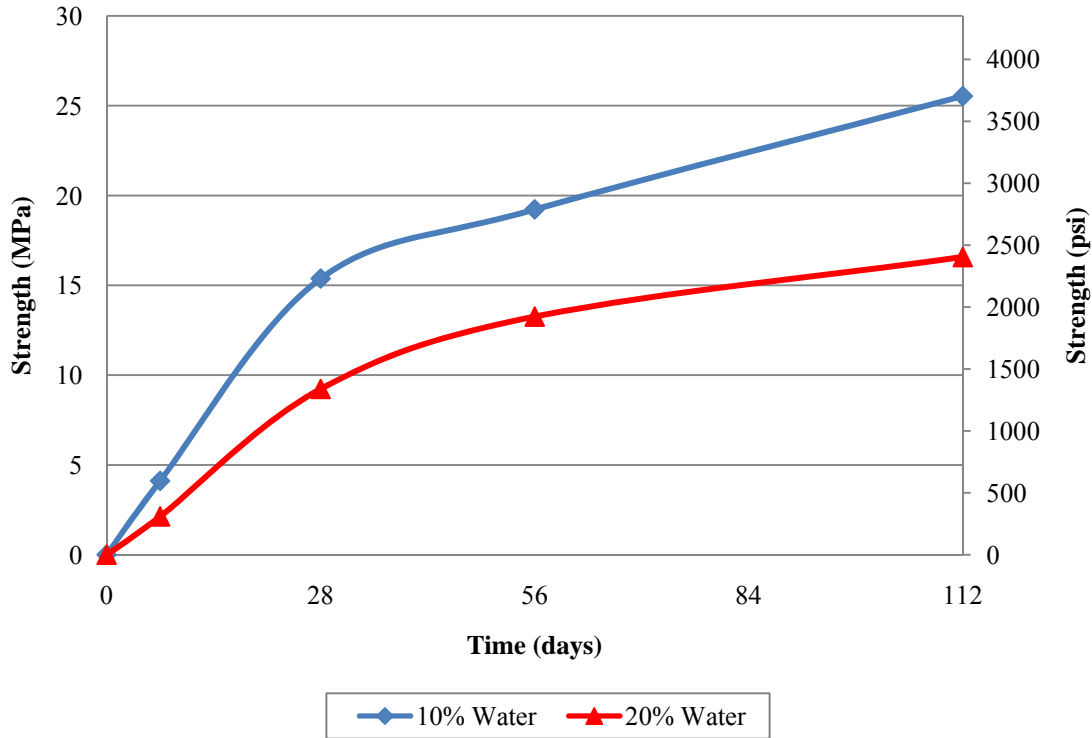
From Figure 6.1, it appeared that the compressive strengths of the mortar cubes increased with an increase in the ultra fine ash percentage of the cement blends (*Clinkerless #3* > *Clinkerless #2a* > *Clinkerless #1*). The 224-day compressive data were recorded, but the cubes were cracking severely as a result of expansion, and their data were affected. The coefficients of variation of the 224-day compression tests of the mortar cubes prepared using the three cement blends were 18.4%, 9.2%, and 18.6% respectively.

### **6.1.2 Confirmation of the Prehydration Technique**

The preliminary *Clinkerless #2a* cement blend was accidentally prehydrated with 20% water by weight of the spent bed instead of the 10% used to prehydrate the other preliminary “Clinkerless” cement blends. Even though the prehydration range suggested by Bland et al. (1987) was 10%-20% water by weight of spent bed, a second batch of mortar cubes were prepared using the 70/30 ratio (spent bed / ultra fine ash) cement blend to obtain consistent results. The refined prehydration procedure described in Section 5.1.2 of this report was implemented in the creation of the second 70/30 ratio “Clinkerless” cement blend, and it was named *Clinkerless #2*.

Figure 6.2 contains the compressive strength data of the preliminary *Clinkerless #2a* cement blend that was prehydrated with 20% water as well as the *Clinkerless #2* cement blend that was prepared using 10% water. Each data point for the 10% blend represents the average of three tests, and each data point for the 20% blend represents the average of two tests.

Figure 6.2 – Compressive strengths of mortar cubes prepared using the 70/30 spent bed / ultra fine ash cement blend prehydrated with 10% and 20% water by weight of spent bed.



From Figure 6.2 it can be seen that the compressive strengths of the mortar cubes prepared using the cement blend prehydrated with 10% water by weight of spent bed were higher than the compressive strengths of the mortar cubes prepared using the cement blend prehydrated with 20% water. The 112-day compressive strength of the blend prehydrated with 10% water by was 25.5 MPa (3700 psi) which was 35 percent higher than the 16.5 MPa (2400 psi) achieved by the blend prehydrated with 20% water at 112 days of curing. The difference in the compressive strengths confirmed the use of 10% water by weight of the spent bed material as the prehydration technique.

### 6.1.3 “Clinkerless” Cement Blends to Reduce Expansion

The mortar cubes prepared using the preliminary “Clinkerless” cement blends showed signs of map cracking between 28 and 56 days in the moist curing room which

was hypothesized to be the result of expansive ettringite formation (see Section 6.5 for chemical analysis of cement blends).

Figure 6.3 – Photograph of map cracking on a mortar cube prepared using the *Clinkerless* #3 cement blend after 56 days in the moist curing room.



Ettringite can cause large expansions when in contact with an outside source of water. There are two theories on the expansive behavior associated with ettringite:

The first theory is that, in the presence of excessive calcium hydroxide, and a high pH, colloidal ettringite crystals attract a large number of water molecules, similar to expansive clays. These water molecules surround the ettringite crystals and cause interparticle repulsion, thus causing an overall expansion of the system without any change in the crystal lattice of the ettringite (Mehta 1973).

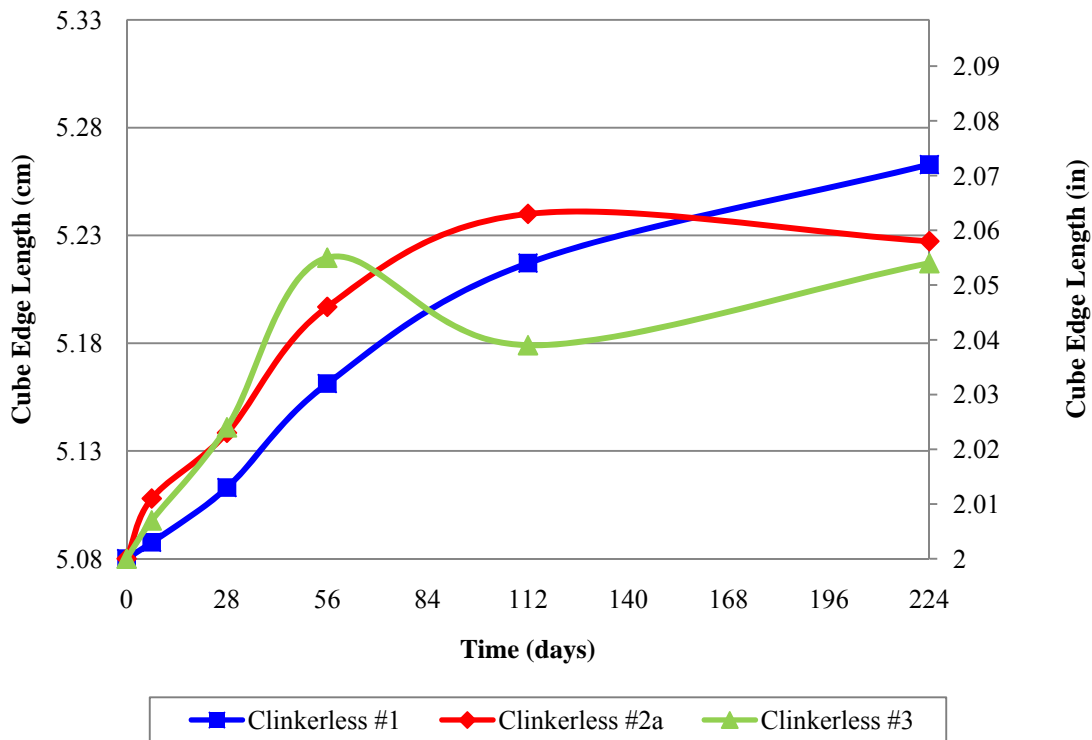
The second theory is that the reacting grains in the original cement paste contact one another through thin films of water. As the grains expand due to topochemical reactions, which involve the modification of a host structure by the introduction of a guest species, they exert pressure on each other at the contact points and cause the increase in volume (Hansen 1973).

To verify the mortar cubes prepared using the preliminary “Clinkerless” cement blends were expanding, the average cube edge lengths were plotted with time. The edge

lengths were recorded each time a compressive strength test was performed. The method was rather crude, but it gave an indication of how the different ratios of spent bed / ultra fine ash affected the volume stability of the mortar cubes over time.

The expansion data have been included in Figure 6.4. Each data point represents the average of four measurements.

Figure 6.4 – Average edge lengths of mortar cubes prepared using the preliminary “Clinkerless” cement blends.



Based on these initial results, two new “Clinkerless” cement blends were produced to try to reduce the expansion and cracking exhibited by the mortar cubes prepared using the preliminary “Clinkerless” cement blends. The intent of the new blends was to “starve” the cement system of either aluminum or lime after 28 to 56 days of curing.

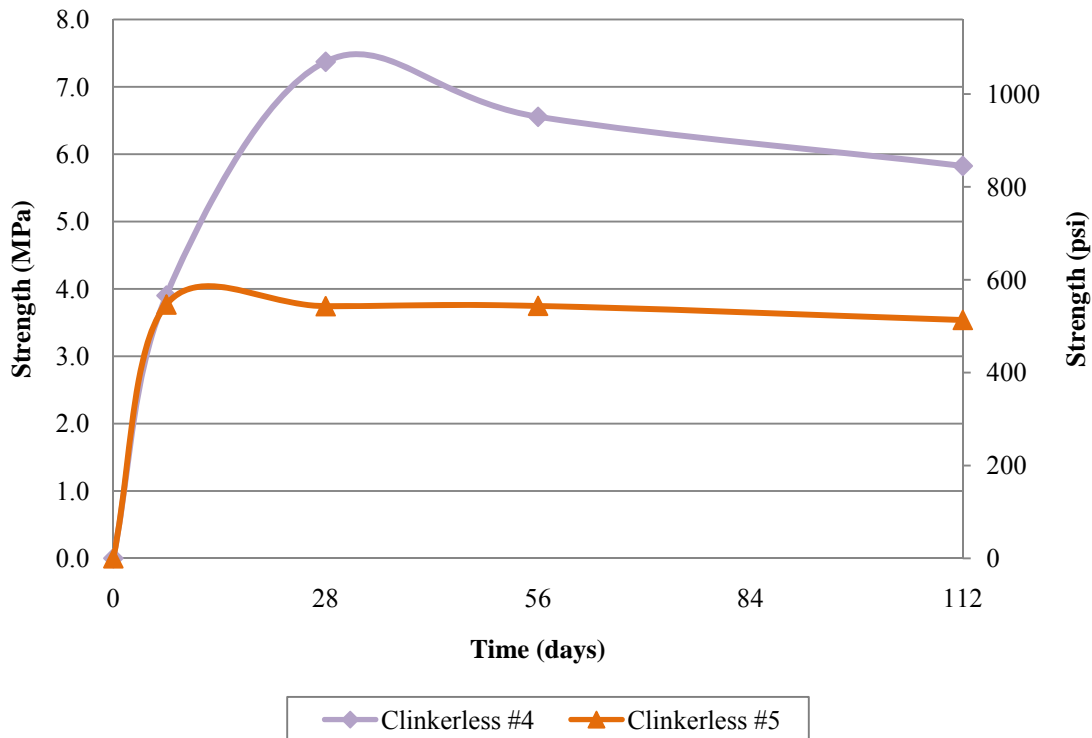
In an attempt to reduce the amount of aluminum present in the cement system, the ultra fine ash was reduced to 10% of the cementing material and the spent bed was increased to 90% of the cementing material. The resulting cement blend was named

*Clinkerless #4*, and its composition was provided in Table 5.2 of this report. On a commercial scale, this rationale may not be effective because aluminum exists in clays, and a concrete system could easily extract aluminum from the environment if exposed to clay, thus expanding at a later time.

An alternative to starving the cement system of aluminum was to starve it of lime in the long-term, which was achieved with *Clinkerless #5* (see Table 5.2) having a spent bed / ultra fine ash ratio of 10/90. In most environments, free lime is not likely to be encountered so the cement system would less likely expand as the result of extracting additional free lime.

The compressive strengths of the “Clinkerless” cement blends that were produced to reduce expansion can be seen in Figure 6.5. Each data point for *Clinkerless #4* represents the average of three tests, and each data point for *Clinkerless #5* represents the average of two tests.

Figure 6.5 – Average compressive strengths of mortar cubes prepared using the “Clinkerless” cement blends that were produced to reduce expansion.



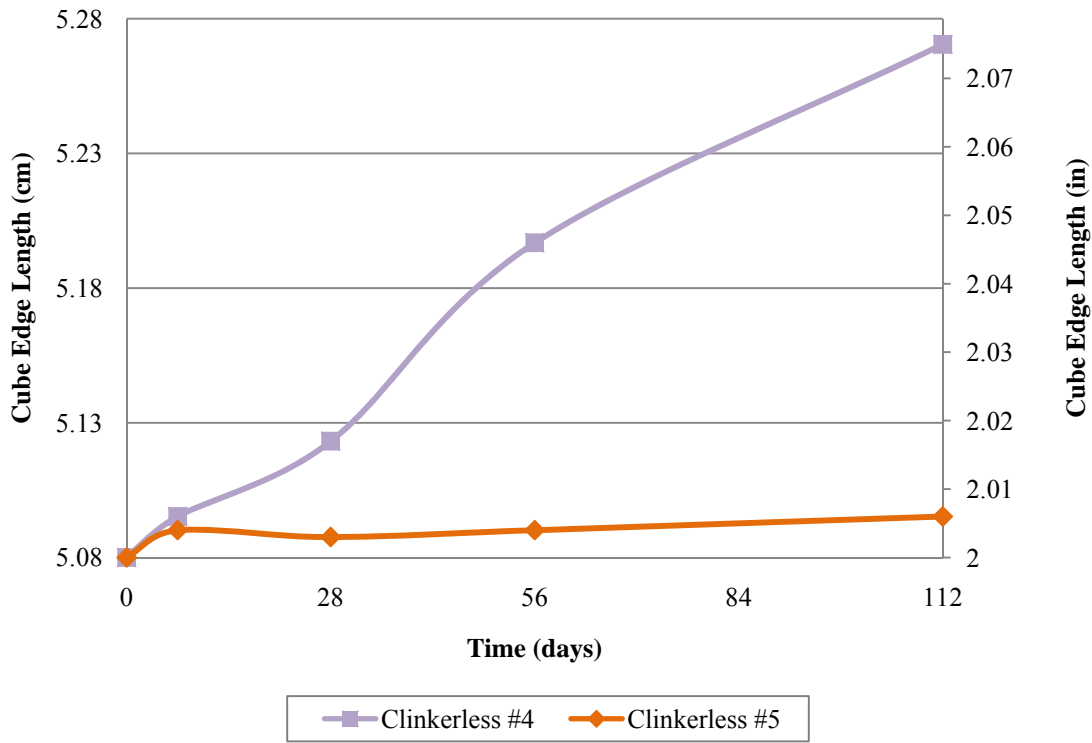


The compressive strengths for both cement blends were less than the strengths achieved by the three preliminary “Clinkerless” cement blends. *Clinkerless #4* had an abundance of lime but very little aluminum to initiate the ettringite reaction. It achieved a compressive strength of 7.38 MPa (1070 psi) at 28 days, but due to excessive cracking, the compressive strength decreased thereafter.

*Clinkerless #5* was the exact opposite of *Clinkerless #4* in that it had an abundance of silica and aluminum but very little lime to form ettringite and other pozzolanic reaction products. The compressive strength of *Clinkerless #5* was 3.79 MPa (550 psi) at seven days (approximately the same as *Clinkerless #4*), but the lime available to continue the reactions was consumed, and thus the reactions ceased. The compressive strength of the *Clinkerless #5* blend did not increase after seven days curing.

The expansion data of the two “Clinkerless” cement blends produced to reduce expansion can be seen in Figure 6.6. The method used to obtain the expansion data was the same as the method used to obtain the expansion data of the preliminary “Clinkerless” cement blends. Each data point for *Clinkerless #4* represents the average of six measurements, and each data point for *Clinkerless #5* represents the average of four measurements.

Figure 6.6 – Average edge lengths of mortar cubes prepared using the “Clinkerless” cement blends that were produced to reduce expansion.



The mortar cubes prepared using the *Clinkerless #4* cement blend, which was 90% spent bed, expanded from an initial average edge length of 5.08 cm (2 in) to 5.27 cm (2.075 in) after 112 days in the moist curing room. Map cracking accompanied the expansion of the mortar cubes.

Conversely, the mortar cubes prepared using the *Clinkerless #5* cement blend only expanded to an average edge length of 5.10 cm (2.006 in) after 112 days in the moist curing room. Because the mortar cubes did not expand, they showed no signs of map cracking.

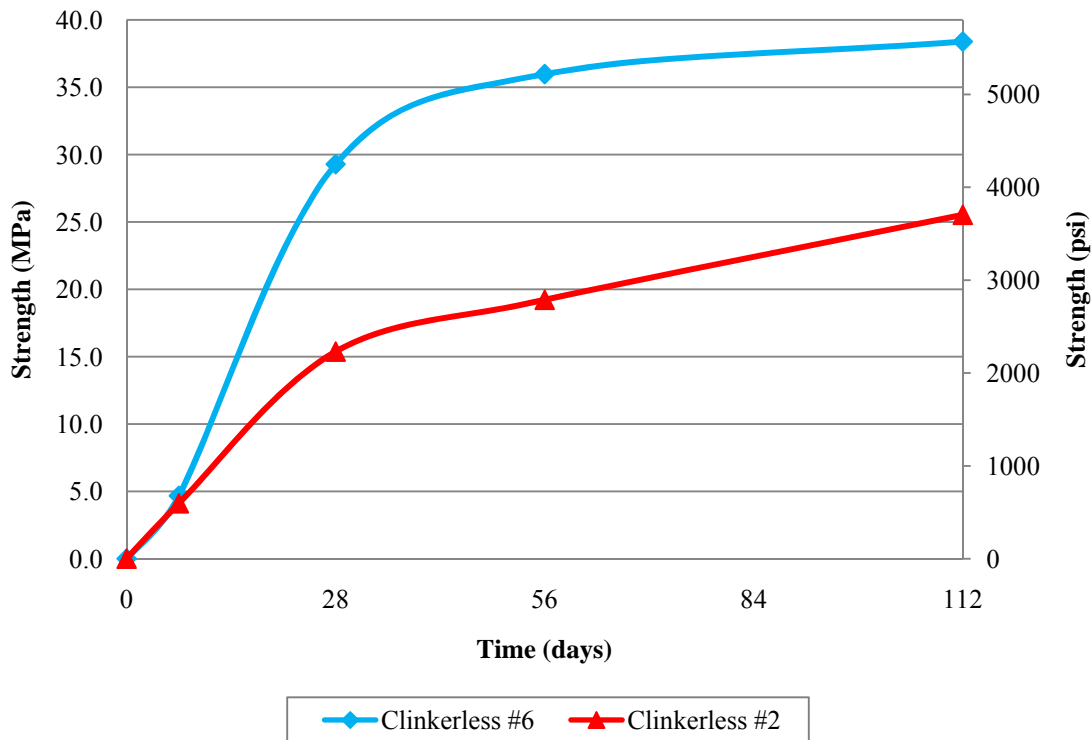
#### 6.1.4 High Strength and Low Expansion “Clinkerless” Cement Blends

In addition to *Clinkerless #2*, *Clinkerless #6* was the second “Clinkerless” cement blend produced in the study to maximize compressive strength while keeping expansion at a minimum. It had a spent bed / ultra fine ash ratio of 40/60, and it gave an understanding of the behavior of cement blends containing slightly more ultra fine ash

than spent bed. The compositions of the two cement blends were included in Table 5.2 of this report.

Figure 6.7 contains the compressive strengths of the mortar cubes prepared using the two high strength and low expansion “Clinkerless” cement blends. Each data point represents the average of three tests.

Figure 6.7 – Compressive strengths of mortar cubes prepared using the high strength and low expansion “Clinkerless” cement blends.



Similar to the preliminary “Clinkerless” cement blends, the initial strength gains attributed to the reaction of the spent bed and ultra fine ash were very slow. The seven day compressive strengths of the two blends were 4.14 MPa (600 psi), but after seven days of moist curing, there was a noticeable difference in the compressive strengths. At a curing time of 28 days, the average compressive strength of mortar cubes prepared using the *Clinkerless #6* blend was 29.30 MPa (4250 psi) compared to an average compressive strength of 15.38 MPa (2230 psi) for the *Clinkerless #2* blend. Most of the strength gain of the *Clinkerless #6* cement blend had been achieved by 28 days, but its 112-day average

compressive strength of 38.40 MPa (5570 psi) was 150% stronger than the 25.52 MPa (3700 psi) compressive strength of the *Clinkerless #2* cement blend.

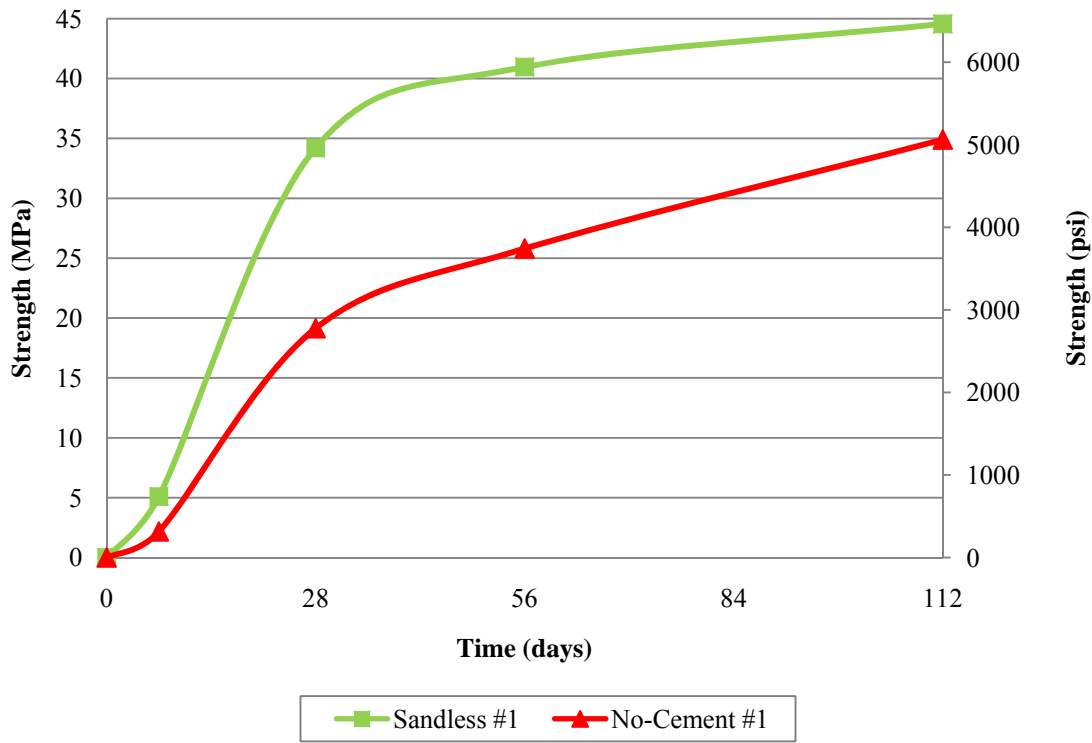
To statistically verify the *Clinkerless #6* cement blend produced higher compressive strengths than the *Clinkerless #2* cement blend, a Two Sample t-Test was performed on the 112-day average compressive strengths of the mortar cubes prepared using the two cement blends because they were the longest-term data available. The null hypothesis tested that the two cement blends had the same compressive strength after 112 days of curing was rejected ( $0.001 < p < 0.005$ ) and it was concluded that the *Clinkerless #6* cement blend was significantly different from *Clinkerless #2* at the error level of 5%.

The long-term strength gains achieved by the high strength and low expansion “Clinkerless” cement blends were encouraging; however, the slow initial compressive strength gains brought about a need for a cementing mechanism that would provide early-term strength compressive strength. Also, the mortar cubes prepared using the high strength and low expansion “Clinkerless” cement blends showed the same signs of expansive map cracking after 56 days in the moist curing room as the preliminary “Clinkerless” cement mortar cubes. The cementing mechanism that would provide early-term strength gains would also have to reduce expansion if the by-product cement blends were to be practical.

## **6.2 Reproducing Previous Research**

Figure 6.8 shows the compressive strengths of the two mortar mixes (Section 5.2) that reproduced previous research in which fluidized bed combustion ash and Class F fly ash were used to make concrete. The 7, 28, and 56-day data points represent the average of two tests, and the 112-day data points represent one test.

Figure 6.8 – Compressive strengths of mortar cubes prepared using the mortar mixes that reproduced previous research by Bland et al. (1987).

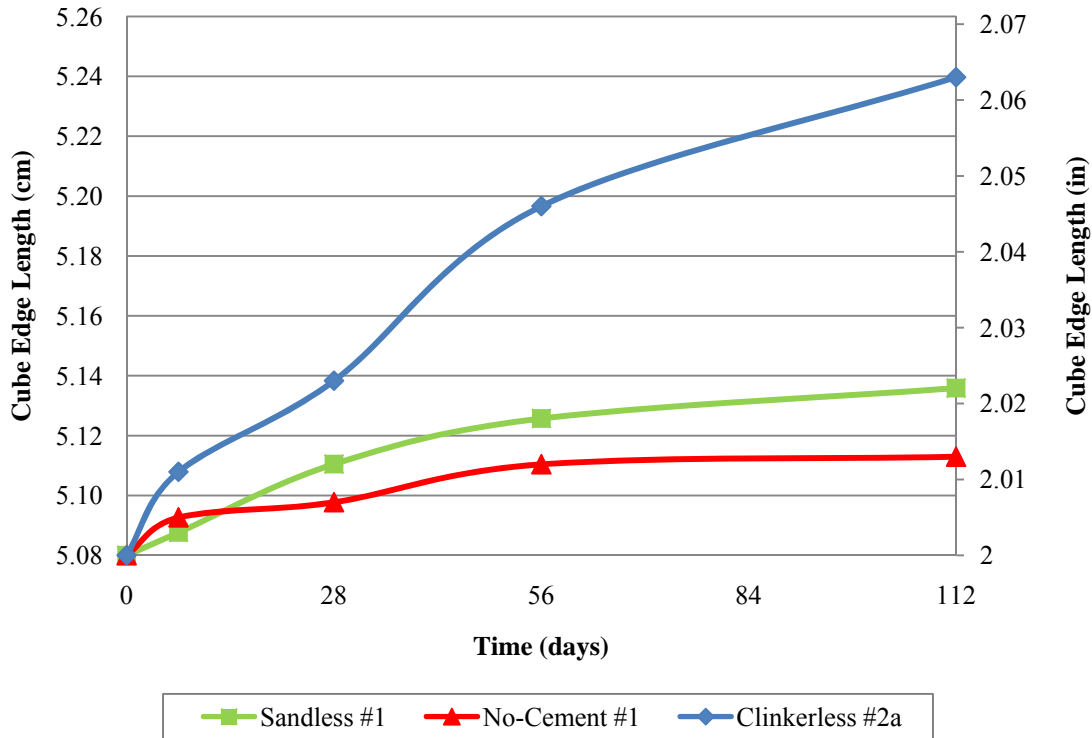


The *No-Cement #1* mortar mix contained less cementitious material than the *Sandless #1* mortar mix, and thus achieved lower compressive strengths. Both mortar mixes experienced slow initial strength gains similar to the “Clinkerless” cement blends presented in this report, indicating that the additional cementitious material did not accelerate the pozzolanic reactions. However, the 100% cementitious material *Sandless #1* mortar mix experienced a compressive strength gain from 5.10 MPa (740 psi) at seven days of curing to 34.47 MPa (5000 psi) at 28 days of curing. The 112-day compressive strength of the *Sandless #1* mortar mix was almost 44.82 MPa (6500 psi).

The primary reason the two mortar mixes were prepared was to determine if they would experience the same expansion problems as the mortar cubes prepared using the “Clinkerless” cement blends. The method used to obtain the expansion data was the same as the method used to obtain the expansion data of the preliminary “Clinkerless” cement blends.

The expansion data of the two mortar mixes are shown in Figure 6.9. The 7, 28, and 56-day data points represent the average of four measurements, and the 112-day data points represent the average of two measurements.

Figure 6.9 – Average edge lengths of mortar cubes prepared using the mortar mixes that reproduced previous research by Bland et al. (1987).



From the figure it appeared the *No-Cement #1* and *Sandless #1* mortar mixes both expanded less than the mortar cubes prepared using the *Clinkerless #2a* cement blend which had approximately the same spent bed / ultra fine ash ratio (70/30). The average cube edge lengths for *No-Cement #1* and *Sandless #1* mortar mixes at 112 days of curing were 5.113 cm (2.013 in) and 5.136 cm (2.022 in) respectively. For comparison, the average cube edge length for *Clinkerless #2a* was 5.240 cm (2.063 in). The *No-Cement #1* mortar mix was 45% cementitious material by weight of solids, and the *Sandless #1* mortar mix was 100% cementitious material by weight of solids. Because the cementitious material was causing the expansion, it was surprising that both the *No-*

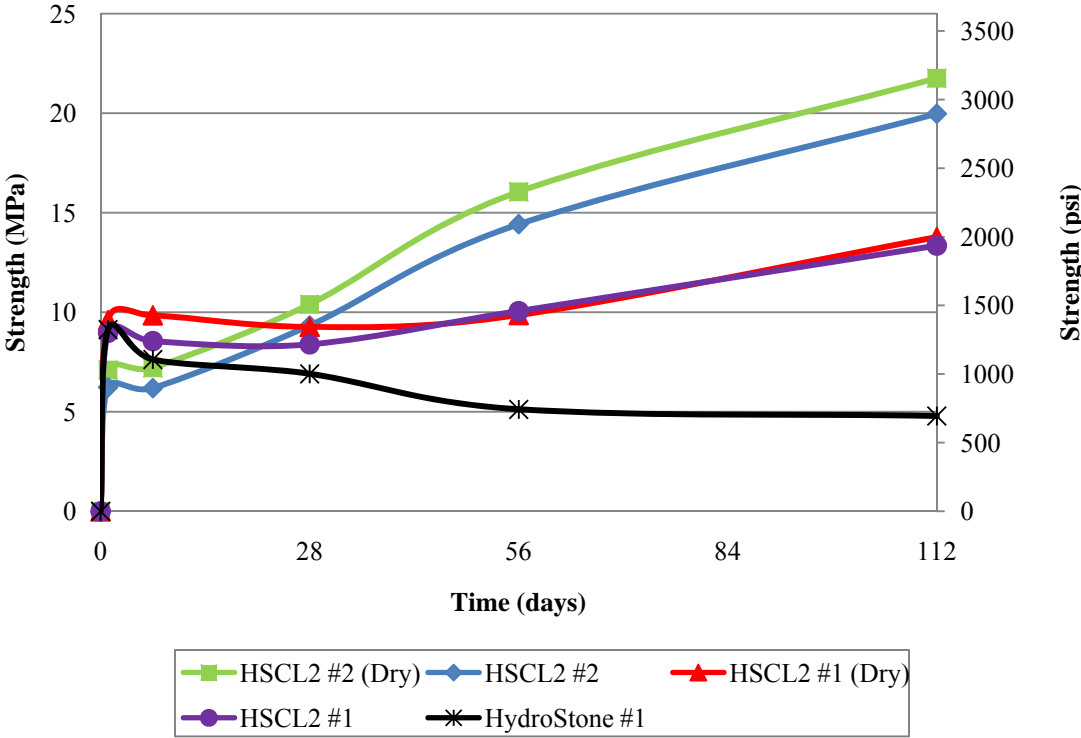
*Cement #1* and *Sandless #1* mortar mixes expanded less than *Clinkerless #2a* which was only 27% cementitious material by weight of solids per ASTM C 109.

However, there remains the possibility of delayed expansion in both the *No-Cement #1* and *Sandless #1* mortar mixes. Because the spent bed was not ground, the particles might contain a large quantity of unreacted lime that has been encased by the chemical reactions taking place on their surfaces. If aluminum and water were to work their way into the interior of the unground spent bed particles, the ettringite reaction could initiate again and cause expansion. The potential was minimized in the “Clinkerless” cement blends by milling the spent bed particles to expose as much of the reactants (e.g. lime) as possible.

### **6.3 Introducing Hemihydrate to the By-Product Cement System**

The compressive strengths of the mortar cubes prepared using the cement blends that contained Hydro-Stone® are shown in figure 6.10 and were valuable in developing the 100% by-product blended cements and served as a baseline. The sealed curing technique discussed in Section 5.3 of this report to dry-cure mortar specimen was designated as “(Dry)” in the blend designation. Each data point for the *HSCL2* cement blends represents the average of three tests, and each data point for *Hydrostone #1* represents the average of two tests.

Figure 6.10 – Compressive strengths of mortar cubes prepared using the cement blends that contained Hydro-Stone®.



The mortar cubes prepared using the *HydroStone #1* cement blend gave the performance of hemihydrate if it was used alone as the cement in the production of mortar cubes. The mortar cubes had an average one-day compressive strength of 9.14 MPa (1325 psi) due to the fast set time of the hemihydrate (it would set in the mixing bowl if a set-retarder was not used). However, after the initial strength gain the hemihydrate did not provide additional strength gains with time. The mortar cubes began to dissolve from the moisture in the curing room, and the compressive strength of the mortar cubes had decreased to 4.07 MPa (590 psi) by 112 days of curing.

The one day average compressive strength of *HSCL2 #1* was 8.96 MPa (1300 psi). It was expected to be less than the one day strength of *HydroStone #1* because the cementitious material of the *HSCL2 #1* cement blend was 75% hemihydrate compared to 100% hemihydrate for the *HydroStone #1* cement blend. The “Clinkerless” portion of the cement blend did not provide much additional strength between one and seven days of curing. However, after seven days of curing the pozzolanic reactions caused the



compressive strength of *HSCL2 #1* to increase with time. After 112 days curing, the average compressive strength of the cement blend was 13.38 MPa (1940 psi).

The cementitious material in the *HSCL2 #2* cement blend was only 50% hemihydrate, and resulted in a one day compressive strength of 6.21 MPa (900 psi) which was less than the one day compressive strength of the *HSCL2 #1* cement blend. But due to the increased percentage of “Clinkerless” material in the blend (50% compared to 25% for the *HSCL2 #1* blend), the compressive strength increased more with time than the *HSCL2 #1* cement blend. After 112 days of curing, the average compressive strength of the *HSCL2 #2* cement blend was 19.99 MPa (2900 psi) which was 1.5 times stronger than the 112-day compressive strength of the *HSCL2 #1* cement blend.

One of the main goals of the Hydro-Stone® cement experiment was to determine which ratio of hemihydrate / “Clinkerless” material in the cement provided the best compressive strength results. A Two Sample t-Test was performed on the 112-day average compressive strengths of the mortar cubes prepared using the *HSCL2 #2* and *HSCL2 #1* cement blends to determine if one of the cement blends produced compressive strengths that were significantly higher than the other blend at the error level of 5%. The comparison was made using the 112-day compressive strengths because they were the longest-term data available. The null hypothesis that the compressive strengths of the two blends were equal was rejected ( $p < 0.001$ ) and it was concluded that the 50 /50 ratio of hemihydrate to “Clinkerless” material provides higher compressive strength results after 112 days of curing.

Both Hydro-Stone® / *Clinkerless #2* cement blends were dry-cured (as explained in Section 5.3) to determine the effect of moisture on their compressive strengths. The strength gain trends for the mortar cubes that were dry-cured were similar to the trends of the cubes that were moist-cured, but the dry-cured mortar cubes produced better compressive strength results. To statistically verify this observation, a Two Sample t-Test was performed on the 112-day average compressive strength of the mortar cubes prepared using the *HSCL2 #2* and *HSCL2 #2(Dry)* cement blends to determine if dry-curing the mortar cubes resulted in a stronger compressive strength. The null hypothesis that the compressive strengths produced by the two blends were equal after 112 days of

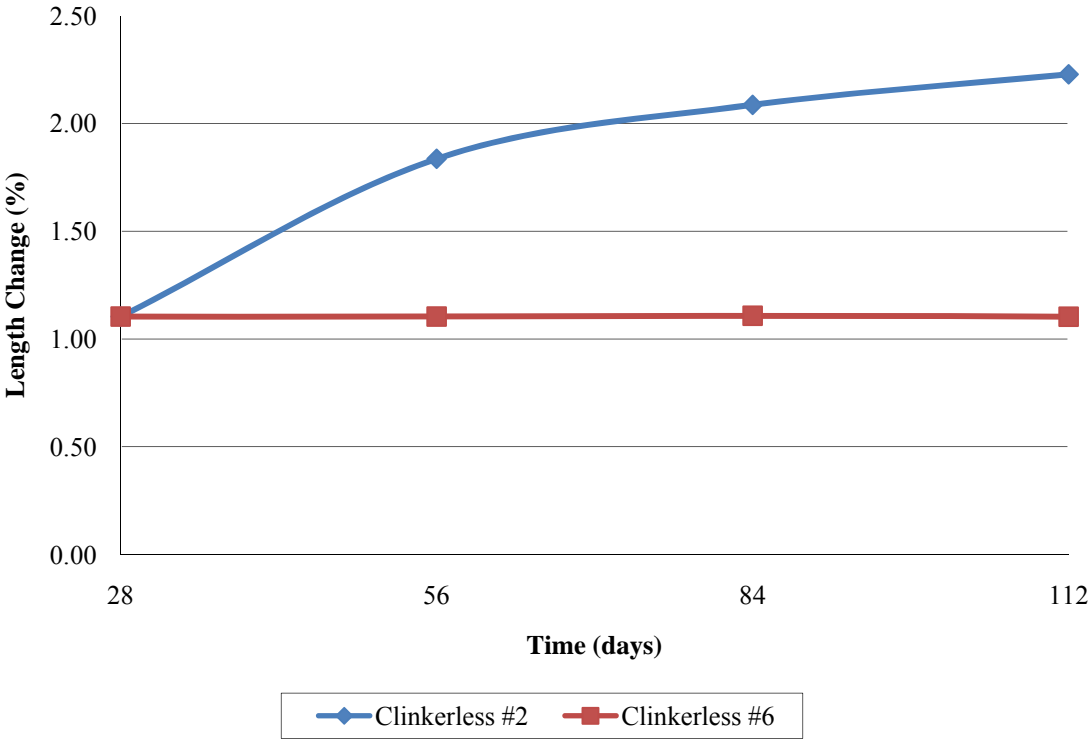
curing was rejected ( $0.025 < p < 0.050$ ) and it was concluded that dry-curing the mortar cubes produced higher compressive strengths at the error level of 5%.

#### **6.4 Expansion Studies**

Figures 6.11 through 6.13 show the expansion data collected using the procedure outlined in ASTM C 157 for the cement blends identified in Section 5.4 of this report. The data were shown in different figures because the expansions of length-change prisms prepared using the “Clinkerless” cement blends (shown in Figures 6.11 and 6.12) were orders of magnitude greater than the expansions of the length-change prisms prepared using the cement blends containing hemihydrate (shown in Figure 6.13).

Figure 6.11 contains the expansion data of length-change prisms prepared using the high strength and low expansion “Clinkerless” cement blends. The 28, 56, and 84-day data points for *Clinkerless #2* represent the average of five measurements, and the 112-day data point represents the average of four measurements. Each data point for *Clinkerless #6* represents the average of four measurements.

Figure 6.11 – Expansion data of length-change prisms prepared using the high strength and low expansion “Clinkerless” cement blends.



The expansions exhibited by the length-change prisms were hypothesized to be the result of the formation of ettringite (see Section 6.5 for verification of ettringite formation). The expansions for the two blends were identical after 28 days of curing with a length-change of 1.10%. However, the prisms prepared using the *Clinkerless #6* cement blend stopped expanding after 28 days of curing, while the prisms prepared using the *Clinkerless #2* cement blend were still expanding at the time of this report. *Clinkerless #2* had expanded 2.23% after 112 days of curing, while *Clinkerless #6* had expanded only 1.10% after 112 days of curing.

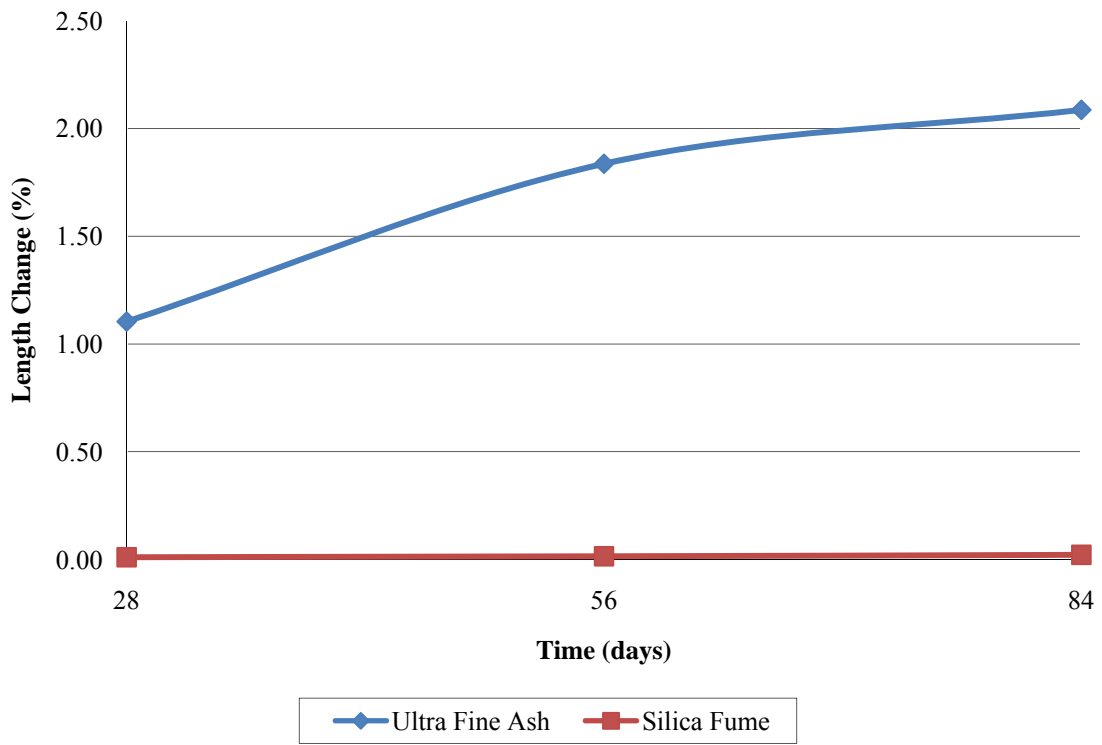
To statistically verify that the *Clinkerless #6* cement blend expanded less than the *Clinkerless #2* cement blend, a Two Sample t-Test was performed on the 112-day expansions of the length-change prisms prepared using the two cement blends because they were the longest-term data available at the time of this report. The null hypothesis that the expansions of the two blends were equal after 112 days of curing was rejected

( $p < 0.001$ ) and it was concluded that *Clinkerless #6* cement blend expanded less than the *Clinkerless #2* cement blend at the error level of 5%.

To provide further indication that ettringite was causing the “Clinkerless” cement blends to expand, silica fume was selected as a pozzolan to investigate if it would cause the same swelling problems experienced with the “Clinkerless” cement blends in which Class F ultra fine ash was used as a pozzolan. Silica fume is a pozzolan that has a high silica content, high specific surface area, and amorphous structure (Hewlett 2001). Because of these characteristics, silica fume has substantial pozzolanic activity, in terms of its capacity of binding lime and its high rate of reaction. The silica fume was expected to react with the lime in the spent bed to form calcium silicate hydrates. Most importantly, it lacked aluminum which is required to form ettringite.

Length-change prisms per ASTM C 157 were prepared using a spent bed / silica fume ratio of 70/30 to compare its expansion with the expansion of the length-change prisms prepared using the *Clinkerless #2* cement blend, which was produced using ultra fine ash as the pozzolan. The expansion data have been included in Figure 6.12. Each data point for the blend produced using ultra fine ash represents the average of five measurements, and each data point for the blend produced using silica fume represents the average of three measurements.

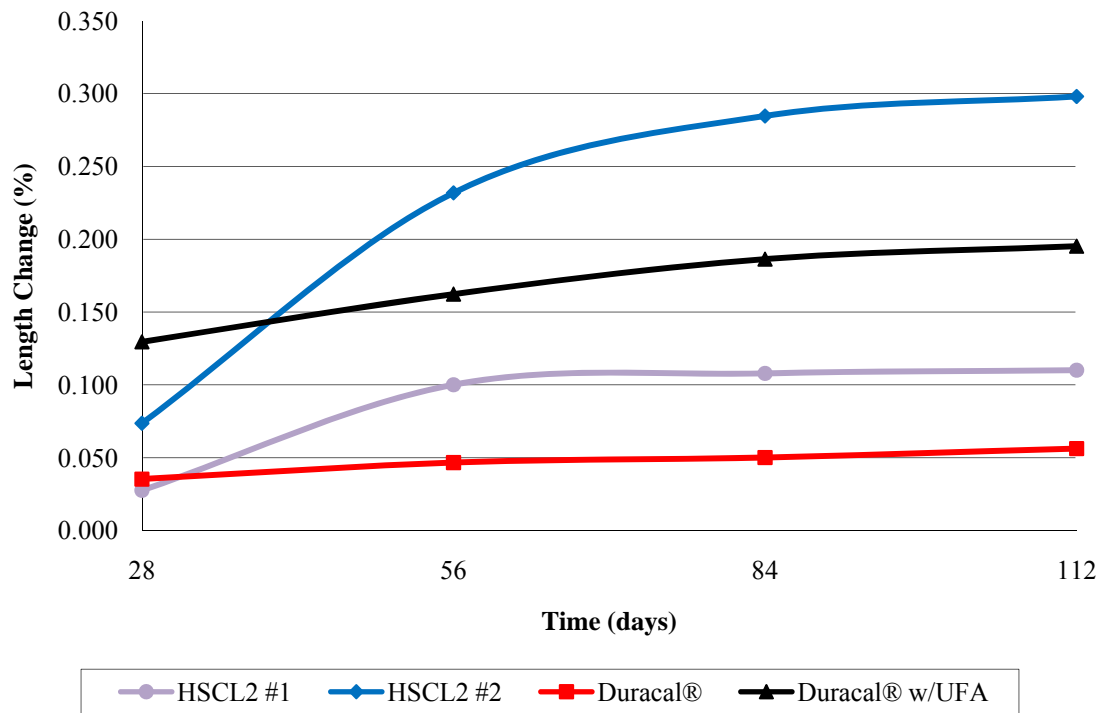
Figure 6.12 – Expansion data of length-change prisms prepared using a 70/30 ratio of spent bed / pozzolan.



Due to the elimination of aluminum from the system by using silica fume instead of ultra fine ash, all of the ingredients required to form ettringite were not present in the cement system, and thus the length-change prisms prepared using silica fume as the pozzolan experienced minimal expansion. After 84 days of curing, the length-change prisms prepared using silica fume as the pozzolan had only expanded 0.02%. Conversely, the length-change prisms prepared using ultra fine ash as the pozzolan had expanded 2.09% after 84 days of curing. These data gave further indication that the ettringite was causing the cement system to expand.

Figure 6.13 compares the expansion data for the Hydro-Stone® / Clinkerless #2 cement blends with the expansion data of the commercially sold Duracal® cement. Each data point for Duracal® represents the average of three measurements. All other data points represent the average of four measurements.

Figure 6.13 – Expansion data of length-change prisms prepared using the two Hydro-Stone® / Clinkerless #2 cement blends and Duracal® cement.



Duracal® was used as the benchmark to compare the expansion data of the cement blends produced in the project because it is a commercially sold portland cement product comprised of approximately 50% hemihydrate and 50 % portland cement. The length-change prisms prepared using the commercially sold cement exhibited the least amount of expansion of the four cement blends (112-day expansion of 0.06%).

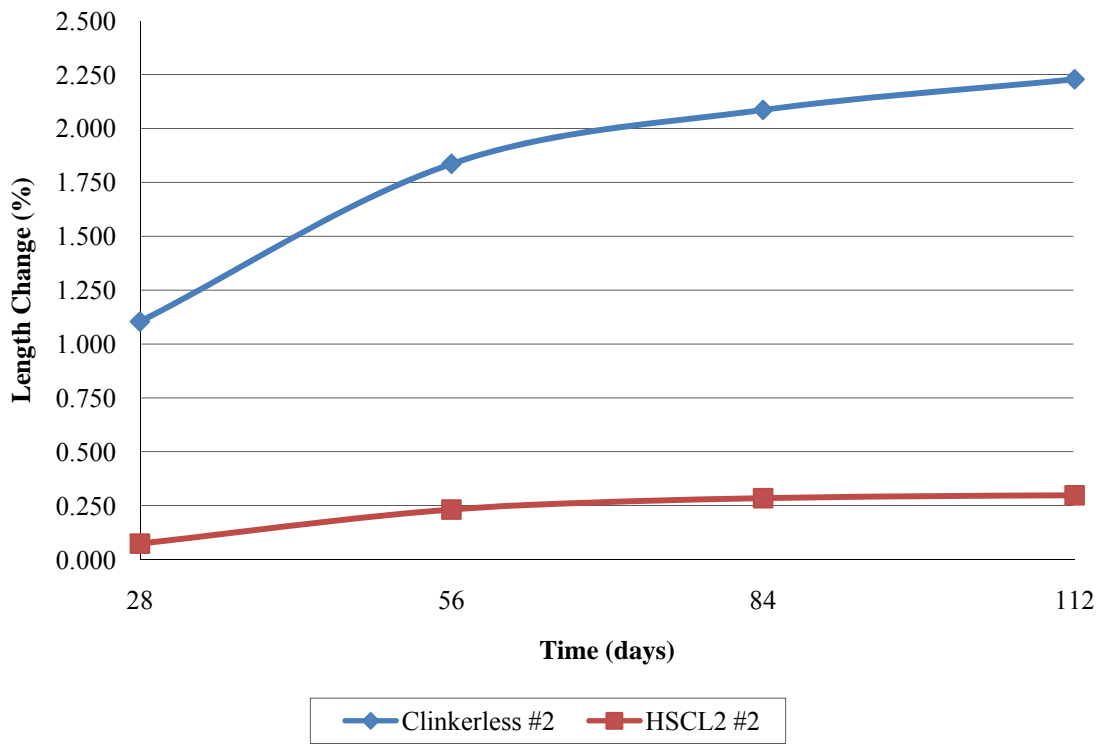
The mortar length-change prisms prepared using the blend of Duracal® with a 25% substitution of Class F ultra fine ash expanded more than the prisms prepared using Duracal®. The 112-day expansion was 0.20% which was 3.33 times greater than the expansion of the length-change prisms prepared using Duracal®. The expansion further agreed with the hypothesis that expansion was attributed to the formation of ettringite. By adding the Class F ultra fine ash to the system, all of the ingredients for the formation of ettringite were present. The portland cement provided the calcium hydroxide, the sulfate was provided by the hemihydrate, and the aluminum was provided by the Class F ultra fine ash.

*HSCL2 #1* was the cement blend that expanded an amount closest to the baseline Duracal® cement. The mechanism causing the expansion of *HSCL2 #1* was the expansion of the *Clinkerless #2* portion of the cement blend. Because the blend was only 25% of the expansive “Clinkerless” material, the 112-day expansion was 0.11%.

The length-change prisms prepared using the *HSCL2 #2* cement blend expanded more than the prisms prepared using the *HSCL2 #1* cement blend because they contained twice the amount of the expansive “Clinkerless” material (50% compared to 25% for *HSCL2 #1*). Because of the increase in “Clinkerless” material present in the cement blend, the 112-day expansion was 0.30% compared to the 0.11% expansion exhibited by the prisms prepared using the *HSCL2 #1* cement blend.

However, just because *HSCL2 #2* expanded more than *HSCL2 #1* did not mean the blend was not worth pursuing. Figure 6.14 contains the expansion data of the length-change prisms prepared using the *HSCL2 #2* cement blend plotted against the expansion data of the length-change prisms prepared using the *Clinkerless #2* cement blend to show the magnitude of the difference in expansion. The 28, 56, and 84-day data points for *Clinkerless #2* represent the average of five measurements, and the 112-day data point represents the average of four measurements. Each data point for *HSCL2 #2* represents the average of four measurements.

Figure 6.14 – Expansion data of length-change prisms prepared using the *Clinkerless #2* and *HSCL2 #2* cement blends.



From Figure 6.14 it can be seen that the length-change prisms prepared using the *HSCL2 #2* cement blend expanded less than the length-change prisms prepared using the *Clinkerless #2* cement blend. The average 112-day expansion of the length-change prisms prepared using the *Clinkerless #2* cement blend was 2.2% compared to 0.30% for the *HSCL2 #2* cement blend. Therefore, by substituting 50% hemihydrate for *Clinkerless #2* in the cement blend, the expansion was reduced by 86%. Just as important, the mortar cubes and length-change prisms prepared using the *HSCL2 #2* cement blend did not crack, unlike the mortar cubes and length-change prisms prepared using the *Clinkerless #2* cement blend.

One of the goals of the Hydro-Stone® cement experiment was to determine if the addition of hemihydrate to the cement blend would significantly reduce expansion while providing early-term strength. A Two Sample t-Test was performed on the 112-day average expansions of the length-change prisms prepared using the *HSCL2 #2* and *Clinkerless #2* cement blends to determine if the substitution of 50% hemihydrate for



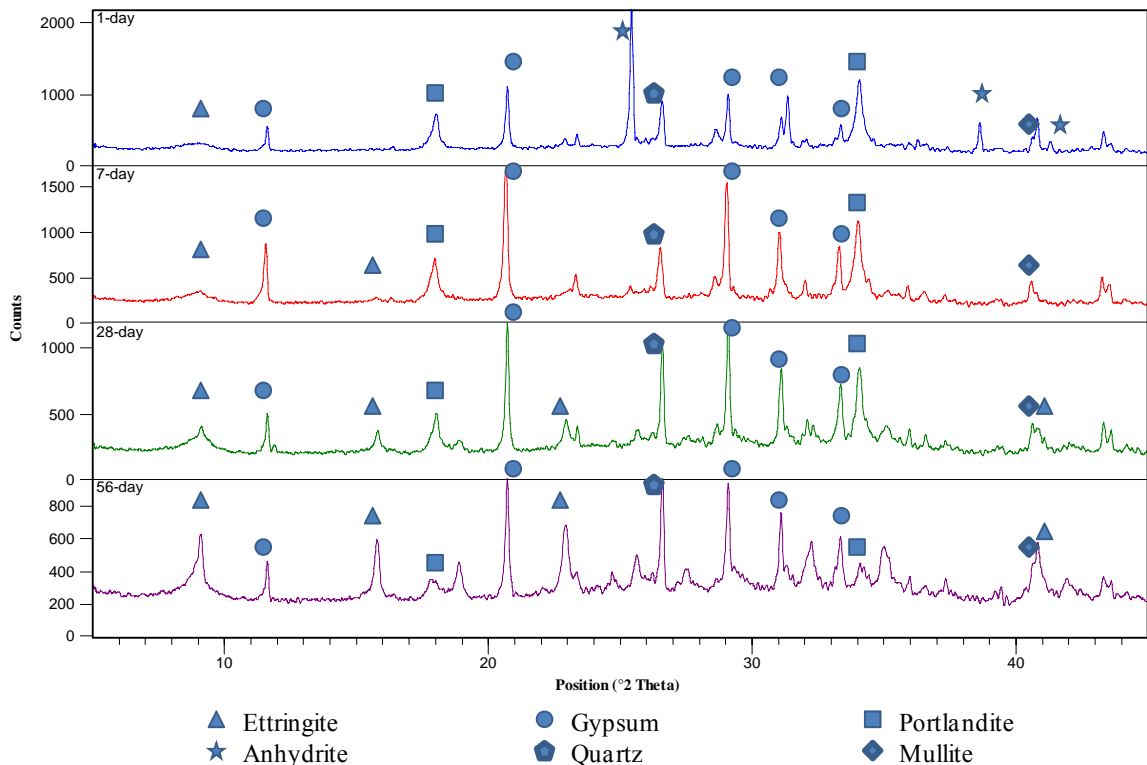
“Clinkerless” material significantly reduced expansion. The 112-day expansion data were compared because they were the longest-term data available. The results proved that in addition to providing initial compressive strength, the addition of hemihydrate to the cement blend also significantly reduced expansion ( $p < 0.001$ ) at the error level of 5%.

## 6.5 Mortar Paste Study

### 6.5.1 X-ray Diffraction Analysis

The XRD plots of the *Clinkerless #2*, *Clinkerless #6*, and *HSCL2 #2* cement blends have been included below to help explain the compressive strength gains and expansion data presented in previous sections. Attention was given to the amount of anhydrite, ettringite, gypsum, and portlandite present in the cements at different ages of curing.

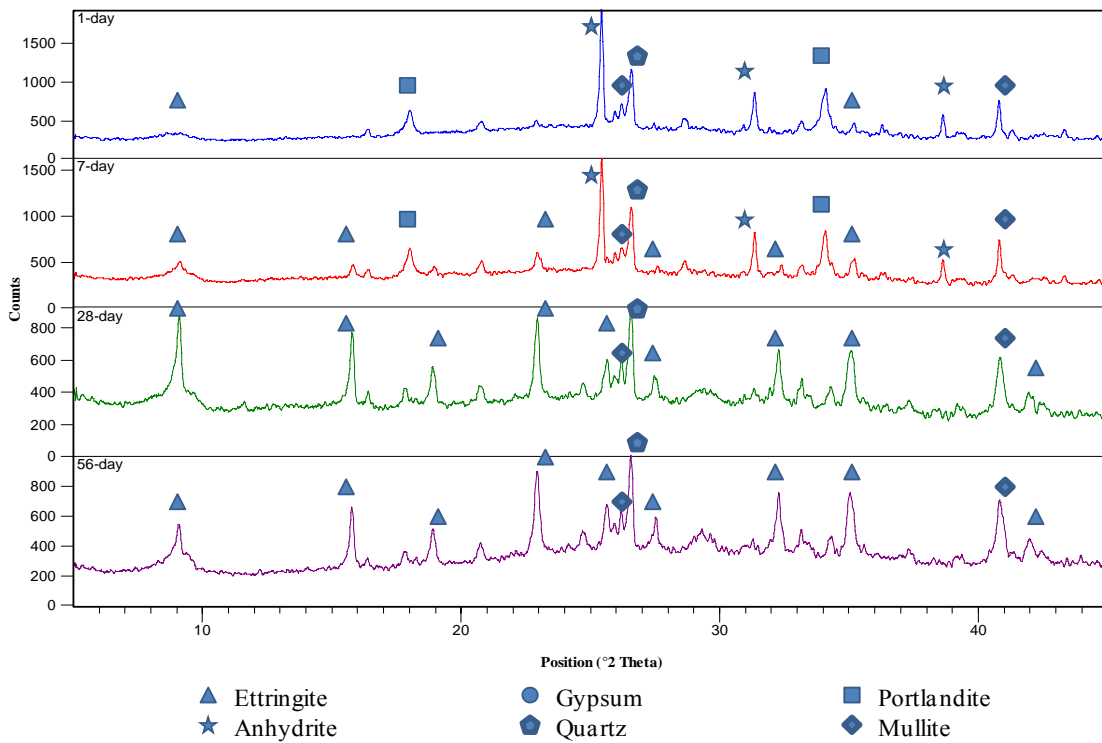
Figure 6.15 – XRD plots of *Clinkerless #2* at different curing ages.



From the XRD plot of *Clinkerless #2*, it can be seen that an abundance of anhydrite was present at one day of curing. After 7 days of curing, the anhydrite had

reacted with water to form gypsum, and some ettringite had also formed. After 28 and 56 days of curing, gypsum was still the most abundant mineral in the system, but the amount of ettringite was increasing. Portlandite, the mineral form of calcium hydroxide and a key component in the formation of ettringite, was still detected after 56 days of curing. The continued expansion of the length-change prisms prepared using the *Clinkerless #2* cement blend beyond 56 days of curing as seen in Figure 6.11, further indicating that ettringite was causing the cement systems to expand.

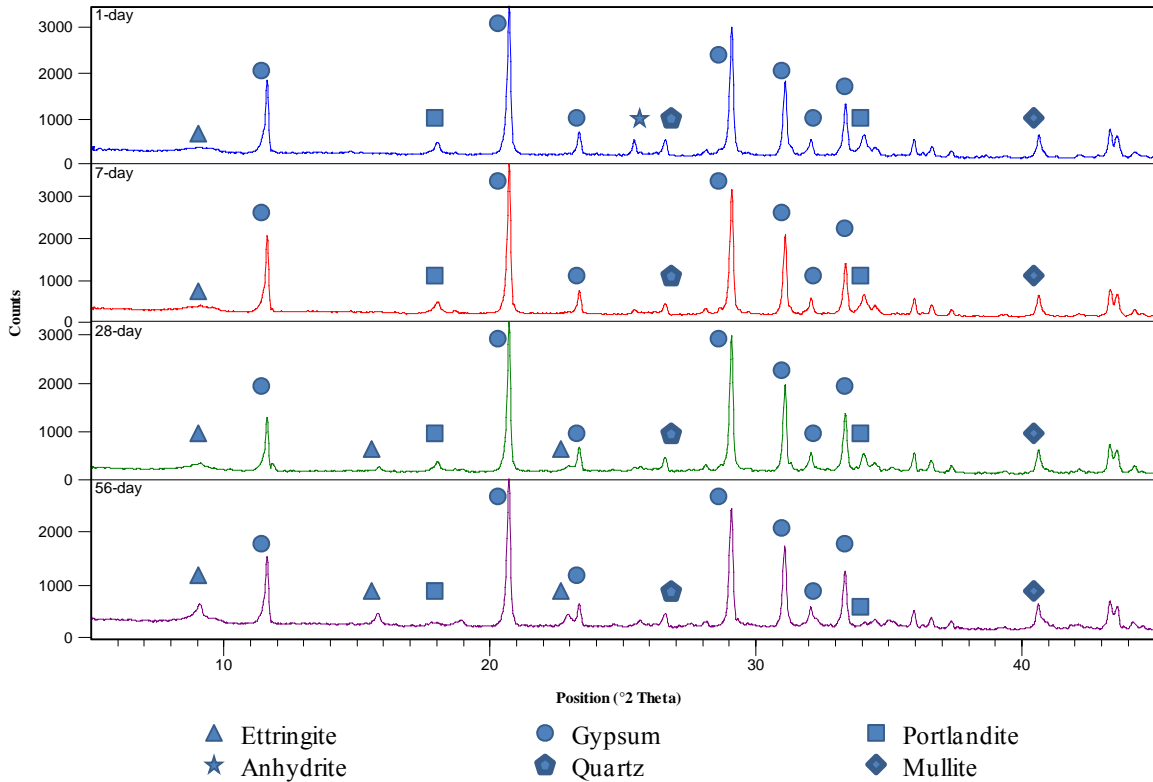
Figure 6.16 – XRD plots of *Clinkerless #6* at different curing ages.



The one-day XRD plot of the *Clinkerless #6* cement blend was similar to the one-day XRD plot of the *Clinkerless #2* cement blend in that anhydrite was the most abundant mineral present. However, after seven days of curing the anhydrite did not convert to gypsum as it had in the sample prepared using the *Clinkerless #2* cement blend. Due to the increased amount of fly ash present, there was much more aluminum dispersed throughout the system that was reacted with portlandite and anhydrite to form ettringite. Ettringite was the most detectable mineral in the system after 7, 28, and 56 days of curing

resulting in higher strength gains than the *Clinkerless #2* cement blend as shown in Figure 6.7. However, portlandite was no longer detected in the system after 28 days of curing which resulted in the formation of ettringite to cease. Further indicating that ettringite formation was causing the cement systems to expand, the length-change prisms prepared using the *Clinkerless #6* cement blend to stop expanding after 28 days of curing as shown in Figure 6.11. After 56 days curing, ettringite was still abundantly present, and a broad amorphous silicate diffraction was increasingly prominent. The minor strength gains exhibited by the mortar cubes prepared using the *Clinkerless #6* cement blend between 56 and 112 days of curing (see Figure 6.7) could have been attributed to the amorphous silicates, along with crystal interlocking and refinement of ettringite and other minerals detected.

Figure 6.17 – XRD plots of *HSCL2 #2* at different curing ages.



A prominent gypsum peak was present on the XRD plot of the *HSCL2 #2* cement blend after one day of curing due to the hydration of hemihydrate. This hydration gave the *HSCL2 #2* cement blend its early compressive strength as seen in Figure 6.10. The

pattern of solid minerals present after 7, 28, and 56 days of curing was similar to the pattern of *Clinkerless #2*, but the detection of the minerals was less because the *HSCL2 #2* cement blend was only 50% “Clinkerless” material.

### 6.5.2 Thermogravimetric Analysis

To further support the hypothesis that the formation of ettringite was causing the cement systems to expand, the results of the thermogravimetric analysis (TGA) have been included in Figures 6.18-6.20 to show the amount of calcium hydroxide was present in the cement blends at different curing ages. The derivative of the thermogravimetric curve was plotted to show the percent weight loss of water per minute at specific temperatures. Calcium hydroxide was indicated by an abrupt weight loss near 450°C (Marsh 1988).

Figure 6.18 – TGA plot of *Clinkerless #2*.

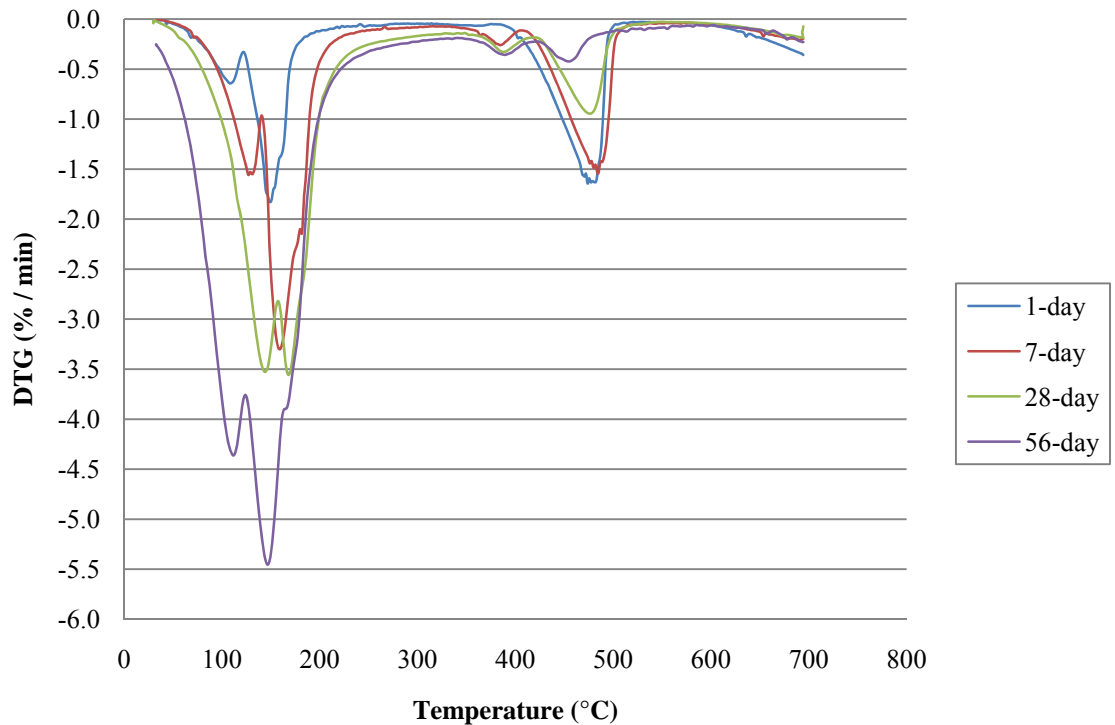


Figure 6.19 – TGA plot of *Clinkerless #6*.

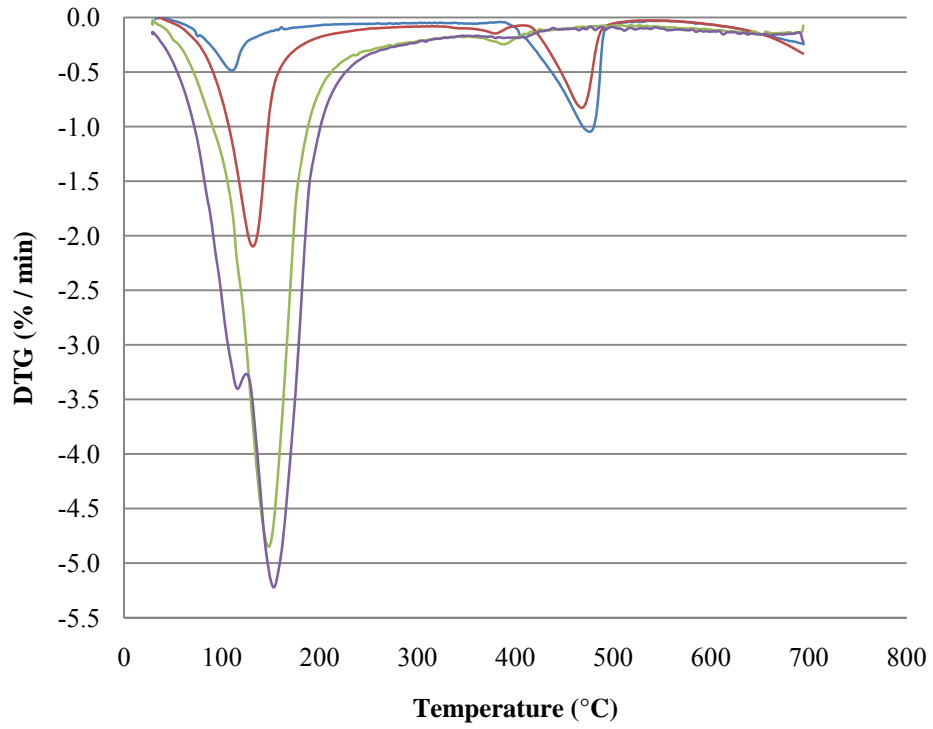
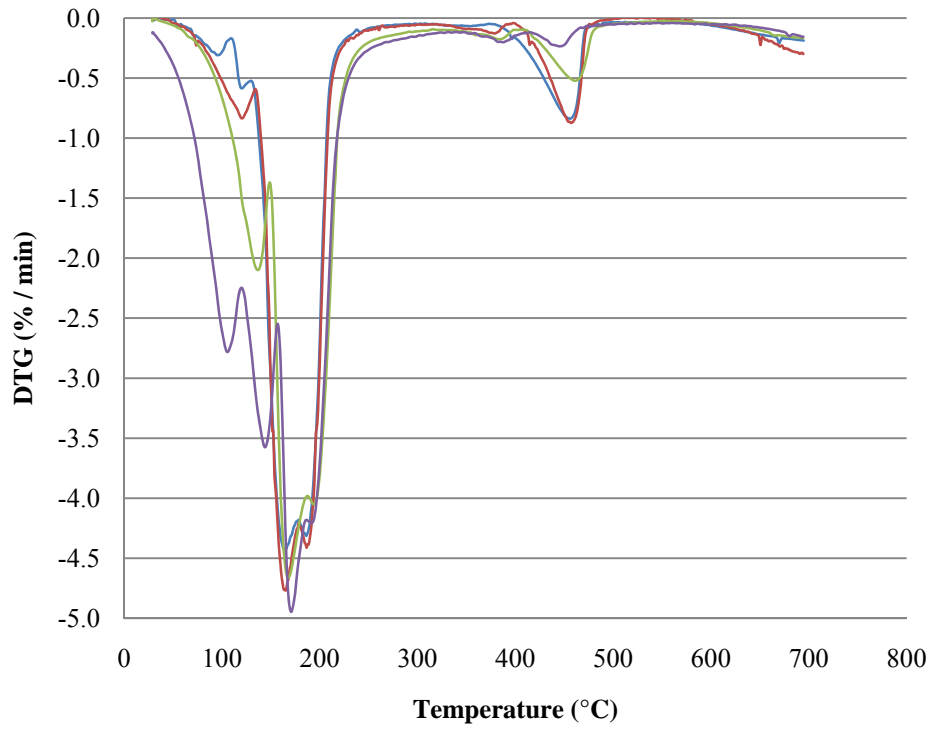


Figure 6.20 – TGA plot of *HSCL2 #2*.



From the figures, it can be seen that the amount of calcium hydroxide present in the cement systems decreased with curing time as it reacted with the aluminum of the ultra fine ash and sulfate of the anhydrite to form ettringite. After 56 days of curing, calcium hydroxide was still detected in the *Clinkerless #2* and *HSCL2 #2* cement blends; however, the amount of calcium hydroxide present in the *Clinkerless #6* cement blend was below detection after 28 days of curing. These data along with the expansion data presented in Section 6.4 of this report were consistent in supporting the hypothesis that the expansion of the cement systems was the result of the formation of ettringite.

The length-change prisms prepared using the *Clinkerless #6* cement blend (Figure 6.11) stopped expanding at 28 days, which was the curing time when calcium hydroxide was no longer detected in the cement blend to form ettringite, and thus cause the prisms to expand. However, the length-change prisms of the *Clinkerless #2* and *HSCL2 #2* cement blends (Figure 6.11 and Figure 6.13 respectively) were still expanding at 56 days curing because calcium hydroxide was still present to form ettringite.

The procedure outlined by Wang (1990) was followed to determine the calcium hydroxide content of the cement blends at different curing ages. The data have been included in the following table.

Table 6.1 – Calcium hydroxide content of cement blends at different curing ages.

	<b>Clinkerless #2</b>	<b>HSCL2 #2</b>	<b>Clinkerless #6</b>
1 - day	17.7 %	7.7 %	10.1 %
7 -day	15.4 %	6.6 %	6.3 %
28 - day	8.2 %	3.9 %	0 %
56 - day	2.2 %	1.0 %	0 %

## **6.6 Procedure for Producing Hemihydrate from FGD Gypsum**

The detailed experimental procedure that was used to produce a supply of hemihydrate from FGD gypsum was described in Section 5.6 of this report. Even though there were patents on procedures for producing hemihydrate from FGD gypsum, the best method needed to be determined for producing hemihydrate in the lab at the UK CAER.

The most effective pressing force used to press the gypsum into pucks was determined using the following: No pressing force, 24.47 kN (5500 lbs) of pressing force,

and 48.93 kN (11000 lbs) of pressing force. Scanning electron microscopy (SEM) photographs of the hemihydrate crystals produced from the various pressing techniques, as well as the crystal structure of gypsum before it was autoclaved, have been included below. Compact hemihydrate crystals were desired because they were less likely to break into smaller pieces when they were mixed with water to form plaster. The proper flow could be obtained with less water demand compared to flaky crystals, which broke apart easily into smaller particles with a higher surface area.

Figure 6.21 – SEM photograph of gypsum crystals before the conversion to hemihydrate.

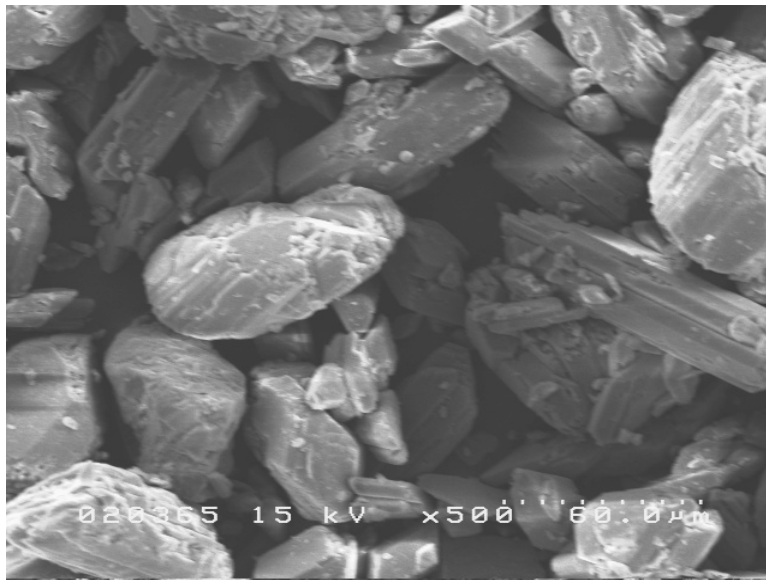


Figure 6.22 – SEM photograph of hemihydrate crystals produced from un-pressed gypsum autoclaved four hours.

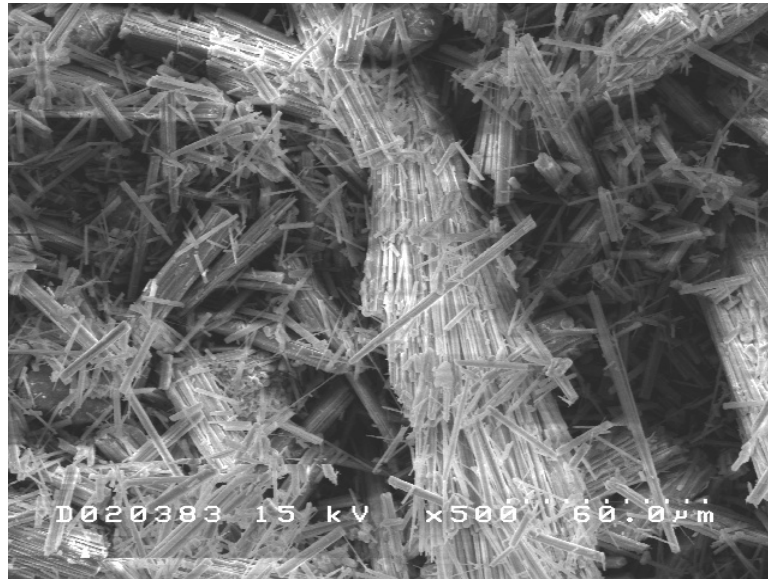


Figure 6.23 – SEM photograph of hemihydrate crystals produced from gypsum that was pressed into pucks with 24.47 kN (5500 lbs) of force, and autoclaved four hours.

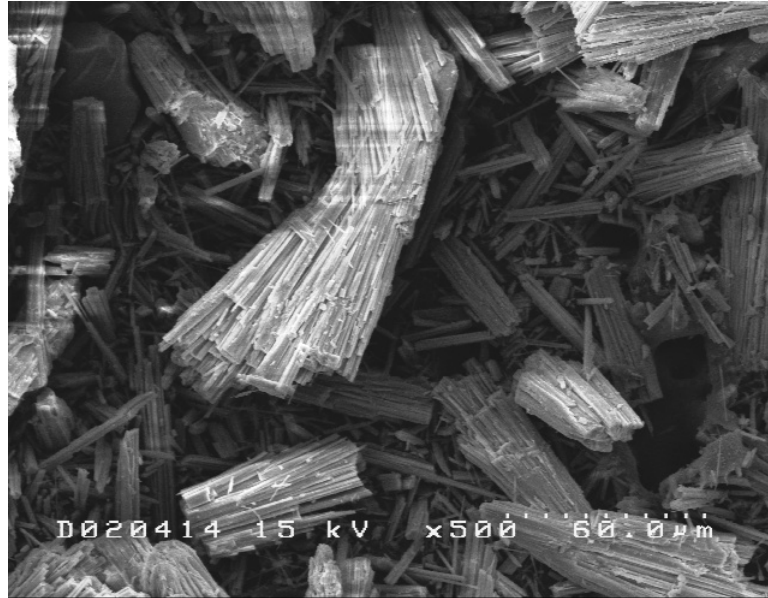




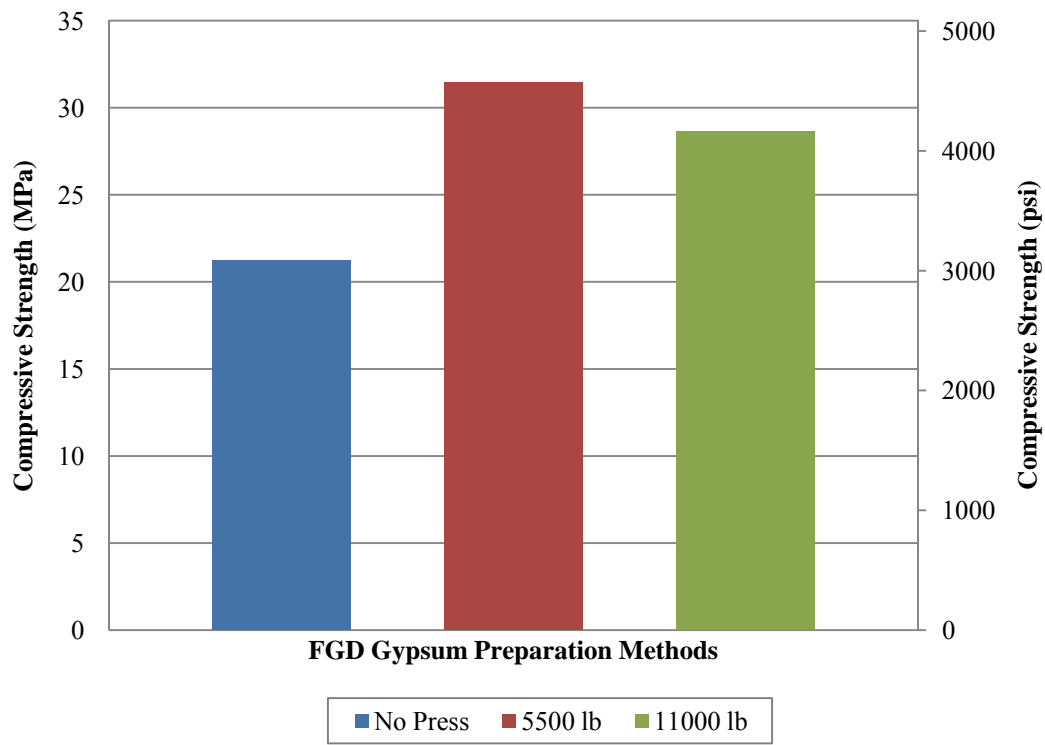
Figure 6.24 – SEM photograph of hemihydrate crystals produced from gypsum that was pressed into pucks with 48.93 kN (11000 lbs) of force, and autoclaved four hours.



From the SEM photographs, it can be seen that compact hemihydrate crystals were produced by pressing the FGD gypsum into pucks before it was autoclaved compared to the un-pressed technique.

In order to determine which preparation technique produced the best compressive strength results, ASTM C 109 was followed in preparing mortar cubes using the hemihydrates produced from the different FGD gypsum pressing techniques. Citric acid was used as a set retarder, and the procedure of ASTM C 472 (ASTM 2000) was followed for curing and testing the mortar cubes. The compressive strength data are shown in Figure 6.25 below. Each column represents the average of six tests.

Figure 6.25 – Compressive strengths of mortar cubes prepared using hemihydrates produced from the different FGD gypsum pressing techniques.

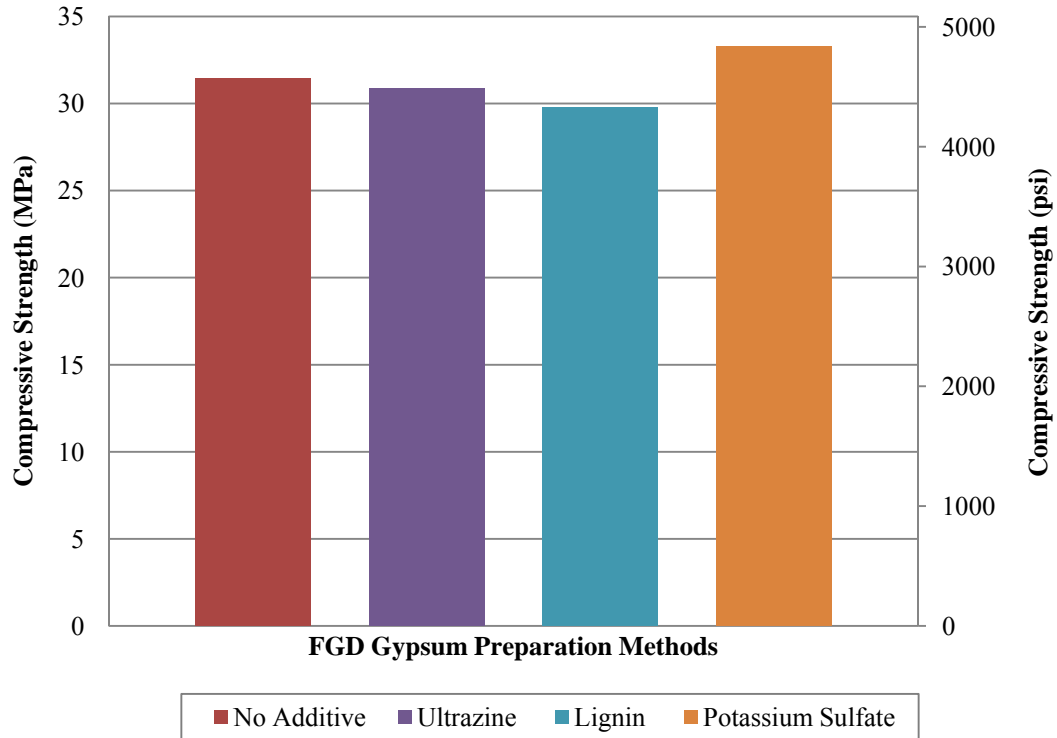


From Figure 6.25, it can be seen that pressing the gypsum into pucks with a force of 24.47 kN (5500 lbs) produced the best compressive strength results. For statistical verification, a Two Sample t-Test was performed on the average compressive strengths of the two gypsum preparation techniques that produced the highest compressive strengths which were: gypsum pressed with 24.47 kN (5500 lbs) of force, and gypsum pressed with 48.93 kN (11000 lbs) of force. The null hypothesis that the mean compressive strengths were equal for the two preparation techniques was rejected ( $p < 0.001$ ), and it was concluded that pressing the gypsum with 24.47 kN (5500 lbs) of force resulted in higher compressive strengths at the error level of 5%.

Work then began on mixing different chemicals with the gypsum before it was autoclaved. Ultrazine, lignin, and potassium sulfate were mixed with deionized water and added to dry gypsum so the resulting moisture content of the gypsum would match the moisture content of the gypsum supply. The procedure outlined in Section 5.6 of this report was then followed in producing hemihydrate from FGD gypsum. The compressive

strengths were measured using the procedure described above and are shown in Figure 6.26. Each column represents the average of six tests.

Figure 6.26 – Compressive strengths of mortar cubes prepared using hemihydrates that were produced from FGD gypsum mixed with chemical additives, and pressed with 24.47 kN (5500 lbs) of force.



To select the best method to be used to produce the hemihydrate, two factors were considered: strength of the hemihydrate and simplicity of the process. From Figure 6.26, it can be seen that the hemihydrate prepared by mixing potassium sulfate with FGD gypsum produced the best compressive strength results. However, mixing the additives into the gypsum was a time-consuming step that would ultimately increase the cost of production. The water : cement ratio of the mortar cubes prepared using the potassium sulfate-enhanced hemihydrate was 0.46, which was lower than the 0.50 water : cement ratio of the mortar cubes prepared using the additive-free hemihydrate.

It was determined that the additive-free hemihydrate could be strengthened at the time of mixing by adding a water-reducing admixture. Furthermore, drying the gypsum

and mixing in the additive took extra time, thus it was determined that pressing additive-free gypsum would be the preparation technique of choice for the project.

## **6.7 Preliminary “Low-Energy, 100% By-Product Cement” Blends**

### **6.7.1 Compressive Strength Results**

Using the results from the cement blends that were produced from the combination of *Clinkerless* #2 and Hydro-Stone®, it was determined that equal amounts of “Clinkerless” cement and hemihydrate would be blended together to make the 100% by-product cement blends. The 50/50 blend of hemihydrate to “Clinkerless” material appeared to produce a less soluble product than the 75/25 blend, and it had better long-term compressive strengths (see Section 6.3).

Before any mortar cubes were prepared using the preliminary “low-energy, 100% by-product cement” blends (compositions given in Table 5.6), the set time of the *0.5HH/0.5CL2 #1* cement blend was determined per ASTM C 807 (ASTM 2000). Sodium citrate was selected as the set retarder. It was determined that the addition of 1.0 g (0.035 oz) sodium citrate per 500 g (17.64 oz) cement gave the mortar cement blend a set time of 3.5 hours which was longer than the two hour set time of the control portland mortar cement.

Figure 6.27 – Setting time of the mortar prepared using the 0.5HH/0.5CL2 #1 cement blend.

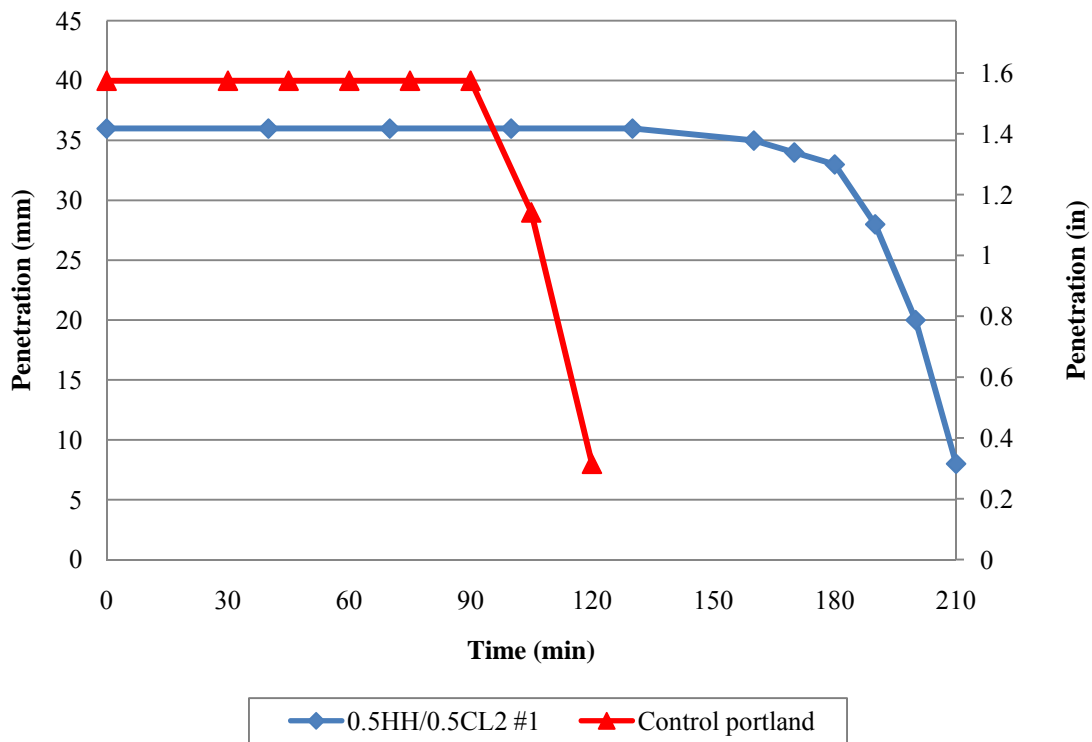
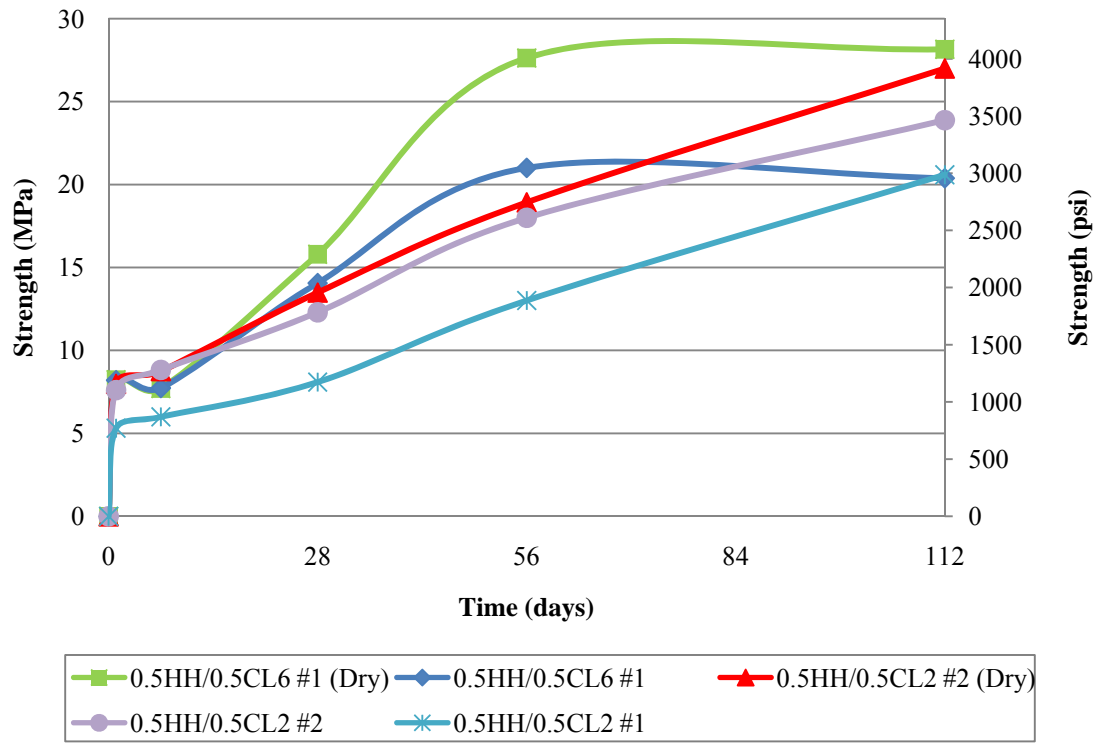


Figure 6.28 contains the compressive strength data for the preliminary “low-energy, 100% by-product cement” blends described in Section 5.7 of this report. The strength-gaining mechanisms for the blended cements produced using the FGD gypsum hemihydrate were the same as the cement blends that were produced using Hydro-Stone® as described in Section 6.3 of this report. The sealed curing technique discussed in Section 5.3 of this report to dry-cure mortar specimen was designated as “(Dry)” in the blend designation. Each data point represents the average of three tests.

Figure 6.28 – Compressive strengths of mortar cubes prepared using the preliminary “low-energy, 100% by-product cement” blends.



After the one day compressive testing of the mortar cubes prepared using the *0.5HH/0.5CL2 #1* cement blend, it was determined the blend was not satisfactory. The goal was a one day compressive strength of 6.89 MPa (1000 psi), but the blend only achieved a one day compressive strength of 5.31 MPa (770 psi).

To increase the compressive strengths of the 100% by-product cement blends, Glenium® 3030 NS was chosen as a water-reducing admixture because of its ability to provide normal, mid-range, or high range water-reduction. The recommended dosage for mid-range water reduction was the addition of 4.0 mL (0.14 oz) per 1.0 kg (35.27 oz) of cement (BASF 2007) which was equivalent to using 2.0 mL (0.07 oz) of Glenium® 3030 NS in a 500 g (17.64 oz) batch of mortar.

With the water-reduction established, a second 100% by-product cement blend was produced using 50% FGD hemihydrate and 50% *Clinkerless #2* named *0.5HH/0.5CL2 #2*. As was shown in Table 5.6 of this report, the water : cement ratio of the mortar mix was reduced from 0.46 to 0.40 with the addition of the water-reducing

admixture. Because of the lower water : cement ratio, the average one day compressive strength of the mortar cubes prepared using the *0.5HH/0.5CL2 #2* cement blend was 7.58 MPa (1100 psi). The lower water : cement ratio also resulted in better long-term compressive strengths of the *0.5HH/0.5CL2 #2* cement blend compared to the *0.5HH/0.5CL2 #1* cement blend. The average 28 and 56 day compressive strengths were 12.27 MPa (1780 psi) and 18.0 MPa (2610 psi) respectively.

*0.5HH/0.5CL6 #1* was a 50 / 50 blend of FGD hemihydrate to *Clinkerless #6*. Mortar cubes were prepared using Glenium® 3030 NS resulting in a water : cement ratio of 0.40 as seen in Table 5.6 of this report. The mortar cubes had a one day compressive strength 8.20 MPa (1190 psi) which was slightly higher than the one day compressive strength of the *0.5HH/0.5CL2 #2*. The compressive strength then increased to 14.07 MPa (2040 psi) after 28 days of curing and to 21.03 MPa (3050 psi) after 56 days of curing due to the formation of ettringite and other pozzolanic reactions.

The compressive strength gains of the mortar cubes that were dry-cured followed the same pattern as the cubes that were cured in the moist curing room. However, to statistically verify that the compressive strength gains of the dry-cured mortar cubes were significantly higher than the mortar cubes that were moist-cured, a Two Sample t-Test was performed on the 112-day average compressive strengths of the mortar cubes prepared using the *0.5HH/0.5CL6 #1(Dry)* and *0.5HH/0.5CL6 #1* cement blends. The 112-day data were selected because they were the longest-term data available. The null hypothesis that the compressive strengths of the mortar cubes were equal for the two curing techniques after 112 days of curing was rejected ( $p < 0.001$ ), and it was concluded that the dry curing technique produced higher compressive strengths at the error level of 5% (as was the case comparing the dry-curing and moist-curing methods of *HSCL2 #2*). The higher compressive strength gains were attributed to the lack of excess moisture present to dissolve the hemihydrate in the dry-curing method.

Once it was statistically verified that the dry-curing method produced higher long-term compressive strengths, the 112-day average compressive strength of the mortar cubes prepared using the *0.5HH/0.5CL6 #1(Dry)* cement blend was compared to the 112-day average compressive strength of the mortar cubes prepared using the *0.5HH/0.5CL62 #2(Dry)* cement blend to determine if the *0.5HH/0.5CL6 #1(Dry)* cement blend produced

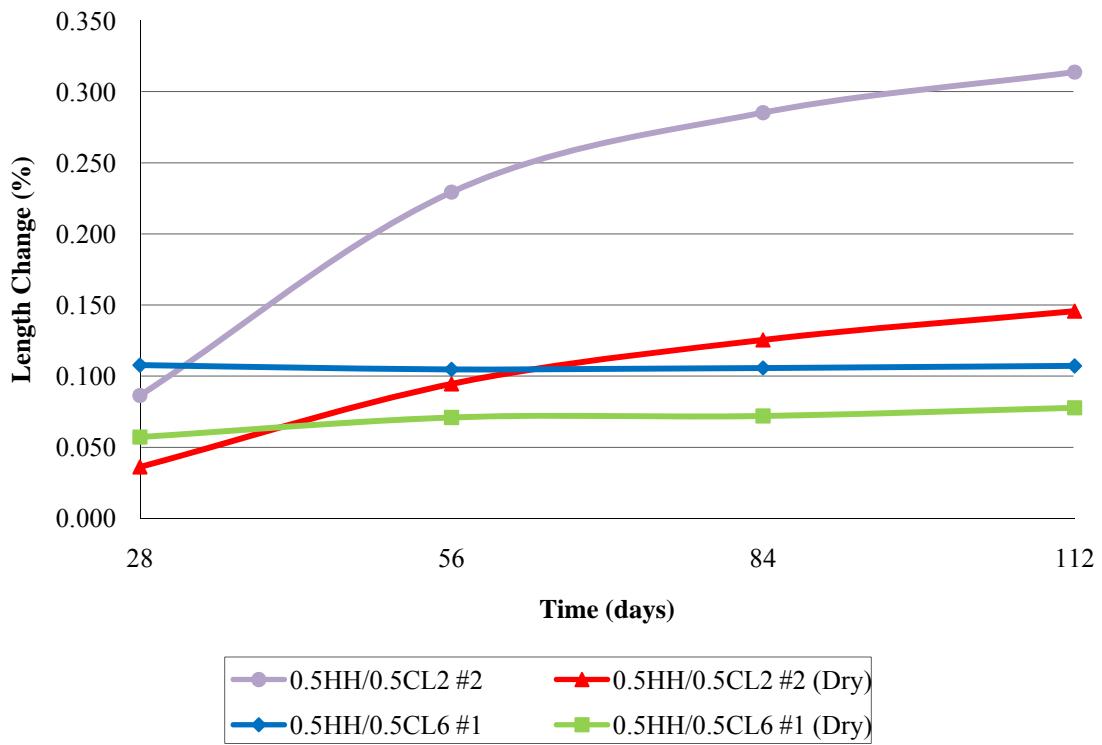
higher compressive strengths. The null hypothesis was failed to be rejected ( $0.100 < p < 0.200$ ), and no statistical verification could be made at the error level of 5%. However, the faster strength gains provided by the *0.5HH/0.5CL6 #1(Dry)* cement blend made it a more desirable candidate for further experimentation.

### **6.7.2 Expansion Results**

Figure 6.29 shows the expansion data of the length-change prisms prepared using the preliminary “low-energy, 100% by-product cement” blends as described in Section 5.7 of this report. The trends in the figure reflect the trends in Figure 6.11 which contained the expansion data of the length-change prisms prepared using the high strength and low expansion “Clinkerless” cement blends, but the overall expansions were less due to inclusion of hemihydrate in the cement blends. Each data point for the specimen that were moist-cured represents the average of four measurements, and each data point for the specimen that were dry-cured represents the average of three measurements.



Figure 6.29 – Expansion data of length-change prisms prepared using the preliminary “low-energy, 100% by-product cement” blends.



The length-change prisms prepared using the *0.5HH/0.5CL2 #2* cement blend had expanded 0.31% after 112 days of curing and were still expanding at the time of this report. However, the 112 day total expansion of the mortar prisms prepared using the *Clinkerless #2* cement blend (See Figure 6.11) was 2.23%. Therefore, by substituting 50% of the cementitious material in the cement blend with hemihydrate, the expansion was reduced by 86%.

The length-change prisms prepared using the *0.5HH/0.5CL2 #2* cement blend that were dry-cured expanded less than the prisms that were moist-cured. After 112 days of curing, the prisms had expanded 0.15%, but as was the case with the prisms that were moist-cured, they were still expanding at the time of this report.

The expansion of the *0.5HH/0.5CL6 #1* cement blend ceased after 28 days of curing due to the total consumption of free lime in the system to form ettringite (see Section 6.5). The prisms expanded 0.11% after 28 days curing, and the expansion was the same after 112 days of curing. The 112-day total expansion of the mortar prisms

prepared using the *Clinkerless #6* cement blend (Figure 6.11) was 1.10%. Therefore, by substituting 50% of the cementitious material in the cement blend with hemihydrate, the expansion was reduced by 90%.

The length-change prisms prepared using the *0.5HH/0.5CL6 #1* cement blend that were dry-cured showed signs of expansion up to 56 days of curing before the expansion began to subside. However the expansion was less severe, with a 28-day expansion of 0.06%, a 56-day expansion of 0.07%, and a 112-day expansion of 0.08%.

A Two Sample t-Test was performed on the 112-day average expansions of the length-change prisms prepared using the *0.5HH/0.5CL6 #1(Dry)* and *0.5HH/0.5CL6 #1* cement blends to determine if the dry-curing technique resulted in less expansion. The 112-day data were compared because they were the longest-term data available at the time of this report. The null hypothesis that the expansions were the same for the two curing techniques was rejected ( $0.025 < p < 0.050$ ), and it was concluded that dry-curing the mortar prisms significantly reduced their expansion at the error level of 5%.

Once it was statistically verified that the dry-curing method resulted in less expansion, the 112-day average expansion of the length-change prisms prepared using the *0.5HH/0.5CL6 #1(Dry)* cement blend were compared to the 112-day average expansion of the length-change prisms prepared using the *0.5HH/0.5CL62 #2(Dry)* cement blend to determine if the *0.5HH/0.5CL6 #1(Dry)* cement blend experienced less expansion. The null hypothesis that the expansions were the same was rejected ( $0.010 < p < 0.025$ ), and it was concluded that the *0.5HH/0.5CL6 #1(Dry)* cement blend expanded less after 112 days of curing at the error level of 5%.

## **6.8 High Strength and Low Expansion “Low-Energy, 100% By-Product Cement”**

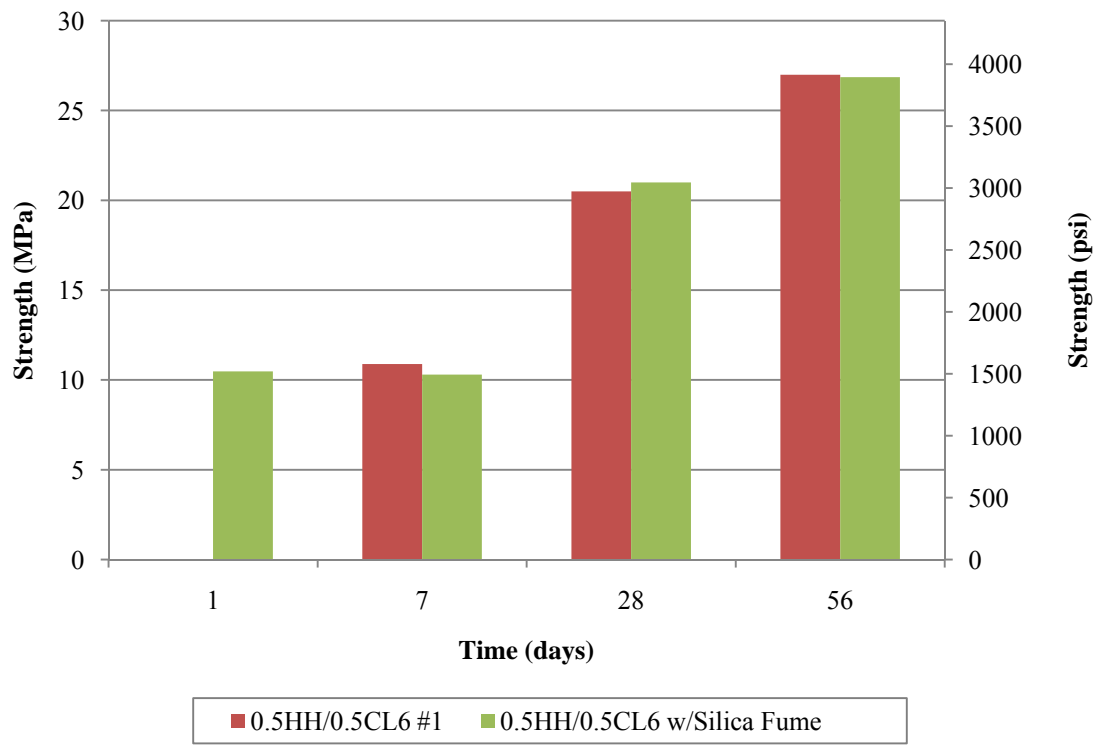
The results of the previous section indicated four key observations: Higher early-term compressive strengths were obtained with the *0.5HH/0.5CL6 #1* cement blend compared to the *0.5HH/0.5CL2 #2* cement blend (as was the case with the *Clinkerless #6* compared to *Clinkerless #2*), the *0.5HH/0.5CL6 #1* cement blend expanded less than the *0.5HH/0.5CL2 #2* cement blend, and keeping excess water off the cement blends increased their compressive strengths and reduced their expansions.

All four observations were considered in the production of the high strength and low expansion “low-energy, 100% by-product cement” mortar mix designs. The *0.5HH/0.5CL6 #1* cement blend was selected because of its higher early-term compressive strength compared to the *0.5HH/0.5CL2 #2* cement blend, and because it expanded less than the *0.5HH/0.5CL2 #2* cement blend. CHRYSO®Pave 100 was included in the mix designs because of its water-reducing capability, and because of its ability to inhibit the flow of water into the cement system, which made the dry-curing technique developed in the lab applicable in the field.

The compressive strengths of the two mixes are displayed in Figure 6.30. Each column for the *0.5HH/0.5CL6 w/ Silica Fume* mix represents the average of three tests. The 7 and 28-day columns for the *0.5HH/0.5CL6 #1* mix represent the average of two tests, while the 56-day column represents the average of three tests.

Due to material constraints, mortar cubes were not prepared to test the one-day compressive strength of the *0.5HH/0.5CL6 #1* mix design. However, its one-day compressive strength was expected to be very similar to the one-day compressive strength of the *0.5HH/0.5CL6 w/Silica Fume* mix design because hemihydrate provided the early-term compressive strength (both of the mortar mix designs contained the same quantity of hemihydrate), and the two mix designs had comparable water : cement ratios. No compressive data beyond 56 days of curing were available at the time of this report.

Figure 6.30 – Compressive strengths of mortar cubes prepared using the high strength and low expansion “low-energy, 100% by-product cement” mortar mix designs.



By using the recommended dosage of the CHRYSO<sup>®</sup>Pave 100, the w/c ratio was lowered from 0.40, which was obtained using the Glenium<sup>®</sup> 3030 NS water-reducing admixture in the preliminary *0.5HH/0.5CL6 #1* mortar cement mix, to 0.36 in the high strength low expansion *0.5HH/0.5CL6 #1* mortar mix design. The lower water : cement ratio increased the 28-day compressive strength from 15.79 MPa (2290 psi) of the preliminary *0.5HH/0.5CL6 #1(Dry)* cement blend at 28 days curing to 20.48 MPa (2970 psi) at 28 days curing for the high strength and low expansion *0.5HH/0.5CL6 #1* mortar cement mix produced using CHRYSO<sup>®</sup>Pave 100.

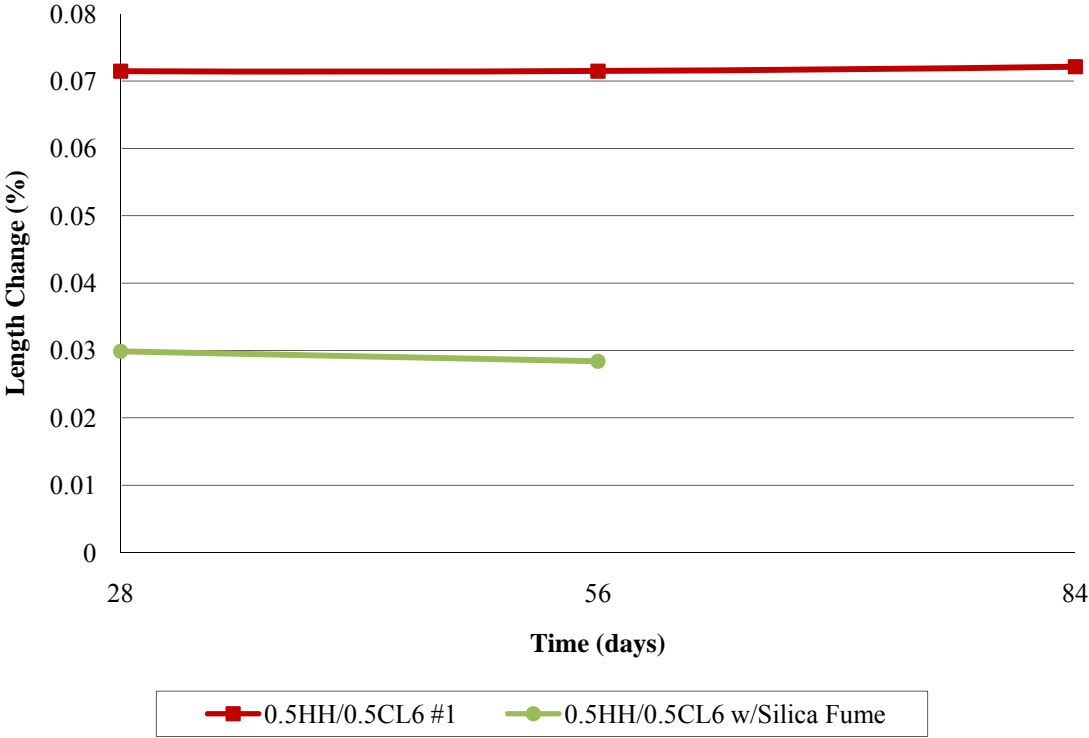
The mortar cubes prepared using the high strength and low expansion *0.5HH/0.5CL6 #1* mortar mix design were moist-cured, but their compressive strengths were very similar to the compressive strengths exhibited by the mortar cubes prepared using the *0.5HH/0.5CL6 #1(Dry)* cement blend (Figure 6.28). The mortar cubes prepared using the *0.5HH/0.5CL6 #1(Dry)* cement blend obtained compressive strengths of 15.79 MPa (2290 psi) and 27.58 MPa (4000 psi) respectively at 28 and 56 days of dry curing.

The compressive strength of the mortar cubes prepared using the high strength and low expansion *0.5HH/0.5CL6 #1* mortar mix design was slightly higher after 28 days of moist curing with a strength of 20.48 MPa (2970 psi), and slightly lower after 56 days of moist curing with a strength of 27.00 MPa (3915 psi). The compressive strength results indicated that CHRYSO<sup>®</sup>Pave 100 could be used to make the dry-curing technique developed in the lab applicable in the field.

The compressive strengths for the *0.5HH/0.5CL6 w/Silica Fume* mortar cement mix, which included a 2.5% substitution of silica fume for ultra fine ash, were similar to the compressive strengths for the high strength and low expansion *0.5HH/0.5CL6 #1* mortar cement mix. However, by adding silica fume to the cement blend, the workability of the mix decreased slightly and required a water : cement ratio of 0.37 to obtain the  $110\% \pm 5\%$  flow required to comply with ASTM C 109.

The expansion data of the mix designs were of equal importance. Figure 6.31 contains the expansion data of length-change prisms prepared using the high strength and low expansion “low-energy, 100% by-product mortar cement” mortar mix designs. Each data point represents the average of three measurements. The 84-day expansion data for the *.5HH/0.5CL6 w/Silica Fume* mortar mix design were not available at the time of this report. However, from the plot it can be seen that the expansion of both “low-energy, 100% by-product cement” mortar mixes ceased at 28 days.

Figure 6.31 – Expansion data of length-change prisms prepared using the high strength and low expansion “low-energy, 100% by-product cement” mortar mix designs.



The length-change prisms of the *0.5HH/0.5CL6 #1* mortar mix had the same 0.07% expansion after 28 days of curing as the prisms from the same cement blend that were dry-cured (preliminary *0.5HH/0.5CL6 #1(Dry)* cement blend shown in Figure 6.29). The expansion results indicated that CHRYSO<sup>®</sup> Pave 100 could be used to make the dry-curing technique developed in the lab applicable in the field.

The length-change prisms prepared using the *0.5HH/0.5CL6 w/Silica Fume* mortar mix expanded even less than the prisms prepared using the *0.5HH/0.5CL6 #1* mortar mix a 28-day expansion of 0.03%. The expansion was approximately the same after 56 days of curing.

## Section 7: Conclusions

From the experimentation and results discussed in this report, the following conclusions were made:

1. The Prehydration technique of 10% water by weight of the spent bed ash, which was the lower-limit of the range suggested by Bland et al. (1987), was successful in reacting with the unslaked lime (CaO) present in the spent bed ash to control the exothermic reaction before mortar was prepared.
2. By reducing the amount of spent bed ash in the “Clinkerless” cement blends, expansion was reduced. However, a sufficient quantity of lime must be present in the cementing system to form ettringite and calcium silicate hydrates to give the system cementing properties. A spent bed / ultra fine ash ratio of 40/60 produced the best compressive strength results of the “Clinkerless” cement blends produced in the study, and it expanded significantly less than the 70/30 “Clinkerless” cement blend.
3. The expansion of the “Clinkerless” cement blends was caused by the formation of ettringite shown by the X-ray diffraction (XRD) and thermogravimetric analysis (TGA) results included in Section 6.5. The system stopped expanding when calcium hydroxide, a component of ettringite formation, was consumed. Further supporting this conclusion was that the length-change prisms, which were prepared using the *Clinkerless* #2 cement blend in which silica fume was substituted for ultra fine ash, did not expand (Figure 6.12).
4. The spent bed / ultra fine ash “Clinkerless” cement blends produced in the study cannot be used alone as mortar cement. Even though long-term compressive strength gains of 38.40 MPa (5570 psi) were obtained after 112 days of curing, mortar cube specimens prepared using the “Clinkerless” cement blends expanded in the presence of water resulting in map cracking after several months of curing.
5. Hemihydrate was successfully produced in the lab from flue gas desulfurization (FGD) gypsum. The method of pressing the gypsum into pucks with 24.47 kN (5500 lbs) of force, autoclaving the pucks for four hours at 130°C (266°F), and drying the pucks at 100°C (212°F) for two days produced a hemihydrate product that was 4% stronger than the commercial hemihydrate used in the research.

6. By introducing hemihydrate to the “Clinkerless” cement blends to create the “low-energy, 100% by-product cement” blends, expansion was reduced up to 90%. After being immersed in water for 112 days, the length-change prisms prepared using the *Clinkerless #6* cement blend expanded 1.10%. Conversely, the prisms prepared using the *0.5HH/0.5CL6 #1* cement blend (50% hemihydrate / 50% *Clinkerless #6*) expanded only 0.11% after 112 days. Most importantly, the mortar specimen prepared using the cement blends that contained 50% hemihydrate did not crack.
7. In addition to preventing the mortar cement blends from cracking, the hemihydrate provided early compressive strength gains that the spent bed / ultra fine ash “Clinkerless” cement blends could not achieve. One day compressive strengths of up to 10.34 MPa (1500 psi) were achieved with the 50% hemihydrate cement blends when a water-reducing admixture was used in the mortar mix.
8. By establishing a dry-curing technique, the compressive strengths of the 100% by-product cement blends were increased, and the expansions were reduced when compared to the traditional moist-curing method. The reduction in expansion was attributed to free water being kept out of the system that would otherwise “fuel” ettringite expansion.
9. The dry-curing technique developed in the lab would be applicable in the field by adding CHRYSO<sup>®</sup>Pave 100 to the mortar cement mix. The mortar specimens were moist-cured in the curing room and behaved similar to the specimen that were cured using the dry-curing technique. Two high strength and low expansion “low-energy, 100% by-product cement” mortar mix designs were successfully developed as candidates for field applications:



Table 7.1 – Mortar mix design of the *0.5HH/0.5CL6 #1* cement blend.

<b>Material</b>	<b>Quantity (SI)</b>	<b>Quantity (US)</b>
Hemihydrate	250 g	8.82 oz
Spent Bed	100 g	3.53 oz
Ultra Fine Ash	150 g	5.29 oz
Sand	1375 g	48.5 oz
Sodium Citrate	1.0 g	0.035 oz
Water	180 mL	6.09 oz
CHRYSO®Pave 100	2.6 mL	0.088 oz

Table 7.2 – Mortar mix design of the *0.5HH/0.5CL6 w/Silica Fume* cement blend.

<b>Material</b>	<b>Quantity (SI)</b>	<b>Quantity (US)</b>
Hemihydrate	250 g	8.82 oz
Spent Bed	100 g	3.53 oz
Ultra Fine Ash	137.5 g	4.85 oz
Silica Fume	12.5 g	0.44 oz
Sand	1375 g	48.5 oz
Sodium Citrate	1.0 g	0.035 oz
Water	180 mL	6.09 oz
CHRYSO®Pave 100	2.6 mL	0.088 oz

## **Section 8: Recommendations for Future Research**

Concrete should be prepared using the two high strength and low expansion “low-energy, 100% by-product cement” mortar mix candidates. Both confined and unconfined compressive strengths, permeability, and volume stability of the concrete should be tested.

A more economically feasible form of Class F fly ash should be investigated for use instead of the more expensive ultra fine ash that was used in this study. The ultra fine ash was used to determine if the concept presented in this report would work. Results using a more traditional Class F fly ash should be obtained to produce a product that is more marketable.

The high solubility of the “low-energy, 100% by-product cement” needs to be further decreased using chemical admixtures. Other admixtures should also be explored to determine if the hemihydrate percentage of the cement blend can be reduced to less than 50%, thus resulting in a less soluble product.

Much of the testing in this report included results up to 112 days of curing. Longer-term data on these samples should be obtained to determine the behaviors of the cement blends beyond 112 days of curing.

In this report, a dry curing technique was developed. Experimentation should be performed to determine the behavior of the dry-cured blends if they are exposed to water after 112 days of curing.

Specific applications should be investigated for the use of the rapid-setting and expansive cements developed in this research project. In some situations, expansive cement is desired. Additionally, adding fibers to the cement blends could create a self-prestressing concrete that could be beneficial in certain applications.

## **Appendix A: Glossary of Terms Used in this Report**

- Circulating fluidized bed combustion (CFBC) – Method of sulfur-dioxide removal that takes place inside the coal combustion zone. The sulfur dioxide removal is achieved by burning the coal in the presence of limestone that calcines in the combustor. The unslaked lime reacts with sulfur dioxide to form anhydrite which is the mineral form of gypsum.
- CFBC spent bed ash – By-product from coal burned in the presence of limestone in the CFBC process. It is a granular material characterized by poor pozzolanic activity, but it is high in free lime making it a candidate to be blended with pozzolans. The material produces an exothermic reaction when wetted with water as the unslaked lime hydrates to calcium hydroxide.
- Clinker – Hydraulic material consisting of at least two-thirds calcium silicates by mass with the remainder consisting of aluminum oxide, iron oxide, and other oxides. Portland cement clinker is produced by burning raw materials in a kiln at 1450°C (2642°F) until the material sinters into lumps.
- Ettringite – White, highly insoluble, complex and sometimes unpredictable mineral with good cementitious properties. Lime, sulfate, and aluminum are the three main components in the formation of ettringite. Ettringite can cause large expansions when in contact with an outside source of water.
- FGD gypsum – By-product from the reaction of calcium carbonate and sulfur dioxide in the flue gas desulfurization process. Originally, the by-product was a calcium sulfite sludge that was not of much use. However, as the technology advanced it was discovered that the sludge could be oxidized and converted into a marketable gypsum product.
- Flue gas desulfurization (FGD) – Method of sulfur-dioxide removal that takes place after coal combustion has occurred. As coal is combusted, sulfur present in the coal reacts with oxygen in the air, and it forms SO<sub>2</sub> that exits the combustor in the flue gas. The flue gas containing SO<sub>2</sub> is an acidic gas; therefore, alkaline materials such as limestone slurries or lime are used to remove the sulfur as the gas passes through the scrubber system.

Fly Ash (Class F) – By-product from the burning of pulverized bituminous coal in a coal-fired boiler. Class F fly ash is a pozzolan and is different from Class C fly ash in that it has no cementing properties because it contains less than 10% lime. The glassy silica and alumina make it an ideal substitution for portland cement with benefits that include: enhanced workability due to the spherical particle shape, reduced bleeding and a lower water : cement ratio, increased ultimate strength, reduced permeability and chloride ion penetration, greater resistance to sulfate attack, greater resistance to alkali-aggregate reactivity, reduced drying shrinkage, and increased ultimate strength.

Hemihydrate – Commonly called Plaster of Paris. The mineral is formed by partially dehydrating gypsum to form the following compound:  $\text{CaSO}_4 \cdot 0.5 \text{H}_2\text{O}$ . When the mineral is mixed with water, it hydrates into gypsum rapidly.

Pozzolan – A siliceous or siliceous and aluminous material which in itself possesses little or no cementitious value but will, in finely divided form and in the presence of moisture, chemically react with calcium hydroxide at ordinary temperatures to form compounds possessing cementitious properties.

Silica Fume – Artificial pozzolan that has a high silica content, high specific surface area, and amorphous structure. Because of these characteristics, silica fume has substantial pozzolanic activity, in terms of its capacity of binding lime and its high reaction rate.

Thermogravimetric Analysis (TGA) – Analysis in which the weight loss of a sample is measured with change in temperature. The quantity of a specific material in a sample can be determined by the weight loss attributed to the dehydration of the material at a known temperature. In the study, the quantity of calcium hydroxide was determined by the weight loss that occurred around  $450^\circ\text{C}$  ( $842^\circ\text{F}$ ).

X-ray Diffraction – Analysis of mineral crystals by the scattering of X-rays that are beamed through a material.

## Appendix B: Raw Experimental Data of Cement Blends Produced in the Study

Table B.1 - Compressive strengths of mortar cubes prepared using the preliminary “Clinkerless” cement blends.

<b>Clinkerless #1 Compressive Strength Data (psi)</b>						
	1-day	7-day	28-day	56-day	112-day	224-day
Cube 1	NA	578	1563	1941	2053	1638
Cube 2	NA	527	1628	1996	1735	2375
Cube 3	NA	NA	NA	NA	NA	2143
Mean Strength	NA	552.5	1595.5	1968.5	1894.0	2052.0
Standard Deviation	NA	36.1	46.0	38.9	224.9	376.8
Coefficient of Var.	NA	6.53	2.88	1.98	11.87	18.36
<b>Clinkerless #2 Compressive Strength Data (psi)</b>						
	1-day	7-day	28-day	56-day	112-day	224-day
Cube 1	NA	318	1322	1940	2381	4093
Cube 2	NA	300	1355	1907	2428	3629
Cube 3	NA	NA	NA	NA	NA	4364
Mean Strength	NA	309.0	1338.5	1923.5	2404.5	4028.7
Standard Deviation	NA	12.7	23.3	23.3	33.2	371.7
Coefficient of Var.	NA	4.12	1.74	1.21	1.38	9.23
<b>Clinkerless #3 Compressive Strength Data (psi)</b>						
	1-day	7-day	28-day	56-day	112-day	224-day
Cube 1	NA	491	2139	2230	5266	5884
Cube 2	NA	439	2121	3078	5235	4685
Cube 3	NA	NA	NA	NA	NA	4099
Mean Strength	NA	465.0	2130.0	2654.0	5250.5	4889.3
Standard Deviation	NA	36.8	12.7	599.6	21.9	909.9
Coefficient of Var.	NA	7.91	0.60	22.59	0.42	18.61

Table B.2 – Edge lengths of mortar cubes prepared using the preliminary “Clinkerless” cement blends.

<b>Clinkerless #1 Expansion Data (in)</b>						
	1-day	7-day	28-day	56-day	112-day	224-day
Cube 1	NA	2.003	2.014	2.033	2.052	2.0795
Cube 2	NA	2.0025	2.0115	2.031	2.0565	2.0635
Cube 3	NA	NA	NA	NA	NA	NA
Average Edge Length	NA	2.003	2.013	2.032	2.054	2.072
<b>Clinkerless #2 Expansion Data (in)</b>						
	1-day	7-day	28-day	56-day	112-day	224-day
Cube 1	NA	2.0125	2.021	2.048	2.063	2.059
Cube 2	NA	2.0085	2.0245	2.043	2.062.5	2.065
Cube 3	NA	NA	NA	NA	NA	2.049
Average Edge Length	NA	2.011	2.023	2.046	2.063	2.058
<b>Clinkerless #3 Expansion Data (in)</b>						
	1-day	7-day	28-day	56-day	112-day	224-day
Cube 1	NA	2.006	2.0225	2.0625	2.0405	2.0625
Cube 2	NA	2.0085	2.0255	2.0475	2.038	2.0425
Cube 3	NA	NA	NA	NA	NA	2.058
Average Edge Length	NA	2.007	2.024	2.055	2.039	2.054

Table B.3 – Compressive strengths of mortar cubes prepared using the “Clinkerless” cement blends that were produced to reduce expansion.

<b>Clinkerless #4 Compressive Strength Data (psi)</b>					
	1-day	7-day	28-day	56-day	112-day
Cube 1	NA	596	1051	980	854
Cube 2	NA	563	1088	922	836
Cube 3	NA	539	NA	NA	NA
Mean Strength	NA	566.0	1069.5	951.0	845.0
Standard Deviation	NA	28.6	26.2	41.0	12.7
Coefficient of Var.	NA	5.0562	2.4463	4.3125	1.5063
<b>Clinkerless #5 Compressive Strength Data (psi)</b>					
	1-day	7-day	28-day	56-day	112-day
Cube 1	NA	541	515	541	543
Cube 2	NA	539	542	536	510
Cube 3	NA	560	572	554	487
Mean Strength	NA	546.7	543.0	543.7	513.3
Standard Deviation	NA	11.6	28.5	9.3	28.1
Coefficient of Var.	NA	2.1202	5.2510	1.7091	5.4835

Table B.4 – Edge lengths of mortar cubes prepared using the “Clinkerless” cement blends that were produced to reduce expansion.

<b>Clinkerless #4 Expansion Data (in)</b>					
	1-day	7-day	28-day	56-day	112-day
Cube 1	NA	2.0068	2.0165	2.0465	2.0755
Cube 2	NA	2.006	2.0175	2.045	2.075
Cube 3	NA	2.0058	NA	NA	NA
Average Edge Length	NA	2.006	2.017	2.046	2.075
<b>Clinkerless #5 Expansion Data (in)</b>					
	1-day	7-day	28-day	56-day	112-day
Cube 1	NA	2.005	2.001	2.004	2.006
Cube 2	NA	2.0065	2.005	2.0045	2.005
Cube 3	NA	2.001	2.003	2.004	2.0065
Average Edge Length	NA	2.004	2.003	2.004	2.006

Table B.5 – Compressive strengths of mortar cubes prepared using the high strength and low expansion “Clinkerless” cement blends.

<b>Clinkerless #2 Compressive Strength Data (psi)</b>					
	<b>1-day</b>	<b>7-day</b>	<b>28-day</b>	<b>56-day</b>	<b>112-day</b>
Cube 1	NA	611	2218	2739	3591
Cube 2	NA	571	2192	2919	3419
Cube 3	NA	607	2281	2707	4101
Mean Strength	NA	596.3	2230.3	2788.3	3703.7
Standard Deviation	NA	22.0	45.8	114.3	354.7
Coefficient of Var.	NA	3.6943	2.0519	4.0987	9.5766
<b>Clinkerless #6 Compressive Strength Data (psi)</b>					
	<b>1-day</b>	<b>7-day</b>	<b>28-day</b>	<b>56-day</b>	<b>112-day</b>
Cube 1	NA	685	4275	5285	5116
Cube 2	NA	680	4222	5419	5830
Cube 3	NA	666	4247	4950	5761
Mean Strength	NA	677.0	4248.0	5218.0	5569.0
Standard Deviation	NA	9.8	26.5	241.6	393.8
Coefficient of Var.	NA	1.4548	0.6242	4.6296	7.0717

Table B.6 – Expansion data of length-change prisms prepared using the high strength and low expansion “Clinkerless” cement blends.

<b>Clinkerless #2 Expansion Data (%)</b>					
	<b>14-day</b>	<b>28-day</b>	<b>56-day</b>	<b>84-day</b>	<b>112-day</b>
Bar 1	0	1.170	1.974	2.247	2.376
Bar 2	0	1.112	1.858	2.123	2.252
Bar 3	0	1.099	1.762	1.993	NA
Bar 4	0	1.08	1.814	2.058	2.166
Bar 5	0	1.060	1.772	2.010	2.120
Average Expansion	0	1.104	1.836	2.086	2.228
<b>Clinkerless #6 Expansion Data (%)</b>					
	<b>7-day</b>	<b>28-day</b>	<b>56-day</b>	<b>84-day</b>	<b>112-day</b>
Bar 1	0	1.090	1.090	1.094	1.090
Bar 2	0	1.063	1.062	1.064	1.061
Bar 3	0	1.176	1.176	1.180	1.175
Bar 4	0	1.090	1.090	1.095	1.089
Average Expansion	0	1.105	1.105	1.108	1.104



Table B.7 – Compressive strengths of mortar mixes that reproduced previous research by Bland et al. (1987).

<b>No-Cement #1 Compressive Strength Data (psi)</b>					
	1-day	7-day	28-day	56-day	112-day
Cube 1	NA	315	2733	3620	5063
Cube 2	NA	NA	2821	3866	NA
Mean Strength	NA	315.0	2777.0	3743.0	5063.0
Standard Deviation	NA	NA	62.2	173.9	NA
Coefficient of Var.	NA	NA	2.24	4.65	NA
<b>Sandless #1 Compressive Strength Data (psi)</b>					
	1-day	7-day	28-day	56-day	112-day
Cube 1	NA	717	4824	6118	6465
Cube 2	NA	759	5101	5766	NA
Mean Strength	NA	738.0	4962.5	5942.0	6465.0
Standard Deviation	NA	29.7	195.9	248.9	NA
Coefficient of Var.	NA	4.02	3.95	4.19	NA

Table B.8 – Cube edge lengths of mortar mixes that reproduced previous research by Bland et al. (1987).

<b>No-Cement #1 Expansion Data (in)</b>					
	1-day	7-day	28-day	56-day	112-day
Cube 1	NA	2	2.007	2.013	2.013
Cube 2	NA	NA	2.0075	2.0115	NA
Average Edge Length	NA	2.005	2.007	2.012	2.013
<b>Sandless #1 Expansion Data (in)</b>					
	1-day	7-day	28-day	56-day	112-day
Cube 1	NA	2.003	2.012	2.019	2.022
Cube 2	NA	2.0035	2.0115	2.016	NA
Average Edge Length	NA	2.003	2.012	2.018	2.022

Table B.9 – Compressive strengths of mortar cubes prepared using the cement blends containing Hydro-Stone®.

<b>HydroStone #1 Compressive Strength Data (psi)</b>					
	1-day	7-day	28-day	56-day	112-day
Cube 1	1273	1183	1021	692	742
Cube 2	1377	1030	983	794	648
Mean Strength	1325.0	1106.5	1002.0	743.0	695.0
Standard Deviation	73.5	108.2	26.9	72.1	66.5
Coefficient of Var.	5.55	9.78	2.68	9.71	9.56
<b>HSCCL2 #1 Compressive Strength Data (psi)</b>					
	1-day	7-day	28-day	56-day	112-day
Cube 1	1352	1267	1206	1463	1889
Cube 2	1247	1215	1237	1472	1872
Cube 3	1304	1239	1207	1441	2049
Mean Strength	1301.0	1240.3	1216.7	1458.7	1936.7
Standard Deviation	52.6	26.0	17.6	15.9	97.7
Coefficient of Var.	4.04	2.10	1.45	1.09	5.04
<b>HSCCL2 #1 (Dry) Compressive Strength Data (psi)</b>					
	1-day	7-day	28-day	56-day	112-day
Cube 1	1495	1438	1293	1410	2021
Cube 2	1376	1433	1372	1446	1963
Cube 3	1309	1414	1367	1436	2011
Mean Strength	1393.3	1428.3	1344.0	1430.7	1998.3
Standard Deviation	94.2	12.7	44.2	18.6	31.0
Coefficient of Var.	6.76	0.89	3.29	1.30	1.55
<b>HSCCL2 #2 Compressive Strength Data (psi)</b>					
	1-day	7-day	28-day	56-day	112-day
Cube 1	871	936	1392	2208	2877
Cube 2	928	941	1330	2096	3012
Cube 3	913	817	1340	1973	2802
Mean Strength	904.0	898.0	1354.0	2092.3	2897.0
Standard Deviation	29.5	70.2	33.3	117.5	106.4
Coefficient of Var.	3.27	7.82	2.46	5.62	0.04
<b>HSCCL2 #2 (Dry) Compressive Strength Data (psi)</b>					
	1-day	7-day	28-day	56-day	112-day
Cube 1	1041	1019	1399	2371	3205
Cube 2	1017	1064	1587	2343	3208
Cube 3	1031	1056	1539	2273	3057
Mean Strength	1029.7	1046.3	1508.3	2329.0	3156.7
Standard Deviation	12.1	24.0	97.7	50.5	86.3
Coefficient of Var.	1.17	2.29	6.48	2.17	2.73

Table B.10 – Expansion data of length-change prisms prepared using the two Hydro-Stone® / Clinkerless #2 cement blends and Duracal® cement.

<b>HSCL2 #1 Expansion Data (%)</b>					
	1-day	28-day	56-day	84-day	112-day
Bar 1	0	0.022	0.094	0.124	0.129
Bar 2	0	0.030	0.104	0.104	0.106
Bar 3	0	0.028	0.101	0.104	0.104
Bar 4	0	0.031	0.102	0.100	0.102
Average Expansion	0	0.028	0.100	0.108	0.110
<b>HSCL2 #2 Expansion Data (%)</b>					
	1-day	28-day	56-day	84-day	112-day
Bar 1	0	0.082	0.228	0.286	0.307
Bar 2	0	0.067	0.230	0.277	0.294
Bar 3	0	0.071	0.240	0.291	0.308
Bar 4	0	0.074	0.229	0.284	0.284
Average Expansion	0	0.074	0.232	0.285	0.298
<b>Duracal® Expansion Data (%)</b>					
	1-day	28-day	56-day	84-day	112-day
Bar 1	0	0.031	0.041	0.046	0.054
Bar 2	0	0.031	0.057	0.053	0.061
Bar 3	0	0.044	0.042	0.051	0.054
Average Expansion	0	0.035	0.047	0.050	0.056
<b>Duracal® w/UFA Expansion Data (%)</b>					
	1-day	28-day	56-day	84-day	112-day
Bar 1	0	0.149	0.188	0.223	0.227
Bar 2	0	0.143	0.184	0.205	0.221
Bar 3	0	0.120	0.139	0.158	0.166
Bar 4	0	0.106	0.138	0.159	0.167
Average Expansion	0	0.130	0.162	0.186	0.195

Table B.11 – Compressive strengths of mortar cubes prepared using hemihydrates that were produced from FGD gypsum, in which different preparation techniques were used.

<b>Compressive Strength Data (psi)</b>						
	No Press	5500 lb	11000 lb	Ultrazine	Lignin	Potassium Sulfate
Cube 1	3032	4757	4270	4705	4565	4833
Cube 2	2762	4469	4151	4538	4275	4686
Cube 3	3225	4398	4226	4376	4502	5008
Cube 4	3264	4611	4137	4287	4524	4920
Cube 5	3091	4400	4182	4455	3895	4560
Cube 6	3102	4734	3954	4483	4163	4936
Mean Strength	3079.3	4561.5	4153.3	4474.0	4320.7	4823.8
Standard Deviation	178.3	162.4	109.3	143.2	261.6	170.0
Coefficient of Var.	5.79	3.56	2.63	3.20	6.05	3.52

Table B.12 – Compressive strengths of mortar cubes prepared using the preliminary “low-energy, 100% by-product cement” blends.

<b>0.5HH/0.5CL2 #1 Compressive Strength Data (psi)</b>					
	1-day	7-day	28-day	56-day	112-day
Cube 1	734	932	1219	1780	3048
Cube 2	761	826	1129	1853	2935
Cube 3	818	852	1173	2030	2978
Mean Strength	771.0	870.0	1173.7	1887.7	2987.0
Standard Deviation	42.9	55.2	45.0	128.6	57.0
Coefficient of Var.	5.56	6.35	3.83	6.81	1.91
<b>0.5HH/0.5CL2 #2 Compressive Strength Data (psi)</b>					
	1-day	7-day	28-day	56-day	112-day
Cube 1	1090	1347	1837	2587	3403
Cube 2	1145	1223	1699	2626	3503
Cube 3	1077	1271	1816	2618	3487
Mean Strength	1104.0	1280.3	1784.0	2610.3	3464.3
Standard Deviation	36.1	62.5	74.4	20.6	53.7
Coefficient of Var.	3.27	4.88	4.17	0.79	1.55
<b>0.5HH/0.5CL2 #2 (Dry) Compressive Strength Data (psi)</b>					
	1-day	7-day	28-day	56-day	112-day
Cube 1	1181	1256	2106	2793	3972
Cube 2	1197	1339	1814	2737	3750
Cube 3	1100	1217	1950	2707	4026
Mean Strength	1159.3	1270.7	1956.7	2745.7	3916.0
Standard Deviation	52.0	62.3	146.1	43.7	146.3
Coefficient of Var.	4.49	4.90	7.47	1.59	3.74
<b>0.5HH/0.5CL6 #1 Compressive Strength Data (psi)</b>					
	1-day	7-day	28-day	56-day	112-day
Cube 1	1253	1137	2047	3082	3039
Cube 2	1289	1140	2070	3082	2970
Cube 3	1028	1088	2000	2976	2859
Mean Strength	1190.0	1121.7	2039.0	3046.7	2956.0
Standard Deviation	141.4	29.2	35.7	61.2	90.8
Coefficient of Var.	11.89	2.60	1.75	2.01	3.07
<b>0.5HH/0.5CL6 #1 (Dry) Compressive Strength Data (psi)</b>					
	1-day	7-day	28-day	56-day	112-day
Cube 1	1199	1057	2291	3992	4085
Cube 2	1287	1154	2279	4024	4160
Cube 3	1099	1144	2305	4007	4008
Mean Strength	1195.0	1118.3	2291.7	4007.7	4084.3
Standard Deviation	94.1	53.4	13.0	16.0	76.0
Coefficient of Var.	7.87	4.77	0.57	0.40	1.86

Table B.13 – Expansion data of length-change prisms prepared using the preliminary “low-energy, 100% by-product cement” blends.

<b>0.5HH/0.5CL2 #2 Expansion Data (%)</b>					
	3-day	28-day	56-day	84-day	112-day
Bar 1	0	0.077	0.209	0.264	0.290
Bar 2	0	0.097	0.258	0.321	0.344
Bar 3	0	0.080	0.217	0.270	0.300
Bar 4	0	0.092	0.233	0.286	0.321
Average Expansion	0	0.086	0.229	0.285	0.314
<b>0.5HH/0.5CL2 #2 (Dry) Expansion Data (%)</b>					
	3-day	28-day	56-day	84-day	112-day
Bar 1	0	0.044	0.107	0.146	0.172
Bar 2	0	0.038	0.097	0.124	0.143
Bar 3	0	0.027	0.080	0.106	0.122
Average Expansion	0	0.036	0.095	0.125	0.146
<b>0.5HH/0.5CL6 #1 Expansion Data (%)</b>					
	3-day	28-day	56-day	84-day	112-day
Bar 1	0	0.122	0.119	0.121	0.123
Bar 2	0	0.110	0.107	0.108	0.109
Bar 3	0	0.102	0.096	0.097	0.098
Bar 4	0	0.097	0.097	0.097	0.099
Average Expansion	0	0.108	0.105	0.106	0.107
<b>0.5HH/0.5CL6 #1 (Dry) Expansion Data (%)</b>					
	3-day	28-day	56-day	84-day	112-day
Bar 1	0	0.061	0.080	0.081	0.089
Bar 2	0	0.058	0.074	0.074	0.081
Bar 3	0	0.052	0.058	0.061	0.064
Average Expansion	0	0.057	0.071	0.072	0.078

Table B.14 – Compressive strengths of mortar cubes prepared using the high strength and low expansion “low-energy, 100% by-product cement” mortar mix designs.

<b>0.5HH/0.5CL6 #1 Compressive Strength Data (psi)</b>				
	1-day	7-day	28-day	56-day
Cube 1	NA	1581	3107	3924
Cube 2	NA	1576	2839	3927
Cube 3	NA	NA	NA	3892
Mean Strength	NA	1578.5	2973.0	3914.3
Standard Deviation	NA	3.5	189.5	19.4
Coefficient of Var.	NA	0.22	6.37	0.50
<b>0.5HH/0.5CL6 w/Silica Fume Compressive Strength Data (psi)</b>				
	1-day	7-day	28-day	56-day
Cube 1	1561	1421	3013	3957
Cube 2	1462	1485	3012	3937
Cube 3	1533	1576	3109	3790
Mean Strength	1518.7	1494.0	3044.7	3894.7
Standard Deviation	51.0	77.9	55.7	91.2
Coefficient of Var.	3.3604	5.21	1.83	2.34

Table B.15 – Expansion data of length-change prisms prepared using the high strength and low expansion “low-energy, 100% by-product cement” mortar mix designs.

<b>0.5HH/0.5CL6 #1 Expansion Data (%)</b>				
	3-day	28-day	56-day	84-day
Bar 1	0	0.068	0.068	0.069
Bar 2	0	0.078	0.078	0.080
Bar 3	0	0.068	0.068	0.068
Average Expansion	0	0.071	0.071	0.072
<b>0.5HH/0.5CL6 w/Silica Fume Expansion Data (%)</b>				
	3-day	28-day	56-day	84-day
Bar 1	0	0.031	0.029	NA
Bar 2	0	0.034	0.032	NA
Bar 3	0	0.025	0.024	NA
Average Expansion	0	0.030	0.028	NA

### Appendix C: Two Sample t-Tests Performed in the Study

112-day compressive strength of mortar cubes prepared using *Clinkerless #6* compared to the 112-day compressive strength of mortar cubes prepared using *Clinkerless #2*.

$\mu_1$  = Average compressive strength of *Clinkerless #6* after 112 days of curing

$\mu_2$  = Average compressive strength of *Clinkerless #2* after 112 days of curing

Data:  $X_1 = 5569$  psi       $X_2 = 3703.7$  psi  
 $s_1^2 = 155078.44$        $s_2^2 = 155078.44$   
 $n_1 = 3$        $n_2 = 3$

$H_0: \mu_1 = \mu_2; \mu_1 - \mu_2 = 0$

$H_a: \mu_1 \neq \mu_2$

Assumption: Populations have a common variance,  $\sigma^2$

Test Statistic:  $X_1 - X_2 = 1865.3$  psi

p-Value:  $s_p^2 = 140445.265$

est. s.d. = 305.99

$t = (X_1 - X_2) / (\text{est. s.d.}) = 6.10$

degrees of freedom =  $(n_1 - 1) + (n_2 - 1) = 4$

►  $0.001 < p < 0.005$

Conclusion: Reject  $H_0$  and conclude that on the average, the 112-day compressive strength of mortar cubes prepared using *Clinkerless #6* is higher than 112-day compressive strength of mortar cubes prepared using *Clinkerless #2* at the error level of 5%.



112-day compressive strength of mortar cubes prepared using *HSCL2 #2* compared to the  
112-day compressive strength of mortar cubes prepared using *HSCL2 #1*.

$\mu_1$  = Average compressive strength of *HSCL2 #2* after 112 days of curing

$\mu_2$  = Average compressive strength of *HSCL2 #1* after 112 days of curing

Data:  $X_1 = 2897.0$  psi       $X_2 = 1936.7$  psi

$s_1^2 = 11320.96$        $s_2^2 = 9545.29$

$n_1 = 3$        $n_2 = 3$

$H_0: \mu_1 = \mu_2; \mu_1 - \mu_2 = 0$

$H_a: \mu_1 \neq \mu_2$

Assumption: Populations have a common variance,  $\sigma^2$

Test Statistic:  $X_1 - X_2 = 960.3$  psi

p-Value:  $s_p^2 = 10433.125$

est. s.d. = 83.40

$t = (X_1 - X_2) / (\text{est. s.d.}) = 11.51$

degrees of freedom =  $(n_1 - 1) + (n_2 - 1) = 4$

►  $p < 0.001$

Conclusion: Reject  $H_0$  and conclude that on the average, the 112-day compressive strength of mortar cubes prepared using *HSCL2 #2* is higher than the 112-day compressive strength of mortar cubes prepared using *HSCL2 #1* at the error level of 5%.

112-day compressive strength of mortar cubes prepared using *HSCL2 #2(Dry)* compared to the 112-day compressive strength of mortar cubes prepared using *HSCL2 #2*.

$\mu_1$  = Average compressive strength of *HSCL2 #2(Dry)* after 112 days of curing

$\mu_2$  = Average compressive strength of *HSCL2 #2* after 112 days of curing

Data:  $X_1 = 3156.7$  psi       $X_2 = 2897.0$  psi

$s_1^2 = 7447.69$        $s_2^2 = 11320.96$

$n_1 = 3$        $n_2 = 3$

$H_0: \mu_1 = \mu_2; \mu_1 - \mu_2 = 0$

$H_a: \mu_1 \neq \mu_2$

Assumption: Populations have a common variance,  $\sigma^2$

Test Statistic:  $X_1 - X_2 = 259.7$  psi

p-Value:  $s_p^2 = 9384.33$

est. s.d. = 79.096

$t = (X_1 - X_2) / (\text{est. s.d.}) = 3.28$

degrees of freedom =  $(n_1 - 1) + (n_2 - 1) = 4$

►  $0.025 < p < 0.050$

Conclusion: Reject  $H_0$  and conclude that on the average, the 112-day compressive strength of mortar cubes prepared using *HSCL2 #2(Dry)* is higher than the 112-day compressive strength of mortar cubes prepared using *HSCL2 #2* at the error level of 5%.

112-day expansion of length-change prisms prepared using *Clinkerless #6* compared to the 112-day expansion of length-change prisms prepared using *Clinkerless #2*.

$\mu_1$  = Average expansion of *Clinkerless #6* after 112 days of curing

$\mu_2$  = Average expansion of *Clinkerless #2* after 112 days of curing

Data:  $X_1 = 1.104\%$        $X_2 = 2.228\%$   
 $s_1^2 = 2.4369 \times 10^{-3}$      $s_2^2 = 0.012662$   
 $n_1 = 4$                        $n_2 = 4$

$H_0: \mu_1 = \mu_2; \mu_1 - \mu_2 = 0$

$H_a: \mu_1 \neq \mu_2$

Assumption: Populations have a common variance,  $\sigma^2$

Test Statistic:  $X_1 - X_2 = -1.124\%$

p-Value:  $s_p^2 = 7.549 \times 10^{-3}$

est. s.d. = 0.061439

$t = (X_1 - X_2) / (\text{est. s.d.}) = 18.3$

degrees of freedom =  $(n_1 - 1) + (n_2 - 1) = 6$

►  $p < 0.001$

Conclusion: Reject  $H_0$  and conclude that on the average, the 112-day expansion of length-change prisms prepared using *Clinkerless #6* is less than the 112-day expansion of length-change prisms prepared using *Clinkerless #2* at the error level of 5%.

112-day expansion of length-change prisms prepared using *HSCL2 #2* compared to the  
112-day expansion of length-change prisms prepared using *Clinkerless #2*.

$\mu_1$  = Average expansion of *HSCL2 #2* after 112 days of curing

$\mu_2$  = Average expansion of *Clinkerless #2* after 112 days of curing

Data:  $X_1 = 0.298\%$                        $X_2 = 2.228\%$   
 $s_1^2 = 1.3092 \times 10^{-3}$                        $s_2^2 = 0.012662$   
 $n_1 = 4$      $n_2 = 4$

$H_0: \mu_1 = \mu_2; \mu_1 - \mu_2 = 0$

$H_a: \mu_1 \neq \mu_2$

Assumption: Populations have a common variance,  $\sigma^2$

Test Statistic:  $X_1 - X_2 = -1.93\%$

p-Value:  $s_p^2 = 6.9396 \times 10^{-3}$

est. s.d. = 0.05655

$t = (X_1 - X_2) / (\text{est. s.d.}) = 34.13$

degrees of freedom =  $(n_1 - 1) + (n_2 - 1) = 6$

►  $p < 0.001$

Conclusion: Reject  $H_0$  and conclude that on the average, the 112-day expansion of length-change prisms prepared using *HSCL2 #2* is less than the 112-day expansion of length-change prisms prepared using *Clinkerless #2* at the error level of 5%.

Compressive strength of mortar cubes prepared using hemihydrate produced from FGD gypsum pucks pressed with 5500 lb of force compared to the compressive strength of mortar cubes prepared using hemihydrate produced from FGD gypsum pucks pressed with 11000 lb of force.

$\mu_1$  = Average compressive strength of 5500 lb force technique

$\mu_2$  = Average compressive strength of 11000 lb force technique

Data:  $X_1 = 4561.5$  psi       $X_2 = 4153.3$  psi

$s_1^2 = 26359.5$        $s_2^2 = 11943.87$

$n_1 = 3$        $n_2 = 3$

$H_0: \mu_1 = \mu_2; \mu_1 - \mu_2 = 0$

$H_a: \mu_1 \neq \mu_2$

Assumption: Populations have a common variance,  $\sigma^2$

Test Statistic:  $X_1 - X_2 = 408.2$  psi

p-Value:  $s_p^2 = 19151.7$

est. s.d. = 79.8993

$t = (X_1 - X_2) / (\text{est. s.d.}) = 5.11$

degrees of freedom =  $(n_1 - 1) + (n_2 - 1) = 10$

►  $p < 0.001$

Conclusion: Reject  $H_0$  and conclude that on the average, the 5500 lb force technique produces hemihydrate that obtains a higher compressive strength than the 11000 lb force technique at the error level of 5%.

112-day compressive strength of mortar cubes prepared using *0.5HH/0.5CL6 #1(Dry)*  
compared to the 112-day compressive strength of mortar cubes prepared using  
*0.5HH/0.5CL6 #1*.

$\mu_1$  = Average compressive strength of *0.5HH/0.5CL6 #1(Dry)* after 112 days of curing

$\mu_2$  = Average compressive strength of *0.5HH/0.5CL6 #1* after 112 days of curing

Data:  $X_1 = 4084.3$  psi       $X_2 = 2956.0$  psi  
 $s_1^2 = 5776.0$        $s_2^2 = 8244.64$   
 $n_1 = 3$        $n_2 = 3$

$H_0: \mu_1 = \mu_2; \mu_1 - \mu_2 = 0$

$H_a: \mu_1 \neq \mu_2$

Assumption: Populations have a common variance,  $\sigma^2$

Test Statistic:  $X_1 - X_2 = 1128.3$  psi

p-Value:  $s_p^2 = 7010.32$

est. s.d. = 68.363

$t = (X_1 - X_2) / (\text{est. s.d.}) = 16.5$

degrees of freedom =  $(n_1 - 1) + (n_2 - 1) = 4$

►  $p < 0.001$

Conclusion: Reject  $H_0$  and conclude that on the average, the 112-day compressive strength of mortar cubes prepared using *0.5HH/0.5CL6 #1(Dry)* is higher than the 112-day compressive strength of mortar cubes prepared using *0.5HH/0.5CL6 #1* at the error level of 5%.

112-day compressive strength of mortar cubes prepared using *0.5HH/0.5CL6 #1(Dry)*  
compared to the 112-day compressive strength of mortar cubes prepared using  
*0.5HH/0.5CL2 #2(Dry)*.

$\mu_1$  = Average compressive strength of *0.5HH/0.5CL6 #1(Dry)* after 112 days of curing

$\mu_2$  = Average compressive strength of *0.5HH/0.5CL2 #2(Dry)* after 112 days of curing

Data:  $X_1 = 4084.3$  psi                       $X_2 = 3916.0$  psi  
 $s_1^2 = 5776.0$                                        $s_2^2 = 21403.7$   
 $n_1 = 3$      $n_2 = 3$

$H_0: \mu_1 = \mu_2; \mu_1 - \mu_2 = 0$

$H_a: \mu_1 \neq \mu_2$

Assumption: Populations have a common variance,  $\sigma^2$

Test Statistic:  $X_1 - X_2 = 168.3$  psi

p-Value:  $s_p^2 = 13589.9$

est. s.d. = 95.184

$t = (X_1 - X_2) / (\text{est. s.d.}) = 1.768$

degrees of freedom =  $(n_1 - 1) + (n_2 - 1) = 4$

►  $0.100 < p < 0.200$

Conclusion: Fail to reject  $H_0$  at the error level of 5%.

112-day expansion of length-change prisms prepared using *0.5HH/0.5CL6 #1(Dry)*  
compared to the 112-day expansion of length-change prisms prepared using  
*0.5HH/0.5CL6 #1*.

$\mu_1$  = Average expansion of *0.5HH/0.5CL6 #1(Dry)* after 112 days of curing

$\mu_2$  = Average expansion of *0.5HH/0.5CL6 #1* after 112 days of curing

Data:  $X_1 = 0.078\%$

$X_2 = 0.107\%$

$s_1^2 = 1.62996 \times 10^{-4}$

$s_2^2 = 1.3491 \times 10^{-4}$

$n_1 = 3$

$n_2 = 4$

$H_0: \mu_1 = \mu_2; \mu_1 - \mu_2 = 0$

$H_a: \mu_1 \neq \mu_2$

Assumption: Populations have a common variance,  $\sigma^2$

Test Statistic:  $X_1 - X_2 = -0.029\%$

p-Value:  $s_p^2 = 1.4614 \times 10^{-4}$

est. s.d. =  $9.233 \times 10^{-3}$

$t = (X_1 - X_2) / (\text{est. s.d.}) = -3.14$

degrees of freedom =  $(n_1 - 1) + (n_2 - 1) = 5$

►  $0.025 < p < 0.050$

Conclusion: Reject  $H_0$  and conclude that on the average, the 112-day expansion of length-change prisms prepared using *0.5HH/0.5CL6 #1(Dry)* is less than the 112-day expansion of length-change prisms prepared using *0.5HH/0.5CL6 #1* at the error level of 5%.



112-day expansion of length-change prisms prepared using *0.5HH/0.5CL6 #1(Dry)*  
compared to the 112-day expansion of length-change prisms prepared using  
*0.5HH/0.5CL2 #2(Dry)*.

$\mu_1$  = Average expansion of *0.5HH/0.5CL6 #1(Dry)* after 112 days of curing

$\mu_2$  = Average expansion of *0.5HH/0.5CL2 #2(Dry)* after 112 days of curing

Data:  $X_1 = 0.078\%$

$X_2 = 0.146\%$

$s_1^2 = 1.62996 \times 10^{-4}$

$s_2^2 = 6.3031 \times 10^{-4}$

$n_1 = 3$

$n_2 = 3$

$H_0: \mu_1 = \mu_2; \mu_1 - \mu_2 = 0$

$H_a: \mu_1 \neq \mu_2$

Assumption: Populations have a common variance,  $\sigma^2$

Test Statistic:  $X_1 - X_2 = -0.068\%$

p-Value:  $s_p^2 = 3.9665 \times 10^{-4}$

est. s.d. = 0.016261

$t = (X_1 - X_2) / (\text{est. s.d.}) = -4.18$

degrees of freedom =  $(n_1 - 1) + (n_2 - 1) = 4$

►  $0.010 < p < 0.025$

Conclusion: Reject  $H_0$  and conclude that on the average, the 112-day expansion of length-change prisms prepared using *0.5HH/0.5CL6 #1(Dry)* is less than the 112-day expansion of length-change prisms prepared using *0.5HH/0.5CL2 #2(Dry)* at the error level of 5%.

## References

- American Coal Ash Association (1995). Fly Ash Facts for Highway Engineers. Report No. FHWA-SA-94-081. F. H. Administration. Washington, DC.
- American Coal Ash Association (2007). 2006 Coal Combustion Product (CCP) Production and Use Survey.
- American Concrete Institute (1994). Controlled low strength materials (CLSM). Report No. 229r-94. A. C. 229. Detroit, Michigan.
- American Society of Testing and Materials (2000). Annual Book of ASTM Standards. Vols. 04.01 and 04.02. West Conshohocken, PA.
- BASF Construction Chemicals LLC (2007). Glenium® 3030 NS Product Data. Master Builders. 23700 Chagrin Boulevard, Cleveland, OH.
- Basu, P. (1999). "Combustion of coal in circulating fluidized-bed boilers: a review." Chemical Engineering Science **54**(22): 5547-5557.
- Berry, E. E., R. T. Hemmings, et al. (1991). Commercialization Potential of AFBC Concrete: Part 2. Volume 2: Mechanistic Basis for Cementing Action. D. M. Golden. Palo Alto, Electric Power Research Institute.
- Bland, A. E. and T. H. Brown (1997). Market Assessment and Technical Feasibility Study of Pressurized Fluidized Bed Combustion Ash Use. Cooperative Agreement DE-FC21-93MC30127. Laramie, Wyoming, Western Research Institute.
- Bland, A. E., C. E. Jones, et al. (1987). Production of No-Cement Concretes Utilizing Fluid Bed Combustion Waste and Power Plant Fly Ash. 9th International Conference on FBC, ASME, Boston, MA.
- Burkard, E. A. (1985). Manufacture of gypsum board from FGD gypsum. United States Patent. USPTO. United States of America, National Gypsum Company. **4,502,901**.
- Butalia, T. S., W. E. Wolfe, et al. (2001). "Evaluation of a dry FGD material as a flowable fill." Fuel **80**(6): 845-850.
- Chryso (2007). CHRYSO®Pave 100 Product Information Sheet. 10600 Hwy 62, Gate 19, Unit 7, Charlestown, IN.
- Deschamps, R. J. (1998). "Using FBC and Stoker Ashes as Roadway Fill: A Case Study." Journal of Geotechnical and Environmental Engineering **124**(11): 1120-1127.
- Energy Information Administration (2008). Summary Reference Case Tables. Annual Energy Outlook 2008 (Revised Early Release) 1-34.
- Gartner, E. (2004). "Industrially interesting approaches to "low-CO<sub>2</sub>" cements." Cement and Concrete Research **34**(9): 1489-1498.
- Giacinto, J. F., P. Petzrick, et al. (2007). Cost Optimization for Mine Void Stabilization Projects: A Deep Mine Case Study. 2007 World of Coal Ash. Northern Kentucky Convention Center, Covington, KY, Center for Applied Energy Research, University of Kentucky.
- Gungor, A. (2008). "Analysis of combustion efficiency in CFB coal combustors." Fuel **87**(7): 1083-1095.
- Hansen, W. C. (1973). "A Discussion of the Paper "Mechanism of Expansion Associated With Ettringite Formation" by P.K. Mehta." Cement and Concrete Research **3**(5): 651-652.

- Hemmings, R. (2007). Introduction to By-Products Produced by Clean Coal Technologies Part 1. Properties. 2007 World of Coal Ash. Northern Kentucky Convention Center, Covington, KY.
- Hemmings, R. (2007). Introduction to By-Products Produced by Clean Coal Technologies Part 2. Applications. 2007 World of Coal Ash. Northern Kentucky Convention Center, Covington, KY.
- Hewlett, P. C. (2001). Lea's Chemistry of Cement and Concrete. Woburn, MA, Butterworth-Heinemann.
- Hopkins, T. C. and T. L. Beckham (1999). Long-Term Performance of a Highway Subgrade Stabilized with an Atmospheric Fluidized Bed Combustion Material. 1999 International Ash Utilization Symposium. Hyatt Regency, Lexington, KY, Center for Applied Energy Research, University of Kentucky: 632-639.
- Koslowski, T. J. (1991). Process for making construction grade calcium sulfate alpha-hemihydrate from moist finely divided gypsum obtained from a power plant flue gas desulfurization. USPTO, Promineral Gesellschaft zur Verwendung von Mineralstoffen mbH & Sicowa Verfahrenstechnik fur Baustoffe GmbH & Co. K.G. **5015449**.
- Marsh, B. K. and R. L. Day (1988). "Pozzolanic and Cementitious Reactions of Fly Ash in Blended Cement Pastes." Cement and Concrete Research **18**(2): 301-310.
- Mehta, P. K. (1973). "Mechanism of Expansion Associated with Ettringite Formation." Cement and Concrete Research **3**(1): 1-6.
- Mehta, P. K. (1980). "Investigations on energy-saving cements." World Cement Technology **11**(5): 166-177.
- Montagnaro, F., M. Nobili, et al. (2008). "Hydration products of FBC wastes as SO<sub>2</sub> sorbents: comparison between ettringite and calcium hydroxide." Fuel Processing Technology **89**(1): 47-54.
- O'Brien, W. E., W. L. Anders, et al. (1984). Marketing of byproduct gypsum from flue gas desulfurization: Pages: 167.
- Payette, R. M., W. E. Wolfe, et al. (1996). Use of clean coal combustion by-products in highway repairs. Land Application Uses of Dry FGD By-Product. Columbus, OH, The Ohio State University.
- Products, G. C. (2007). Recover® Hydration stabilizer ASTM C494 Type D Product Information. 62 Whittemore Avenue, Cambridge, MA.
- Shang, J. Q. and H. Wang (2005). Coal Fly Ash as Contaminant Barrier for Reactive Mine Tailings. 2005 World of Coal Ash. Lexington Convention Center, Lexington, KY.
- Siriwardane, H. J., S. S. Kannan, et al. (2003). "Use of Waste Material for Control of Acid Mine Drainage and Subsidence." Journal of Environmental Engineering **129**(10): 910-915.
- Solem-Tishmack, J. K., G. J. McCarthy, et al. (1995). "High-Calcium Coal Combustion By-Products: Engineering Properties, Ettringite Formation, and Potential Application in Solidification and Stabilization of Selenium and Boron." Cement and Concrete Research **25**(3): 658-670.

- Stuart, B. J., G. Novak, et al. (1999). Use of Flue Gas Desulfurization By-Product for Mine Sealing and Abatement of Acid Mine Drainage. 1999 International Ash Utilization Symposium. Hyatt Regency, Lexington, KY, Center for Applied Energy Research, University of Kentucky.
- Swan, C., G. Topping, et al. (2007). Flowable Fills Developed With High Volumes of Fly Ash. 2007 World of Coal Ash. Northern Kentucky Convention Center, Covington, Ky, Center for Applied Energy Research, University of Kentucky.
- United States Environmental Protection Agency (1990). Title IV - Acid Deposition Control. Clean Air Act.
- United States Gypsum Company (2003). Duracal® Material Safety Data Sheet. 125 South Franklin Street Chicago, IL, Industrial Gypsum Division.
- United States Gypsum Company (2003). Hydro-Stone® Material Safety Data Sheet. 125 South Franklin Street Chicago, IL, Industrial Gypsum Division.
- Walker, H., P. Taerakul, et al. (2005). Short- and Long-Term Behavior of Fixated FGD Material Grout at the Roberts-Dawson Mine. 2005 World of Coal Ash. Lexington Convention Center, Lexington, KY.
- Wang, H. (1990). Alkali-Silica Reaction-Mechanism. Significance of Chemical and Mineral Admixtures. Department of Civil Engineering. Calgary, Alberta, The University of Calgary.
- Warner, N., J. F. Giacinto, et al. (2007). Effects of Acid Mine Drainage on CCP Grout: A Bench-Scale Weathering Experiment. 2007 World of Coal Ash. Northern Kentucky Convention Center, Covington, KY, Center for Applied Energy Research, University of Kentucky.
- Weinberg, A. and R. Hemmings (1997). Hydration and Weathering reactions in by-products from clean coal technologies: effects on material properties, US Department of Energy.
- Wolfe, W. E., R. J. Lee, et al. (2001). The Effect of Ettringite Formation on Expansion Properties of Compacted Spray Dryer Ash. 2001 International Ash Utilization Symposium. Hyatt Regency, Lexington, KY, Center for Applied Energy Research, University of Kentucky.
- Wolfe, W. E., R. W. Poston, et al. (2001). The Behavior of Coal Combustion Products in Structural Fills - A Case History. 2001 International Ash Symposium. Hyatt Regency, Lexington, KY, Center for Applied Energy Research, University of Kentucky.

**Vita**

Name: David Edward Rust

Born: January 12, 1984 / Cincinnati, Ohio

Education: Bachelor's of Science in Civil and Environmental Engineering from the  
University of Cincinnati (2002 – 2007)

Professional Positions: Project Engineer at Palmer Engineering Company (2008)

Professional Honor: Engineer in Training (2007)